NEWSLETTERS ON

Stratigraphy

Volume 43 No. 3

ISSN 0078-0421

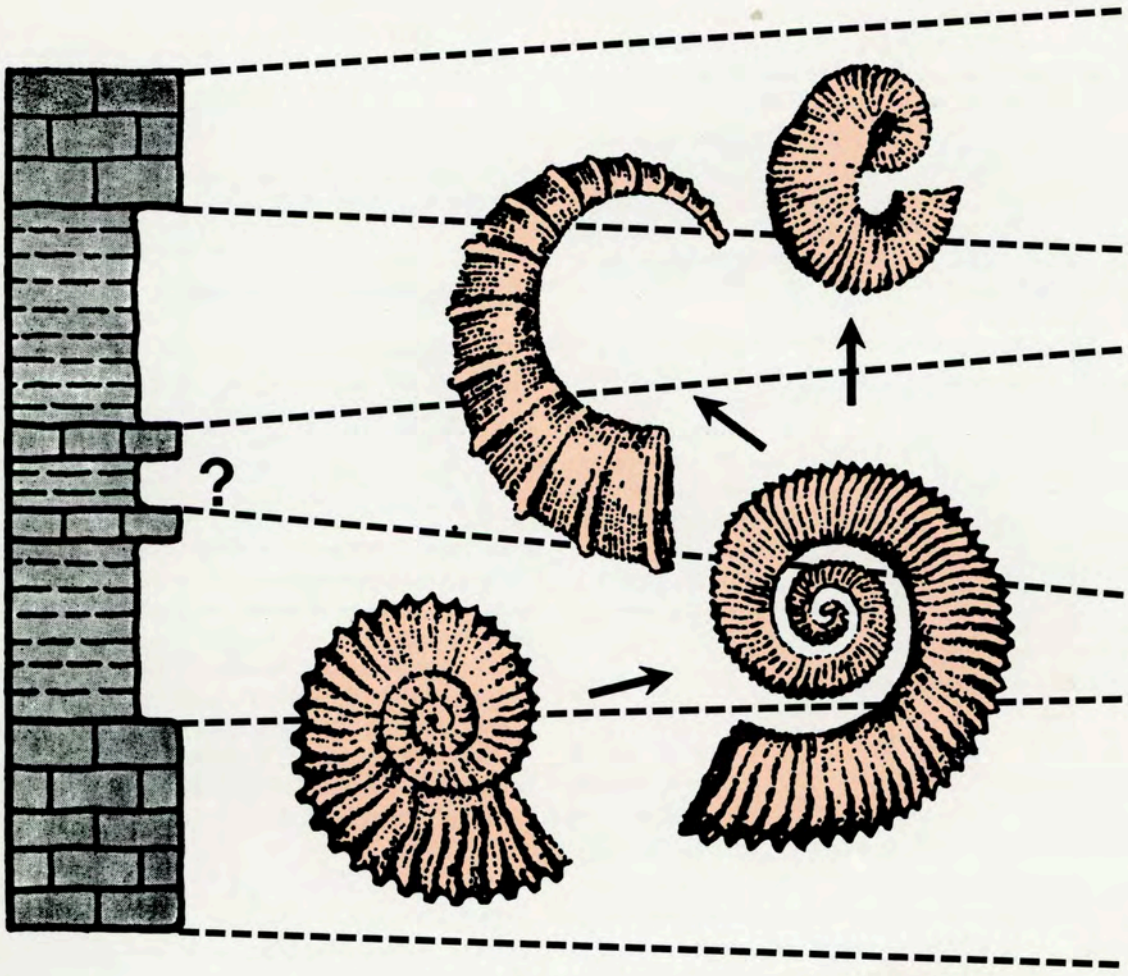

Edited by
J. Erbacher, Hannover and J. Pross, Frankfurt

Gebrüder Borntraeger · Berlin · Stuttgart 2010

Newsletters on Stratigraphy
Instructions to Authors

Manuscript Submission/Copyright

Submission of a manuscript for publication in **Newsletters on Stratigraphy** is considered binding assurance that this work has not been and will not be published elsewhere in this form and length.

With acceptance and publication of a manuscript the exclusive copyright for every language and country is transferred to the publishers. The copyright covers the exclusive rights to reproduce and distribute the article including reprints, microfilm or any other reproduction and translations.

Manuscripts should not exceed 8,000 words without prior agreement from the Editorial Team. In a cover letter accompanying the submitted manuscript, please supply the names and addresses (including E-mail addresses) of 4 potential reviewers. Please send your manuscript to one of the members of the **Editorial Team**:

Dr. Jochen Erbacher
Bundesanstalt für Geowissenschaften und Rohstoffe
Stilleweg 2
30655 Hannover (Germany)
jochen.erbacher@bgr.de

Prof. Dr. Jörg Pross
Johann Wolfgang Goethe-Universität
Institut für Geowissenschaften
Altenhoeferallee 1
60438 Frankfurt (Germany)
joerg.pross@em.uni-frankfurt.de

Contributors to Special Issues are asked to submit their manuscripts directly to the Guest Editor(s).

Manuscript Preparation

Please make sure that your text is written in good English (American and British English are equally acceptable, but please avoid a mixture of both). If the English falls short of the standards of *Newsletters on Stratigraphy*, the Editorial Team will be unable to send the manuscript out for review and will instead return it to the authors for improvement.

Title Page. Please provide the following information on the title page (in the order given)
Title. Please avoid abbreviations and formulae whenever possible.
Author Names and Affiliations. Please present the authors' addresses below the authors' names. Indicate all affiliations with a lower-case superscript letter immediately after the author's name and in front of the respective address. Provide the full postal address of each affiliation, including the country name, and, if available, the e-mail address of each author.

Printer: Laupp & Göbel, Nehren/Tübingen – Printed in Germany

Newsletter on Stratigraphy
Vol. **43/3:** 207–233, April 2010

Magnetostratigraphy – concepts, definitions, and applications

Cor G. Langereis, Wout Krijgsman, Giovanni Muttoni, and Manfred Menning

With 12 figures

Abstract. The most characteristic feature of the Earth's magnetic field is that it reverses polarity at irregular intervals, producing a 'bar code' of alternating normal (north directed) and reverse (south directed) polarity chrons with characteristic durations. Magnetostratigraphy refers to the application of the well-known principles of stratigraphy to the pattern of polarity reversals registered in a rock succession by means of natural magnetic acquisition processes. This requires that the rock faithfully recorded the ancient magnetic field at the time of its formation, a prerequisite that must be verified in the laboratory by means of palaeomagnetic and rock magnetic techniques.

A sequence of intervals of alternatively normal or reverse polarity characterized by irregular (non-periodic) duration constitutes a distinctive pattern functional for correlations. Over the last 35 Myr, polarity intervals show a mean duration of ~ 300,000 years, but large variations occur from 20,000 yr to several Myr and even up to tens of Myr. By correlating the polarity reversal pattern retrieved in a rock succession to a reference geomagnetic polarity time scale (GPTS), calibrated by radioisotopic methods and/or orbital tuning, the age of the rock succession can be derived. Magnetostratigraphy and correlation to the GPTS constitute a standard dating tool in Earth sciences, applicable to a wide variety of sedimentary (but also volcanic) rock types formed under different environmental conditions (continental, lacustrine, marine). It is therefore the stratigraphic tool of choice to perform correlations between continental and marine realms. Finally, we emphasise that magnetostratigraphy, as any other stratigraphic tool, works at best when integrated with other dating tools, as illustrated by the case studies discussed in this paper.

Part one – Concepts, definitions, and applications

Introduction

Dating and time control are essential in all disciplines of the Earth Sciences, since they allow to correlate rock sequences from distant localities and different (marine and continental) realms. Moreover, accurate time control is the sine qua non to understand rates of change of natural processes and thus to determine the underlying mechanisms that explain our observations. Biostratigraphy of different faunal and floral systems has been used since the 1,840 s to erect the relative geological age of sedimentary rocks and hence to perform correlations among them. Radioisotopic dating, originally applied mostly to igneous rocks, has become increasingly sophisticated and can now count on a wide variety of isotopic decay systems capable to provide numerical ages also in sedimentary rocks formed under

Author's addresses:
Cor G. Langereis, Wout Krijgsman, Palaeomagnetic Laboratory "Fort Hoofddijk", University of Utrecht, 3584 CD Utrecht, The Netherlands, E-Mail: langer@geo.uu.nl, krijgsma@geo.uu.nl; Giovanni Muttoni, Department of Earth Sciences, University of Milano, 20133 Milano, Italy, E-Mail: giovanni.muttoni1@unimi.it, Manfred Menning, GFZ German Research Center for Geosciences, 14473 Potsdam, Germany, E-Mail: menne@gfz-potsdam.de

DOI: 10.1127/0078-0421/2010/0043-0207

0078-0421/10/0043-0207 $ 6.75

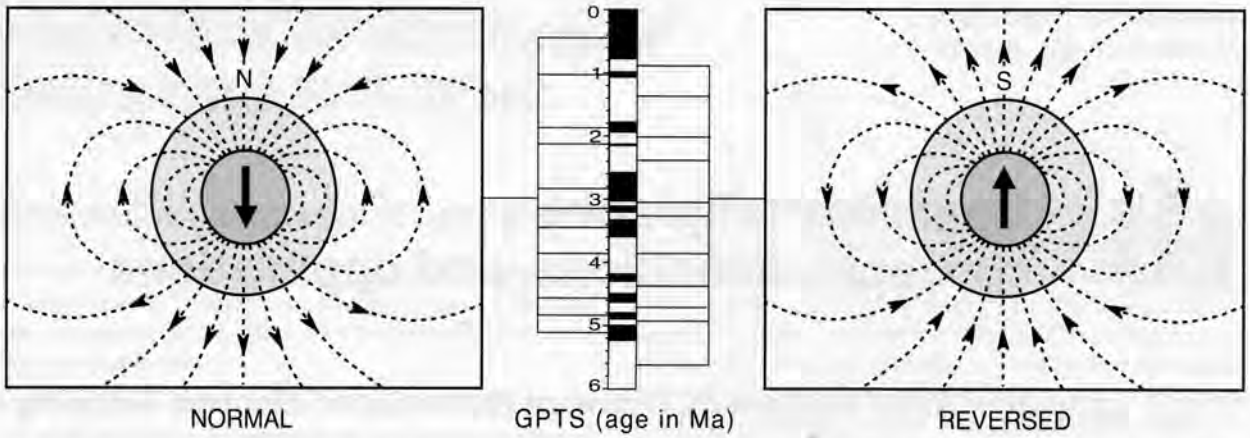

Fig. 1. Schematic representation of the geomagnetic field of a geocentric axial dipole ('bar magnet'). During normal polarity of the field the average magnetic north pole is at the geographic north pole, and a compass aligns along magnetic field lines. Historically, the north pole is referred to as the pole attracting the 'north seeking' needle of a compass, but physically it is a south pole. During normal polarity, the inclination is positive (downward directed) in the northern hemisphere and negative (upward directed) in the southern hemisphere. Conversely, during reversed polarity, the compass needle points south, and the inclination is negative in the northern and positive in the southern hemisphere. In the geomagnetic polarity time scale (column in the middle), periods of normal polarity are conventionally represented by black intervals, reversed intervals by white intervals.

favorable environmental conditions. In this paper, we describe the principles of magnetostratigraphy defined as a dating tool that uses the record of polarity (normal or reverse) of the ancient geomagnetic field registered in igneous or sedimentary rock sequences by natural magnetic acquisition processes.

The most distinctive property of the Earth's magnetic field is that it can reverse polarity (Fig. 1). During the siege of Lucera (Apulia, Italy) by the armies of Charles d'Anjou, an army engineer called Pierre Pèlerin de Maricourt, better known as Petrus Peregrinus ('Peter the Pilgrim'), made a remarkable series of observations. He described the dipolar nature of a (magnetised) spherical lodestone, and showed that the magnetic force of this natural dipole is strongest and vertical at the poles. In 1269, he reported his findings in the Epistola de Magnete – regarded as the first scientific treatise ever written – and became the first to formulate the law by which poles with same magnetic charge repel whereas poles with opposite charge attract. In 1600, William Gilbert published the results of his experimental studies on magnetism entitled De Magnete, Magneticisque Corporibus, et de Magno Magnete Tellure. He investigated the variation in inclination over the surface of a spherical lodestone and concluded for the first time that 'magnus magnes ipse est globus terrestris' (the Earth's globe itself is a great magnet). Apart from the spherical form of the Earth, magnetism was the first physical property attributed to the body of the Earth as a whole. Newton's theory of gravitation came 87 years later with the publication of his 'Philosophiæ Naturalis Principia Mathematica. A pleasantly readable article on a more elaborate history of magnetism is by Stern (2002).

Palaeomagnetic studies of igneous rocks provided the first reliable information on polarity reversals. In 1906, Bernard Brunhes, at that time director of the Puy-de-Dôme Observatory (France), observed lava flows magnetised in a direction approximately antiparallel to the present geomagnetic field, and suggested that this was caused by a reversal of the field itself, rather than by a self-reversal mechanism of the rock. In 1929, Motonori Matuyama demonstrated that young Quaternary lavas were magnetised in the same direction as the present field (normal polarity), whereas older lavas were magnetised in the opposite direction. But it was only in the early 1,950 s that Jan Hospers with his study of Icelandic basalts succeeded to convince many in the geophysics community that reversed magnetism in rocks was not caused by a self-reversal processes but was a record of times when the Earth's magnetic field had reversed polarity state (Hospers 1951). He was the first to realise that the polarity of lava flows could be a powerful stratigraphic correlation tool (cf. Irving 1988; Stern 2002), while Khramov (1958) realised that by correlating volcanic and sedimentary rock successions worldwide, it could be possible to develop a single geochronological palaeomagnetic time scale valid for

the whole Earth. The first geomagnetic polarity time scales (GPTS) began to take shape when the combined use of radioisotopic dating and magnetostratigraphy was adopted on lava flows (Fig. 2; Cox et al. 1963, 1964). Improved techniques and the undertaking of extensive palaeomagnetic investigations in many parts of the world have significantly increased the amount of palaeomagnetic information and have now provided a very detailed Geomagnetic Polarity Time Scale (e.g. Opdyke and Channell 1996), of which the Neogene part is fully astronomically calibrated (Lourens et al., 2004) through the extensive use of cyclostratigraphy (e.g. Strasser et al. 2006).

More than one century after the first reversal of the Earth's magnetic field was discovered by Brunhes (1906), more than half a century after the start of the modern era of magnetostratigraphy (Hospers 1951), and almost half a century after the first development of the modern GPTS (Cox 1963), it can be concluded that magnetostratigraphy has evolved into an indispensable stratigraphic tool for Earth Sciences.

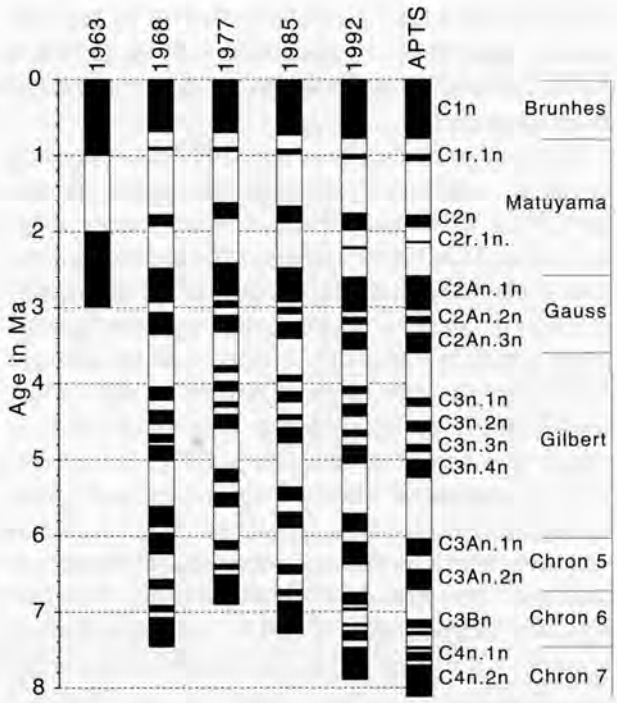

Fig. 2. Development of the geomagnetic polarity time scale (GPTS) over the last half century of study. The initial assumption of periodic behaviour (Cox, 1963) was soon abandoned as new data became available. The first modern GPTS based on marine magnetic anomaly patterns was established by Heirtzler et al. (1968). Subsequent revisions by Labreque et al. (1977), Berggren et al. (1985), Cande, Kent (1992) show improved age control and increased resolution. A major breakthrough came with the astronomical polarity time scale (APTS) in which every individual reversal is accurately dated (e.g. Hilgen et al., 1997). Black (white) intervals denote normal (reversed) polarity; for chron nomenclature, see text.

The palaeomagnetic signal

The Earth's magnetic field is generated in the liquid outer core through a dynamo process that is maintained by convective fluid motion. At the surface of the Earth, the field can be conveniently described as a dipole field, which is equivalent to having a bar magnet at the centre of the Earth. Such a dipole accounts for approximately 90% of the observed field. The remaining 10% derives from higher order terms: the non-dipole field. At any one time, the best fitting geocentric dipole axis does not coincide exactly with the rotation axis of the Earth, but averaged over several thousand years, we may assume the dipole to be both geocentric and axial (Merrill et al. 1996). Initially, it was believed that the field reversed periodically, but as more results on lava flows became available, it became clear that geomagnetic reversals occur randomly. It is precisely this random character that confers stratigraphic value to a measured polarity reversal sequence. A polarity reversal typically takes several thousands of years to occur, fast enough to be considered globally synchronous on geological time scales. The field itself is sign invariant whereby the same configuration of the geodynamo can produce either normal or reverse polarity. What causes the field to reverse is still debated, but recent hypotheses suggest that lateral changes in heat flow at the core-mantle boundary play an important role (e.g. Gubbins 1999). Although polarity reversals occur at irregular times, the reversal frequency can change considerably over geological time spans. For instance, the polarity reversal frequency has increased since 80 Ma from approximately 1 rev/Myr to 5 rev/My in more recent times. In the Cretaceous, from 124.5 to 84 Ma, no reversals occurred and the field maintained stable normal polarity for some 40 Myr. This Cretaceous Superchron is known in ocean-floor magnetic anomaly profiles as the Cretaceous Normal Quiet Zone.

The ancient geomagnetic field can be registered in rocks at the time of their formation. Rocks commonly contain magnetic minerals, usually iron (hydr)oxydes or iron sulphides. During rock-forming processes, these magnetic minerals (or more accurately, their magnetic domains) statistically align with the then am-

bient field, and are subsequently 'locked in' the rock system, thus preserving the direction of the field as a natural remanent magnetisation (NRM): the palaeomagnetic signal.

We distinguish three basic types of NRM, depending on the mechanism of palaeomagnetic signal acquisition: TRM, CRM and DRM. A thermoremanent magnetisation (TRM) is the magnetisation acquired when a rock cools below the Curie temperature of its magnetic minerals, thereby 'locking' the magnetic domains along positions statistically aligned with the ambient field and producing a magnetic remanence that at room temperature may be stable for billions of years. A chemical remanent magnetisation (CRM) is the magnetisation acquired when a magnetic mineral grows through a critical 'blocking volume' or grain size at which the field is locked in and the acquired remanence may again be stable over billions of years. A detrital remanent magnetisation (DRM) is the magnetisation acquired when magnetic grains of detrital origin are deposited. Magnetic grains responsible for a DRM can also form directly in the water column as magnetosomes: intra-cellular chains of magnetic minerals made by magnetotactic bacteria (e.g. Vasiliev et al. 2008). Detrital magnetic grains statistically align with the ambient field as long as they are in the water column or in the soft water-saturated topmost layer of the sediment. Upon compaction and dewatering, the grains are mechanically fixated in a 'lock-in depth zone' and will preserve the direction of the ambient field. Within the sediment, authigenic or diagenetic formation of magnetic minerals may take place which also record the field. This may occur in an early stage, but also well after deposition, deeper within the sediment. In the latter case, this may cause an apparent delay of the NRM acquisition which can distort the magnetic record.

Demagnetisation, laboratory tests, and field tests

Frequently, the total NRM is the vector sum of different magnetic components (Fig. 3). This is because the primary NRM, i.e., the magnetisation originated at the time of rock formation, may be overprinted by magnetic components acquired later in geologic history through weathering reactions at room temperature or thermochemical reactions associated with tectonic or burial processes. An overprint component can be removed through 'magnetic cleaning' techniques. These are primarily the thermal demagnetisation technique and the alternating magnetic field (AF) demagnetisation technique (e.g. Zijderveld 1967; Langereis et al. 1989; Butler 1992; Tauxe 1998). During demagnetisation experiments, samples are subjected to stepwise increasing values of temperature or alternating field in a zero magnetic field (field-free) space. The residual magnetisation is measured after each demagnetisation step and the resultant changes in direction and intensity are displayed and analysed in order to reconstruct the complete component structure of the NRM. Some palaeomagnetic laboratories have recently invested in automatic measurement systems, which enable continuous measurements of large amounts of samples. Automated and repeating measurement schemes yield previously unattainable amounts of information, and may give results even from low-intensity limestones (e.g. Gong et al. 2008) provided such systems are designed to maintain low noise levels during measurements.

The results of stepwise demagnetisation are commonly visualized and analyzed using the so-called Zijderveld diagrams (after Zijderveld 1967), also known as vector end-point demagnetisation diagrams (Fig. 3). In these diagrams, both the intensity and directional changes of the NRM occurring during demagnetisation are displayed at the same time. Magnetic components are then extracted from the Zijderveld diagrams using least-square analysis (Kirschvink 1980), and the most stable and consistent component that can be isolated is referred to as the characteristic remanent magnetisation (ChRM). This ChRM is further investigated to establish if it represents a record of the geomagnetic field at, or close to, the time of rock formation, or a secondary magnetisation acquired later in geologic history by post-depositional processes. To assess the primary nature of the ChRM, and hence its suitability for magnetostratigraphic studies, rock magnetic experiments and reliability tests are usually carried out. Rock magnetic experiments are aimed at determining the fundamental characteristics of the minerals bearing the magnetic remanence (e.g., type, grain size, etc.). A review of these methods is beyond the scope of this paper but can be found in appropriate text books (e.g. Butler 1992) or review papers. The three most important reliability tests for magnetostratigraphy are:

Consistency test. A natural remanent magnetisation component is considered primary in origin when it defines a sequence of polarity reversals that is laterally traceable by independent means (e.g. lithostratigraphy) between distant sections from different parts of the basin.

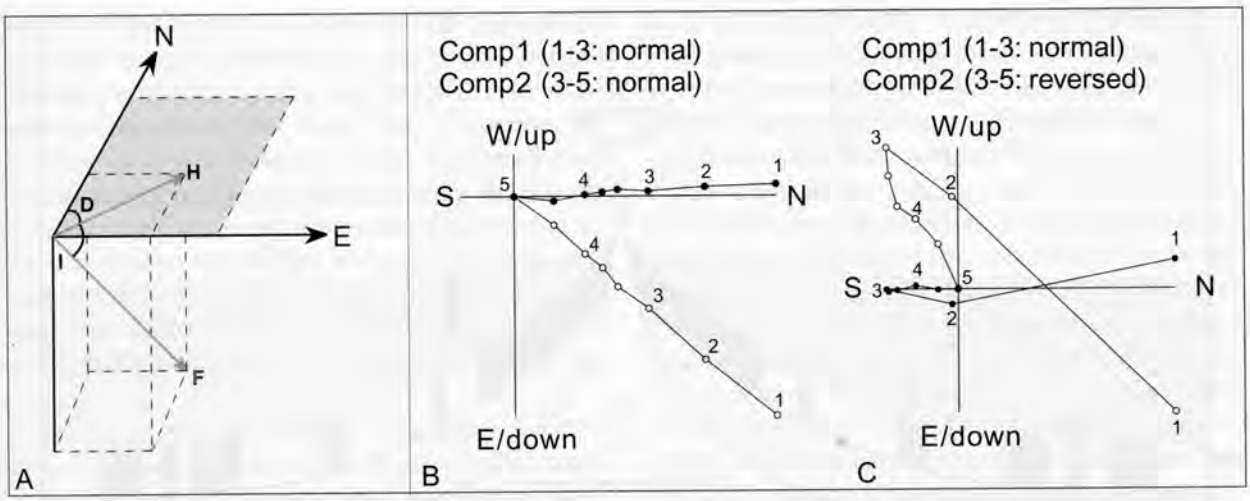

Fig. 3. (A) The magnetic field on any point on the Earth's surface is a vector (F) which possesses a component in the horizontal plane called the horizontal component (H) which makes an angle (D) with the geographical meridian. The declination (D) is an angle from north measured eastward ranging from 0° to 360°. The inclination (I) is the angle made by the magnetic vector with the horizontal. By convention, it is positive if the north-seeking vector points downward and negative if it points upward. (B) and (C) To resolve the different magnetic components that can be acquired in a rock during its geological history, rock samples are subjected to a process of stepwise demagnetisation. The standard method for presentation and analysis of the results is called Zijderveld diagrams (after Zijderveld, 1967). Changes in the magnetisation vector during demagnetisation involve both its direction and its intensity; orthogonal vector Zijderveld diagrams show the changes in both. The endpoint of the vector measured after each demagnetisation step is projected both onto the horizontal plane (closed symbols) and onto the vertical plane (open symbols). Difference vectors (lines between end points) then show the behaviour of the total vector upon stepwise removal of the magnetisation. Conventionally, she solid points are these endpoints when projected onto the horizontal plane containing axes NS and EW, whereas the open points are these endpoints when projected onto the vertical plane containing axes NS (or EW), and up-down. Although many variations exist in literature, the only sensible projected axes combinations are W/up vs. NS and N/up vs. EW.

Reversal test. The observation of characteristic remanence directions with different polarity and, in particular, the occurrence of antiparallel (within statistical error) directions is taken as a strong indication for the primary origin of that ChRM. This test is greatly enhanced if a polarity zonation can be established, and if this zonation is independent of possible changes in the composition of the rock.

Fold test. If the ChRM directions from differently tilted beds converge after correction for the dip of the strata, this remanence was acquired before tilting. Strictly speaking, this fold test does not directly prove a primary origin of this component, but only that it dates from before tilting.

The Geomagnetic Polarity Time Scale

For the construction of the 'bar code' pattern of magnetic polarity intervals, geophysicists rely on two fundamentally different records of geomagnetic polarity history: the marine magnetic anomaly record and the magnetostratigraphic record. Surveys over the ocean basins carried out from the 1950's onward found linear magnetic anomalies, parallel to mid-oceanic ridges, using magnetometers towed behind research vessels (Cox et al. 1963; Heirtzler et al. 1968). During the early 1960s, it was suggested, and soon after confirmed, that these anomalies resulted from the remanent magnetisation of the oceanic crust. This remanence is acquired during the process of sea-floor spreading, when uprising magma beneath the axis of the oceanic ridges cools through the Curie temperatures of its constituent ferromagnetic minerals in presence of the ambient geomagnetic field, thus acquiring its direction and polarity. The continuous process of rising and cooling of magma at the ridge results in magnetisaed crust of alternating normal and reverse polarity, which produces a slight increase or decrease of the measured field: the marine magnetic anomalies (Fig. 4a). It was also found that the magnetic anomaly pattern is generally symmetric on both sides of the ridge, and, most importantly, that it provides a remarkably continuous record of

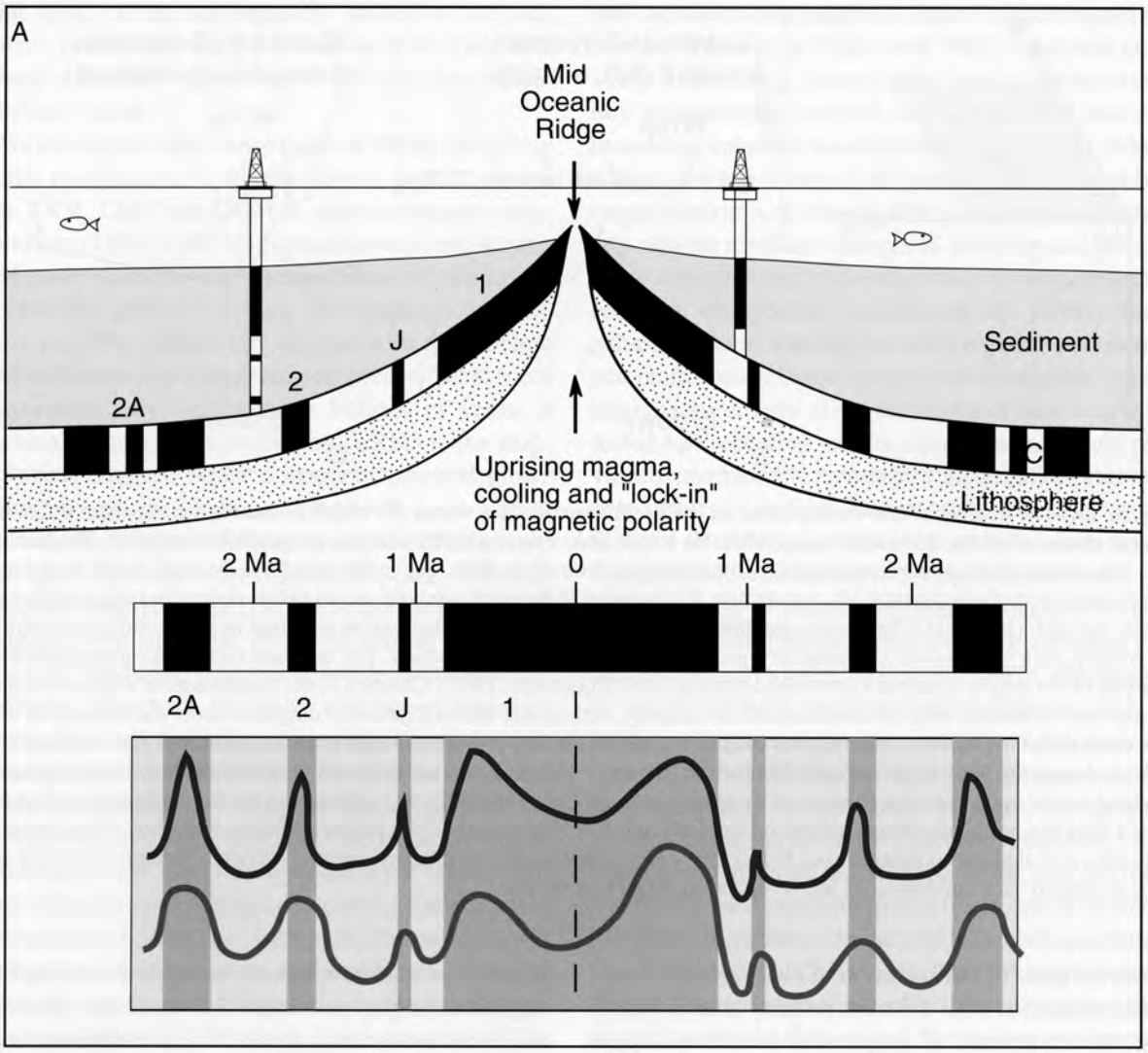
A
Mid
Oceanic
Ridge
1
J
2
2A
Sediment
C
Lithosphere
Uprising magma,
cooling and "lock-in"
of magnetic polarity
2 Ma
1 Ma
0
1 Ma
2 Ma
2A
2
J
1

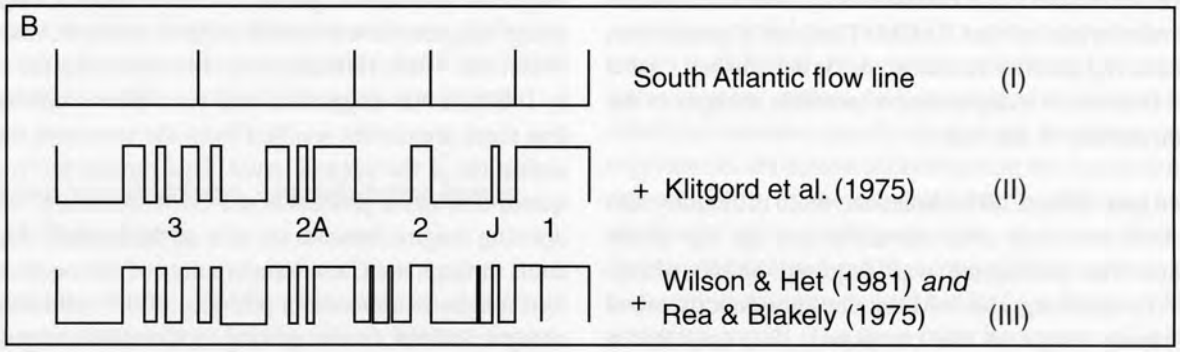
B
South Atlantic flow line (I)
+ Klitgord et al. (1975) (II)
3
2A
2
J
1
+ Wilson & Het (1981) and
Rea & Blakely (1975) (III)

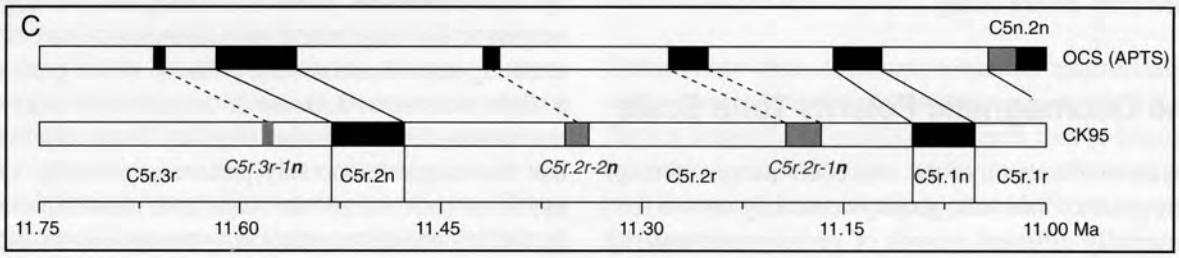
C
C5n.2n
OCS (APTS)
CK95
C5r.3r
C5r.3r-1n
C5r.2n
C5r.2r-2n
C5r.2r
C5r.2r-1n
C5r.1n
C5r.1r
11.75
11.60
11.45
11.30
11.15
11.00 Ma

the geomagnetic reversal sequence. The template of magnetic anomaly patterns from the ocean floor has remained central for constructing the GPTS from magnetic polarity chron M0r in the Early Cretaceous onward (~ 124.5–0 Ma; He et al. 2008). Combined magnetostratigraphic, biostratigraphic, and radioisotopic results of deep-sea sediments and land-based sections have confirmed and refined the general validity and accuracy of the GPTS (e.g. LaBreque et al. 1977; Berggren et al. 1985). The development of the GPTS reflects increasing detail and gradually improved age control.

The latest development in constructing a GPTS comes from orbital tuning of the sediment record, the so called Astronomically calibrated Polarity Time Scale (APTS) (Hilgen et al. 1997). The APTS is now almost complete for the Neogene (Lourens et al. 2004) and has been developed for the Late Triassic (Kent and Olsen 1999; Olsen and Kent 1999). It differs essentially from the conventional GPTS, in the sense that each reversal boundary – or any other geological boundary, e.g. biostratigraphic datum levels or stage and epoch boundaries – is dated individually. This time scale has the inherent promise of increasingly advancing our understanding of the climate system, because cyclostratigraphy and orbital tuning rely on deciphering environmental changes driven by climate change, which in turn is orbitally forced. The main feature of an APTS is that the age of each reversal is directly determined, rather than interpolated between radioisotopic calibration points. This has important consequences for changes in spreading rates of plate pairs, as sea floor spreading rates can now be more accurately determined. Indeed, Wilson (1993) found that the use of astronomical ages resulted in very small and physically realistic spreading rate variations. As a result, the discrepancy in plate-motion rates from the global plate tectonic model (NUVEL-1; DeMets et al. 1990) with respect to those derived from geodesy has become much smaller, and NUVEL-1 has been updated (to NUVEL-1A; DeMets et al. 1994) to incorporate the new astronomical ages.

Periods of a predominant (normal or reverse) polarity are called chrons, and the four youngest ones are named after leading scientists in the field of palaeomagnetism or geomagnetism, i.e. Brunhes, who suggested the existence of field reversals, Matuyama, who proved this, Gauss, who mathematically described the field, and Gilbert, who discovered that the Earth itself is a big magnet. The Brunhes to Gauss chron sequence contain short intervals of opposite polarity called subchrons, which are named after the locality where they were discovered, e.g. the Olduvai normal polarity subchron within the Matuyama reverse polarity chron is named after the Olduvai Gorge (Tanzania), or the Kaena reverse polarity subchron within the Gauss normal polarity chron named after Kaena Point (Hawaii).

Older chrons were not named but numbered according to the anomaly numbers originally given by Heirtzler et al. (1968). Cande and Kent (1992) developed a consistent (sub)chron nomenclature that is now used as the standard (details in their Appendix: Nomenclature). A more recent revision of the Cande and Kent (1992) time scale was made by Cande and Kent (1995) in which they adopted the orbitally tuned timescale (Shackleton et al. 1990; Hilgen 1991a, b) for the last 5.3 Myr.

Tiny wiggles, cryptochrons and subchrons

The magnetic anomaly template over the last 84 Myr was thoroughly revised by Cande and Kent (1992), up to the Cretaceous Normal Superchron (Cretaceous

Fig. 4. A) Formation of marine magnetic anomalies during seafloor spreading. The oceanic crust is formed at the ridge crest, and while spreading away from the ridge it is covered by an increasing thickness of oceanic sediments. The black (white) blocks of oceanic crust represent the original normal (reversed) polarity of the thermoremanent magnetisation (TRM) acquired upon cooling at the ridge. The black and white blocks in the drill holes represent normal and reversed polarity depositional remanent magnetisation (DRM) acquired during deposition of the marine sediments. Normal polarity anomalies are given numbers and refer to anomaly 1 (Brunhes Chron), 2 (Olduvai subchron) and 2A (Gauss Chron); J = Jaramillo subchron. B) Stacks of marine magnetic anomaly profiles (red line) are used to model (blue line) the polarity sequence. B) Categories used by Cande and Kent (1992): category I = major anomalies along a synthetic reference flow line in the South Atlantic, II = filling in details from the best South Atlantic profiles (Klitgord et al. 1975), III = further details from (often deep-tow) anomaly profiles from fast-spreading ridges (Wilson and Hey, 1981, Rea and Blakely, 1975). C) Example of Chron-Subchron-Cryptochron nomenclature: reversed Chron C5r, with normal subchrons C5r.1n and C5r.2n. Cryptochrons C5r.2r-1, C5r.2r-2 and C5r.3r-1 elevated to the status of subchrons C5r.2r-1n, C5r.2r-2n and C5r.3r-1n (after Abdul Aziz and Langereis 2004).

Quiet Zone in magnetic anomaly profiles). They constructed a synthetic flow line in the South Atlantic, with first order distances built up from a combination of finite rotation poles, designated as category I intervals. On these intervals, they projected the best quality profiles surveyed in this ocean basin, providing category II intervals (Fig. 4b). Since spreading rates in the Atlantic are relatively slow, they subsequently filled in the category II intervals with high-resolution profiles from fast spreading ridges (their category III). This enabled them to include much more detail on short polarity intervals (or subchrons), for instance around 7 Ma (Fig. 2). In total, they used 9 calibration points to construct their GPTS, including for the first time as youngest tie point an astronomically calibrated age for the Gauss/Matuyama boundary.

The reliability and completeness of the GPTS is crucial for geochronology but also for understanding the long-term statistical properties of the geomagnetic field. The shortest polarity intervals in the GPTS are typically on the order of 30 kyr in duration, but the magnetic anomaly patterns of fast spreading oceanic plates indicate that smaller-scale variations exist as well. They have been referred to as what they look like: tiny wiggles (LaBrecque et al. 1977); these very short and low intensity anomalies have an uncertain origin. Tiny wiggles may represent very short subchrons of the field, as has been proven for some of them (e.g. the Cobb Mt. subchron at 1.21 Ma, or the Réunion subchron at 2.13–2.15 Ma), or just represent intensity fluctuations of the geomagnetic field, causing the oceanic crust to be less (or more) strongly magnetised. Because of their uncertain or unverified nature, these were called cryptochrons (Cande and Kent, 1992). The cryptochrons have a designation (–1, –2, etc.) following the primary (sub)chron nomenclature. For example, three new cryptochrons were recently discovered in the reversed Chron C5r in Middle-Late Miocene continental deposits of Spain (Abdul Aziz et al. 2004; Abdul Aziz and Langereis 2004) (Fig. 4C). Chron C5r contains two normal polarity subchrons (C5r.1n and C5r.2n) and is consequently divided in three reversed polarity intervals (C5r.1r, C5r.2r and C5r.3r). Since two of the cryptochrons were found in C5r.2r, they are denoted C5r.2r-1 and C5r.2r-2, from young to old. The third cryptochron in C5r.3r then must become C5r.3r-1. Cande and Kent (1992) proposed that a cryptochron can be elevated to the status of subchron if it corresponds to a magnetostratigraphically documented pair of reversals. Since this was the case in the Spanish deposits, the cryptochrons therein found were designated as subchrons and acquired a polarity suffix: C5r.2r-1n – C5r.2r-2n and C5r.3r-1n.

The origin of many cryptochrons has not yet been confirmed by magnetostratigraphic studies. On the other hand, there is firm evidence for excursions and reversal excursions. The term excursion is used for virtual geomagnetic poles (VGP) deviating more than 45° from geographical north (Verosub and Banerjee 1977), while it is termed a reversal excursion for VGPs that deviate in excess of 90° from geographical north (Merrill and McFadden 1994) and possibly reaching (near) opposite polarity. Invariably, reversal excursions are associated with low palaeointensities of the geomagnetic field, both in the Brunhes and in the Matuyama Chrons (Guyodo and Valet, 1999; Channell et al. 2002). Reversal excursions have a typical duration of 3–6 kyr (Langereis et al. 1997), which is usually much too short to be detected in marine magnetic anomaly profiles, and explains why so few excursions have been detected, even as tiny wiggles. Excursions are most frequently observed within the Brunhes normal polarity Chron (0–781 ka), but this is in part because of the chronostratigraphic coverage of DSDP and ODP holes, which decreases more or less exponentially with depth, and in part because of our higher confidence in assuming that excursions of reverse polarity are primary in origin and not due to e.g. overprinting by the normal polarity present-day field. In any case, reversal excursions or even short subchrons are as a rule not suitable for magnetostratigraphic correlation because of their elusive nature inherent to their very short duration (Roberts and Winkelhofer 2004).

Part two – Case studies

We present three case studies to illustrate the use of magnetostratigraphy as a dating and correlating tool. Each case study comes from a different area with a different geological age and depositional setting. The first study deals with the Neogene part of the GPTS, which is based on the direct dating of polarity reversals and biostratigraphic datums using astronomical curves in the Monte dei Corvi section, Italy (Hüsing et al. 2007, 2009a). This case study provides a state-of-the-art example of integrated stratigraphy with orbitally controlled resolution. The second case study is from the middle Triassic Seceda core, Italy (Muttoni et al. 2004a), which provides an example of a multi-disciplinary and integrated stratigraphic approach. The third case study deals with the Carboniferous-Permian Re-

versed Superchron (PCRS), and discusses the state-of-the-art stratigraphy of its lower and upper boundaries. In addition, it provides an updated stratigraphic chart for the late Permian, and a newly interpreted record of the Illawarra reversal that marks the end of the PCRS.

Cenozoic case study: The Middle Miocene Monte dei Corvi section, Italy

Sedimentary cycles reflect climatic oscillations that are ultimately controlled by the Earth's orbital cycles as described by the Milankovitch theory, and are accordingly known also as astrocycles (Strasser et al. 2006). Perturbations in the Earth's orbit and rotation axis are climatically important because they affect the global, seasonal, and latitudinal distribution of the incoming solar insolation. They are held responsible for the Pleistocene ice ages but also affect low-latitude climatic systems such as monsoons. Orbitally forced climatic oscillations are recorded in sedimentary archives through changes in sediment properties, fossil communities, and chemical characteristics (Strasser et al. 2006). While Earth scientists can read the geological archives to reconstruct palaeoclimate, astronomers have formulated astronomical solutions that include both the solar-planetary system and the Earth-Moon system. With these astronomical solutions, they compute the past variations in precession, obliquity, and eccentricity (Varadi et al. 2003; Laskar et al. 2004). As a logical next step, sedimentary archives can be dated by matching patterns of palaeoclimatic variability with patterns in the computed astronomical curves. This astronomical tuning of the sedimentary record results in timescales that are largely independent of radioisotopic dating (Lourens et al. 2004; Kuiper et al. 2008).

Initially, research focused mostly on the Pliocene-Pleistocene – using palaeoclimatic records from Ocean Drilling Project sites in the eastern equatorial Pacific and North Atlantic (Shackleton et al. 1990) and sedimentary cycle patterns in Pliocene-Miocene marine successions exposed on land in the Mediterranean area (Hilgen 1991a, b; Hilgen et al. 1995; Krijgsman et al. 1995, 1999; Hüsing et al. 2007, 2009a). In the Mediterranean area, well-known sections such as Capo Rossello, Eraclea Minoa, Singa, and Vrica were used to construct detailed magnetostratigraphic records (Langereis and Hilgen 1991). These sections consist of carbonates and sapropels (brownish-colored layers enriched in organic carbon) arranged in a remarkably clear cyclic pattern that is controlled by precession and eccentricity. The next goal was to extend the Mediterranean-based APTS into the Miocene. Suitable upper Miocene sections were identified on land on the islands of Crete, Gavdos, and Sicily, and provided a straightforward calibration of their cyclic sedimentary pattern and magnetostratigraphy to the astronomical curves (Hilgen et al. 1995). The resulting time scale embraces in continuity the interval between 9.7 and 6.8 Ma, whereas a "Messinian Gap" is present from 6.8 to 5.3 Ma. This gap is explained by the less favourable sediments (e.g., diatomites, evaporites) deposited during the so-called Messinian Salinity Crisis and the notoriously complex depositional history of the Mediterranean during this time interval (Krijgsman et al. 1999). The classic Messinian sediments, however, also displayed distinct sedimentary cyclicities, holding great promise for astronomical dating. Cyclostratigraphic and detailed palaeoclimatic studies revealed that the sedimentary cycles of the Messinian pre-evaporites and evaporites are dominantly controlled by precession-induced changes in circum-Mediterranean climate (Krijgsman et al. 1999, 2001). Closing the Messinian gap resulted in an APTS for the last ~ 10 Myr, which comprised a precisely dated record of the palaeoceanographic and palaeoclimatologic changes occurring in the Mediterranean region at that time. Magneto-cyclostratigraphic dating consequently allowed marine-continental (Abdul Aziz et al. 2004) and Mediterranean-Paratethys (Vasiliev et al. 2004) correlations of unprecedented high resolution, in which the many fossil and palaeoclimate data from continental, lacustrine, and brackish-water settings could be correlated to the global marine proxy records.

Another application of the astronomical polarity timescale has been the dating of Neogene stage boundaries via their Global boundary Stratotype Section and Point (GSSP), many of which have recently been defined in the Mediterranean, like the base of the Zanclean Stage and base of the Pliocene Series (Van Couvering et al. 2000). The availability of a good astrochronology has effectively become a prerequisite for the definition of a GSSP. Another example is shown by the Tortonian GSSP, which has recently been placed at the mid-point of the sapropel in basic cycle 76 in the Monte dei Corvi Beach section near Ancona, Italy (Hilgen et al. 2005). Here, a detailed and integrated stratigraphy of calcareous plankton biostratigraphy, magnetostratigraphy, and cyclostratigraphy has been established (Hilgen et al. 2003).

versed Superchron (PCRS), and discusses the state-of-the-art stratigraphy of its lower and upper boundaries. In addition, it provides an updated stratigraphic chart for the late Permian, and a newly interpreted record of the Illawarra reversal that marks the end of the PCRS.

Cenozoic case study: The Middle Miocene Monte dei Corvi section, Italy

Sedimentary cycles reflect climatic oscillations that are ultimately controlled by the Earth's orbital cycles as described by the Milankovitch theory, and are accordingly known also as astrocycles (Strasser et al. 2006). Perturbations in the Earth's orbit and rotation axis are climatically important because they affect the global, seasonal, and latitudinal distribution of the incoming solar insolation. They are held responsible for the Pleistocene ice ages but also affect low-latitude climatic systems such as monsoons. Orbitally forced climatic oscillations are recorded in sedimentary archives through changes in sediment properties, fossil communities, and chemical characteristics (Strasser et al. 2006). While Earth scientists can read the geological archives to reconstruct palaeoclimate, astronomers have formulated astronomical solutions that include both the solar-planetary system and the Earth-Moon system. With these astronomical solutions, they compute the past variations in precession, obliquity, and eccentricity (Varadi et al. 2003; Laskar et al. 2004). As a logical next step, sedimentary archives can be dated by matching patterns of palaeoclimatic variability with patterns in the computed astronomical curves. This astronomical tuning of the sedimentary record results in timescales that are largely independent of radioisotopic dating (Lourens et al. 2004; Kuiper et al. 2008).

Initially, research focused mostly on the Pliocene-Pleistocene – using palaeoclimatic records from Ocean Drilling Project sites in the eastern equatorial Pacific and North Atlantic (Shackleton et al. 1990) and sedimentary cycle patterns in Pliocene-Miocene marine successions exposed on land in the Mediterranean area (Hilgen 1991a, b; Hilgen et al. 1995; Krijgsman et al. 1995, 1999; Hüsing et al. 2007, 2009a). In the Mediterranean area, well-known sections such as Capo Rossello, Eraclea Minoa, Singa, and Vrica were used to construct detailed magnetostratigraphic records (Langereis and Hilgen 1991). These sections consist of carbonates and sapropels (brownish-colored layers enriched in organic carbon) arranged in a remarkably clear cyclic pattern that is controlled by precession and eccentricity. The next goal was to extend the Mediterranean-based APTS into the Miocene. Suitable upper Miocene sections were identified on land on the islands of Crete, Gavdos, and Sicily, and provided a straightforward calibration of their cyclic sedimentary pattern and magnetostratigraphy to the astronomical curves (Hilgen et al. 1995). The resulting time scale embraces in continuity the interval between 9.7 and 6.8 Ma, whereas a "Messinian Gap" is present from 6.8 to 5.3 Ma. This gap is explained by the less favourable sediments (e.g., diatomites, evaporites) deposited during the so-called Messinian Salinity Crisis and the notoriously complex depositional history of the Mediterranean during this time interval (Krijgsman et al. 1999). The classic Messinian sediments, however, also displayed distinct sedimentary cyclicities, holding great promise for astronomical dating. Cyclostratigraphic and detailed palaeoclimatic studies revealed that the sedimentary cycles of the Messinian pre-evaporites and evaporites are dominantly controlled by precession-induced changes in circum-Mediterranean climate (Krijgsman et al. 1999, 2001). Closing the Messinian gap resulted in an APTS for the last ~ 10 Myr, which comprised a precisely dated record of the palaeoceanographic and palaeoclimatologic changes occurring in the Mediterranean region at that time. Magneto-cyclostratigraphic dating consequently allowed marine-continental (Abdul Aziz et al. 2004) and Mediterranean-Paratethys (Vasiliev et al. 2004) correlations of unprecedented high resolution, in which the many fossil and palaeoclimate data from continental, lacustrine, and brackish-water settings could be correlated to the global marine proxy records.

Another application of the astronomical polarity timescale has been the dating of Neogene stage boundaries via their Global boundary Stratotype Section and Point (GSSP), many of which have recently been defined in the Mediterranean, like the base of the Zanclean Stage and base of the Pliocene Series (Van Couvering et al. 2000). The availability of a good astrochronology has effectively become a prerequisite for the definition of a GSSP. Another example is shown by the Tortonian GSSP, which has recently been placed at the mid-point of the sapropel in basic cycle 76 in the Monte dei Corvi Beach section near Ancona, Italy (Hilgen et al. 2005). Here, a detailed and integrated stratigraphy of calcareous plankton biostratigraphy, magnetostratigraphy, and cyclostratigraphy has been established (Hilgen et al. 2003).

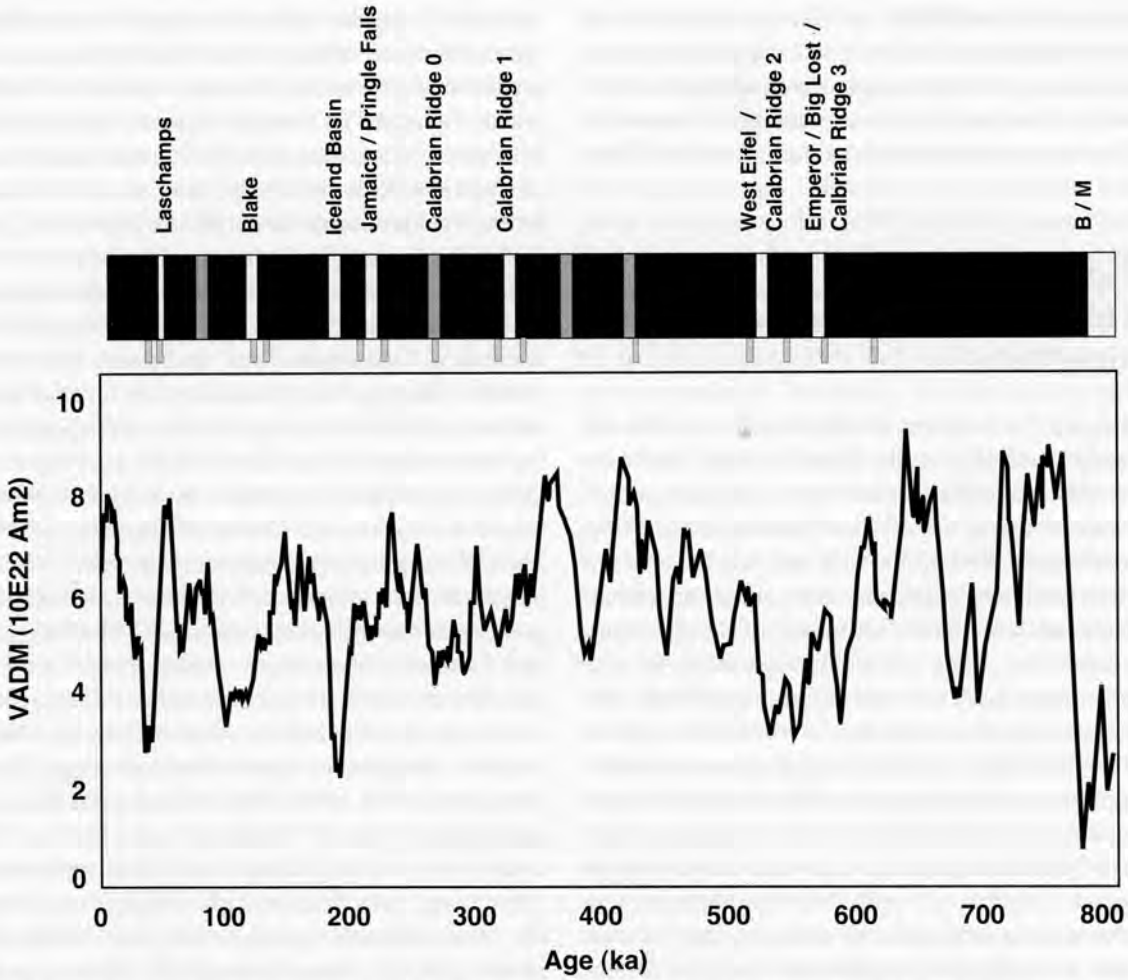

Fig. 5. Virtual Axial Dipole Moment (VADM) of the field for the past 800 kyr (Guyodo and Valet 1999). Low intensities are typically correlated with the occurrence of reversal excursions, short periods where the virtual geomagnetic pole deviates more than 90° from the north geographic pole (white intervals are well confirmed reversal excursions, grey intervals require confirmation; Langereis et al., 1997). Small grey bars outside the column are excursions from ODP cores found by Lund et al. (1998). B/M is Brunhes-Matuyama boundary, showing very low intensities – down to 10% of the stable polarity field – during the reversal.

This section has now been extended upwards to include the Tortonian-Messinian boundary and therefore the entire Tortonian Stage (Hüsing et al. 2009a). Palaeomagnetic results revealed a characteristic low-temperature component characterized by dual polarity, mostly carried by a Fe-sulphide (greigite), but in the younger interval by greigite and magnetite (Hüsing et al. 2009b). The different magnetic minerals carrying the NRM reflect the palaeoenvironment of deposition, whereby oxic, suboxic to anoxic, and anoxic conditions determined the occurrence of, respectively, magnetite, magnetite and greigite, and greigite as recorders of the Earth's magnetic field. The resultant magnetostratigraphy, calibrated to the Astronomically Tuned Neogene Time Scale, shows that the section ranges at least from Chron C5An.2n up to C3Br.2n. The Monte dei Corvi section is the only continuous Tortonian section in the Mediterranean area and is therefore suggested as the Tortonian Reference Section (Fig. 6) (Hüsing et al. 2009a). The correlation of the Tortonian GSSP to the middle part of Chron C5r.2n guarantees global correlation potentials, and the astronomical tuning performed on a precessional scale using the La2004(1,1) solution (Laskar et al. 2004) yielded astronomical ages of each basic cycle and, hence, of the calcareous plankton events and magnetic reversal boundaries with uncertainties on the order of a few thousand years. As a result, the age of the Tortonian GSSP is now 11.625 Ma,

superseding the previously published estimate of 11.608 Ma (Hilgen et al. 2005). This clearly illustrates that continuous refinements of the geological timescale is a forever ongoing research effort.

Mesozoic case study: The Middle Triassic Seceda section, an integrated stratigraphic study from the Dolomites, Italy

Middle Triassic magnetostratigraphy and biostratigraphy in both Tethyan marine and continental sequences received considerable attention during the last decade. In the compilation of Muttoni et al. (2000), a total of ~42 superposed and biostratigraphically calibrated polarity zones were recognised in 15 partially overlapping Tethyan marine sections spanning a late Early Triassic to late Middle Triassic interval of perhaps 10–15 Myr. This compilation was a preliminary attempt to compile a standard Middle Triassic GPTS.

Research by different groups continued since then in both Tethyan and Boreal marine realms (Nawrocki and Szulc 2000; Hounslow and McIntosh 2003; Muttoni et al. 2004a; Gradinaru et al. 2007; Hounslow et al. 2007) as well as in the Germanic (Central European) Basin (Szurlies et al. 2003; Szurlies 2007). As a result, the sequence of polarity reversals for some Middle Triassic time intervals is relatively well established. For example, excellent matching of magnetostratigraphies has been found for the Olenekian-Anisian boundary interval between Albania (Muttoni et al. 1996) and Romania (Gradinaru et al. 2007). Another illustrative example of a laterally reproducible magnetostratigraphy comes from Anisian-Ladinian boundary sections from the Dolomites, Italy (Muttoni et al. 2004a), and is briefly summarised hereafter.

Magnetostratigraphic investigations on biostratigraphically dated Tethyan limestones and radioisotopically dated tuff intervals of Middle Triassic age from the Dolomites started in the late 1,990 s (Muttoni et al. 1997). A ~ 110 m long core was drilled at Mount Seceda in the northwestern Dolomites (Brack et al. 2000). With over 90% recovery, the core offered a unique opportunity to reconstruct a consistent portion of the Middle Triassic time scale in stratigraphic continuity (Muttoni et al. 2004a). The conodont biostratigraphy of the laterally equivalent outcrop section could be integrated by means of magneto- and lithostratigraphic correlations (Fig. 7). A logical next step was the correlation with data from previously studied sections from the Dolomites (Frötschbach, Pedraces, Belvedere), but also from Trentino (Margon-Val Gola), and from the Brescian Alps (Bagolino), as is illustrated in figure 8.

The Seceda core spans a complete succession of Buchenstein Beds limestone members and associated Pietra Verde volcaniclastic layers. Two ash layers located in these intervals yielded accurate U-Pb age data (Mundil et al. 1996, Brack et al. 1996), indicating an average sediment accumulation rate of ~ 1 cm/kyr (Fig. 7). Palaeomagnetic analyses were performed on numerous samples from the oriented core. A characteristic remanent magnetisation component could be established and rock magnetic experiments supported its primary origin (Muttoni et al. 2004a). Moreover, the palaeomagnetic mean directions from the Seceda core and from the Frötschbach, Pedraces and Belvedere sections (Brack and Muttoni 2000) pass the fold test, giving even more confidence in the origin of the palaeomagnetic signal. These observations support the successful magneto- and lithostratigraphic correlations between distant sections and suggest that the Buchenstein Beds carry an original Triassic magnetisation, acquired well before the Cenozoic Alpine deformation.

According to the general palaeogeographic evolution of Pangea during the Permian and Triassic, the Dolomites as part of the African promontory of Adria were located in the northern hemisphere during Middle Triassic times, an assessment that is essential for interpreting magnetic polarity. A sequence of 24 polarity zones was recognized at Seceda (Fig. 7) and was successfully correlated to magnetostratigraphic sequences developed in other sections from the Dolomites and Trentino by using also laterally traceable lithostratigraphic marker beds such as tuff levels (Tc, Td, Te) and limestone beds (Fig. 8). This integrated stratigraphy allowed piecing together sections across virtually the entire eastern Southern Alps, and allowed the construction of a reference magnetostratigraphy. Merging the U-Pb dates from Seceda and the faunal associations from all sections notably augmented the numerical and biostratigraphic definition of the Anisian-Ladinian boundary interval. The resulting composite sequence was found to cover an Anisian-Ladinian time span of ~ 4 Myr, where geochronological and magnetostratigraphic control indicate a frequency of 4 reversals per Myr.

The integrated Anisian-Ladinian chronology contributed to resolve the "Latemar controversy": a debate on the duration of deposition of the Latemar carbonate

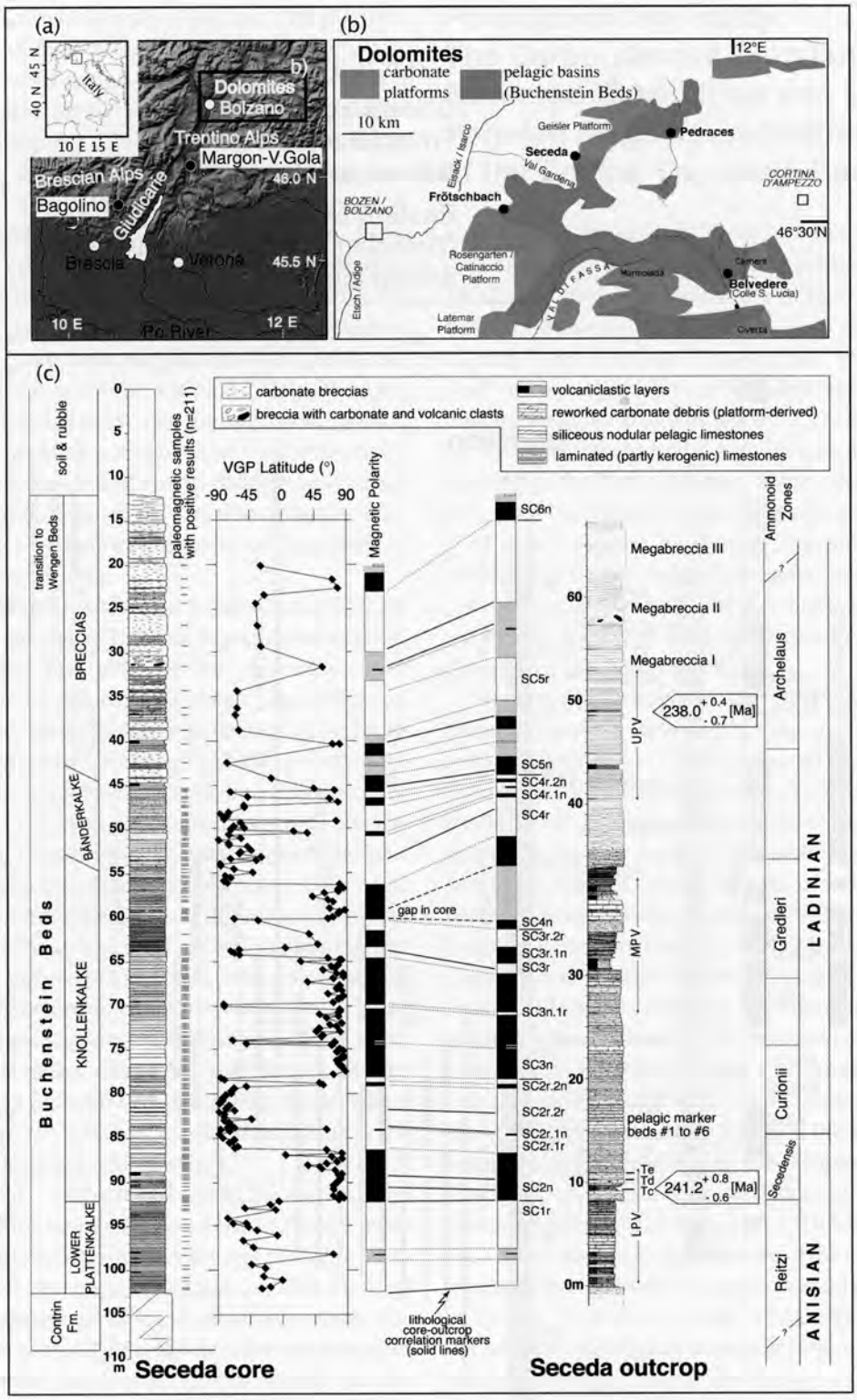

Fig. 7. A) Alpine region with location of the stratigraphic sections: Seceda, Frötschbach, Pedraces, Belvedere, and Rosengarten (Dolomites); Margon-Val Gola (Trentino); Bagolino (Brescian Alps). B) Sections in the Dolomites are placed with respect to the distribution of Ladinian carbonate platforms and pelagic basins. C) Lithology and magnetostratigraphy of the Seceda core and outcrop (Muttoni et al. 2004a). VGP latitudes are derived from the characteristic magnetic component; black (white) is normal (reverse) polarity, grey represents intervals with no data. U-Pb single zircon age data are from Mundil et al. (1996).

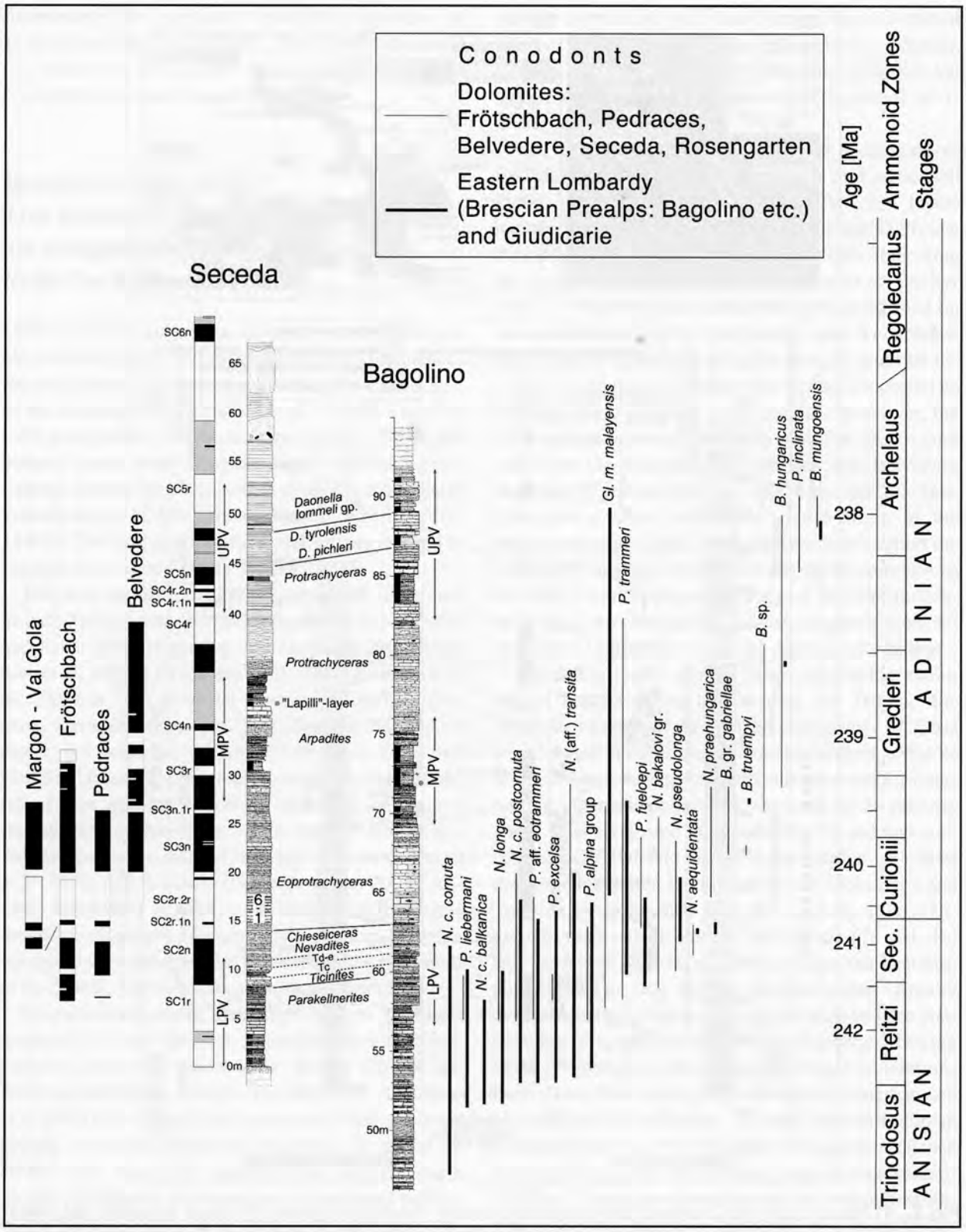

Fig. 8. Integrated Anisian-Ladinian boundary stratigraphy and biochronology. Biostratigraphic data from the Dolomites are projected onto the Seceda outcrop reference stratigraphy, while those from the Brescian Alps and Giudicarie are projected onto the Bagolino reference stratigraphy. Numerical ages are derived from interpolation of dates from Mundil et al. (1996). For details, see Muttoni et al. (2004a) and references therein.

platform from the Dolomites (Fig. 7b). The platform interior – a 470 m thick lagoonal succession of ~ 600 shallowing-upward cycles – was attributed a 9–12 Myr record of precessional forcing of sea level change (Hinnov and Goldhammer 1991; Preto et al. 2001). However, the U-Pb dating of volcanoclastic layers suggests instead that the ~ 600 Latemar cycles cover only a few million years (Brack et al. 1996; Mundil et al. 1996, 2003). An independent astrochronological interpretation of sedimentary cycles in the Muschelkalk of Central Europe coupled with biostratigraphic correlations with Tethyan successions suggest that the Latemar sequence was deposited in maximum 2.6 Myr (Menning et al. 2005). Interestingly, two sophisticated modern techniques to measure geologic time – astrochronology and U-Pb single-crystal zircon dating – lead to age estimates of the duration of the Latemar carbonate platform that differ by almost one order of magnitude: a significant discrepancy.

Kent et al. (2004) performed a magnetostratigraphic analysis of the entire Latemar lagoonal succession, which indicated that most of the succession is of normal magnetic polarity. Although the effects of lightnings and possible thermochemical overprints complicate the picture, Kent et al. (2004) regarded the Latemar results to represent the original polarity of the geomagnetic field. The predominant normal polarity together with biostratigraphic and lithostratigraphic correlations with the adjacent Buchenstein Beds basin led them to consider the Latemar deposition as coeval with Chron SC2n at Seceda (Fig. 7). Considering that no significant normal polarity bias or low reversal frequency have been documented for the Middle Triassic in global palaeomagnetic compilations, Kent et al. (2004) concluded that Chron SC2n at Seceda and the time-equivalent Latemar deposits cannot be anywhere near as long as 9–12 Myr as was implied by the original cyclostratigraphic interpretation.

A duration of ~ 1 Myr for Chron SC2n derives from a straightforward interpretation of the U-Pb age model for Buchenstein deposition. This age model is compatible with all other age constraints, except those of the Latemar. Based on this and other arguments discussed in Kent et al. (2004), and a follow-up comment by Hinnov (2006), Kent et al. (2006) argued that the long duration of Latemar deposition suggested by conventional cycle counting is in error. The recent Concise GTS2008 time scale (Ogg et al. 2008), which supersedes the GTS2004 time scale (Gradstein et al. 2004), now uses the U-Pb data from the Dolomites as age constraints for the Middle Triassic.

Palaeozoic case study: The Carboniferous-Permian Reversed Superchron and Late Permian magneto-cyclostratigraphy of the Central European Basin

Late Carboniferous and Permian rocks were already investigated in various places around the world in the 1950's and 1960's because many of them have a stable and strong magnetisation. These early results indicated that North America, Europe, and several parts of Asia were positioned significantly more to the south than nowadays, and that opposite rotations had occurred in North America and Europe caused by the opening of the North Atlantic. These observations significantly contributed to the development of the theory of plate tectonics. In addition, the dominance of reverse polarity in Permo-Carboniferous rocks led to propose the existence of the Kiaman Magnetic Interval (Irving and Parry 1963) or Carboniferous-Permian Reversed Superchron (CPRS).

The lower boundary of the CPRS was originally named Patterson Reversal (Irving and Parry 1963), until Opdyke et al. (2000) detected normal polarity in younger rocks of the same area. A global analysis and synthesis of 27 magnetostratigraphic records of Carboniferous age has shown that there is at present no consensus on where to place the base of the CPRS: it has been observed in early Bashkirian (SE Australia), late Bashkirian (eastern Canada), early Moscovian (Central Europe), and middle Moscovian rocks (Ukraine) (see Figs. 9, 10). In the GTS2004, the boundary is rather arbitrarily placed close to the Moscovian-Kasimovian boundary at 306.7 Ma, within a reverse polarity interval (Davydov et al. 2004). It would instead be more logical to place the base of the CPRS at the youngest level bearing normal polarity in the Moscovian (middle Kashirian of eastern Europe; Khramov et al. 1974), which would result in an age of ~ 310 Ma according to GTS 2004. Alternatively, the base of the CPRS could be placed at the top of the youngest normal polarity chron in the late Baskirian around 312 Ma. The most recent update of the geological time scale (Ogg et al. 2008), accessible through Time Scale Creator 4.0 (www.tscreator.com), assumes that nearly all short normal subchrons reported between 314 and 299 Ma are questionable, and a result, it places the base of the CPRS at 313.6 Ma within the late Bashkirian (Fig. 10). Approximately five short normal polarity zones could be present within the CPRS (Menning 1995), but these are now

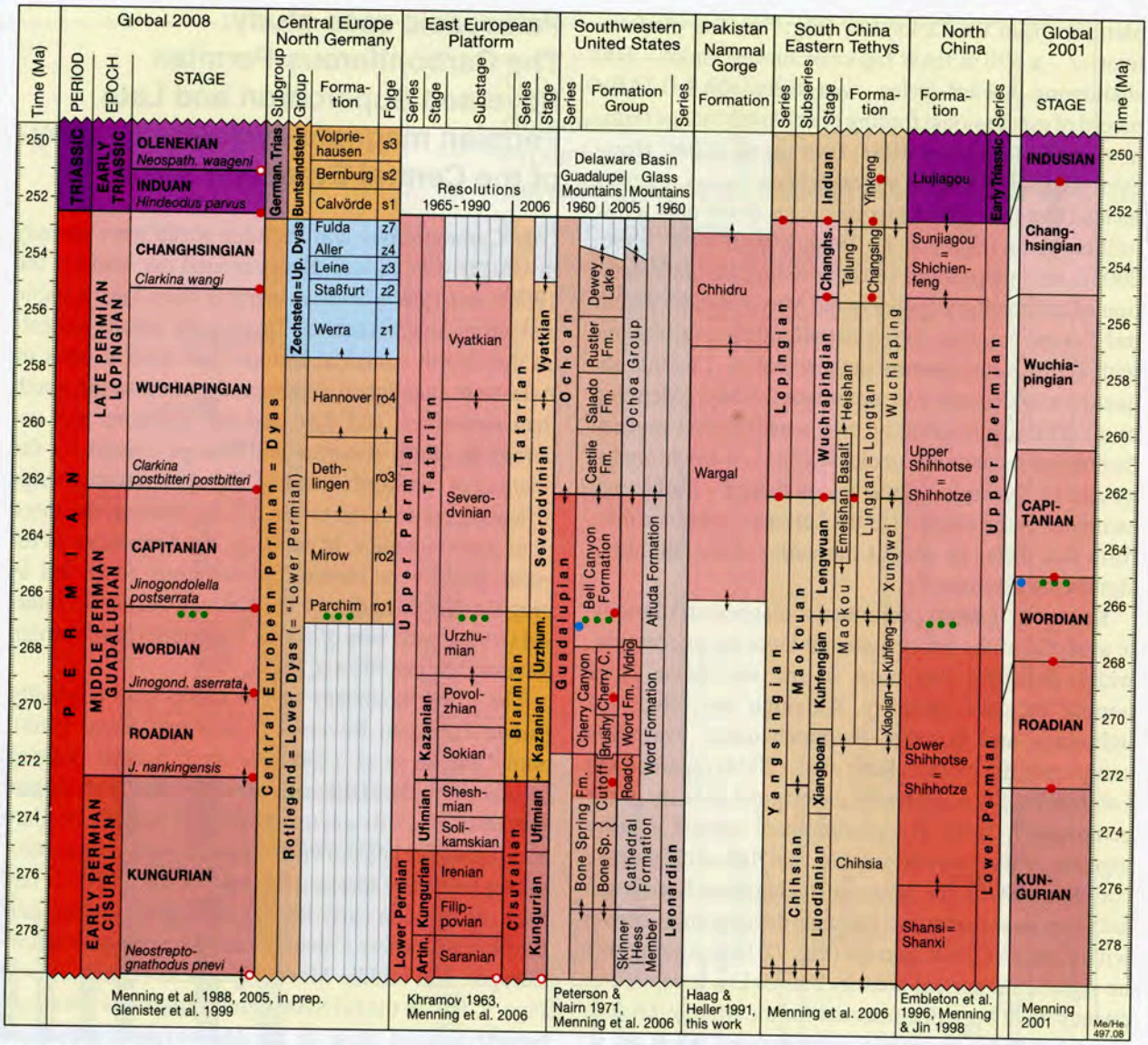

Fig. 9. Permian Global Stratigraphic Scale as used in the Devonian-Carboniferous-Permian Correlation Chart 2006 (DCP 2006) and Regional Stratigraphic Scales. Full red dots: GSSP; open red dots: GSSP proposed; green dots: Illawarra Reversal; blue dot: Pb-U age of Bowring et al. 1988; arrows: uncertain position of a boundary according to the numerical time scale or a global stage boundary. In the global column the index fossils for the stage boundaries are presented as adopted respectively proposed. The terms of the Global Stratigraphic Scale (GSS) are in capital letters to distinguish them from regional terms from which they were derived: unfortunately, commonly they cover different time spans.

reduced to two reliable zones in Time Scale Creator 4.0, although no clear argumentation or references are given in support of this interpretation. Clearly, the lower boundary of the CPRS requires verification in multiple, globally distributed sections.

The upper boundary of the CPRS was named Illawarra Reversal (Irving and Parry 1963). Initially, it seemed to occur near the Permian-Triassic boundary, and this led to speculations on a connection with the late Permian mass extinction (Peterson and Nairn 1971). This inference ignored the well-documented position of the Illawarra Reversal in the lower Tatarian of eastern Europe (Khramov 1963), being significantly older than the Permian-Triassic boundary. Later, varying positions have been suggested: Kungurian, Ufimian, Kazanian of eastern Europe, early Wordian, late Wordian, early Capitanian (see Fig. 10). These positions are not based on new field and laboratory work but mainly

on re-interpretations of existing data combined with successive geological time scales that have significantly different numerical ages. The Illawarra Reversal is a first class time marker when detected reliably and it is the anchor point for the middle and late Permian part of the Devonian-Carboniferous-Permian Correlation Chart (DCP 2003; Menning et al. 2006; DCP 2006, Fig. 9). For most of the Permian, however, the absence of reversals excludes the use of magnetostratigraphy, and other stratigraphic techniques are required. Successions of different environments (e.g. marine, limnic, fluvial, sabkha, volcanic) can then for example be correlated through climatic change. Recently, a first attempt at such a correlation between European Permian sections was carried out based on climatic and environmental information (Schneider et al. 2006).

The relative age of the Illawarra Reversal was estimated to be 10 ± 4 Myr older than the Permian-Triassic boundary (Menning 1986), which has an U-Pb SHRIMP age of 251.2 ± 3.4 Ma (Claoué-Long et al. 1991). Meanwhile, the age of the Permian-Triassic boundary was lowered to ~ 252.5 Ma based on a U/Pb age of 252.6 ± 0.2 Ma from a tuff layer located slightly below the boundary (Mundil et al. 2004). A volcanic tuff from just below the Illawarra Reversal at Nipple Hill (Texas) provided an U-Pb age of 265.3 ± 0.2 Ma (Bowring et al. 1998). Using the ages of ~ 310 (or 314) Ma for the base and ~ 265 Ma for the top, results in a duration of 45 (or 50) Myr for the CPRS. The positions of the boundaries of the PCRS compare well with those of Irving (1971), but he arrived at a longer duration of 60 Myr (290–230 Ma) based on the time scales of his time. The CPRS is thus the longest time span of the Phanerozoic Eon in which one polarity dominates. This duration is some 5–10 Myr longer that of its normal polarity pendant, the Cretaceous Normal Superchron, ranging 124.5–84 Ma (Ogg et al. 2004)

A reliable polarity time scale for post-Illawarra times spanning 265–252.5 Ma is not yet available, but

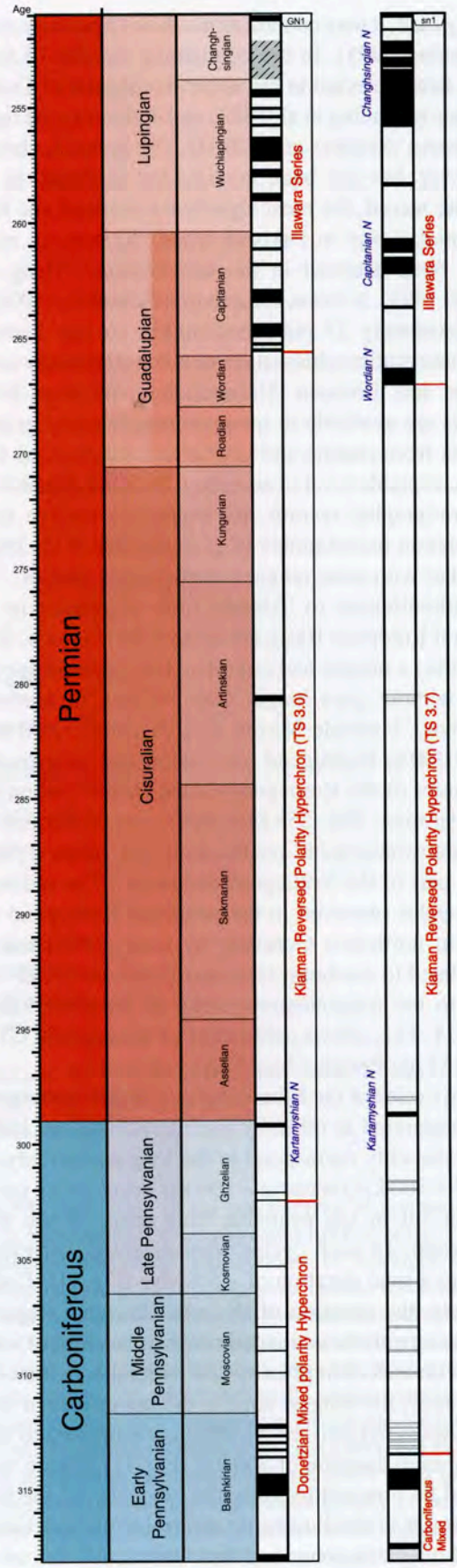

Fig. 10. Two versions of the Carboniferous-Permian Reversed Superchron, on the left the polarity time scale according to GTS2004 (Gradstein et al. 2004), made with Time Scale Creator 3.0, i.e. according to the 2004 version. On the right according to Time Scale Creator 4.0 (www.tscreator.org), providing an update of GTS2004, i.e. the Concise GTS2008 (Ogg et al. 2008). It appears that in the latest version the subchrons preceeding the lower boundary CPRS of GTS2004 are considered uncertain. Also the Illawarra series postdating the PCRS has significantly changed in both timing and number of reversals, according to a new compilation of Steiner (2006).

in any case, it may contain as much as 15 polarity zones (Menning 1995). In the continental record, 10 zones have been detected in the upper Rotliegend of Central Europe (Menning et al. 1988) and 4 zones in the upper Zechstein (Szurlies et al. 2003). The lower Zechstein, however, has not been investigated in detail. In the marine record, the most significant results come from Nammal Gorge in Pakistan where 10 polarity zones have been detected in the late Permian (Haag and Heller 1991). A recent compilation by Steiner (2006) of approximately 27 published middle to late Permian magnetostratigraphies suggests some 10 polarity zones in the late Permian. Unfortunately, no short-living fossils are available to integrate magnetostratigraphic results from marine and continental successions with any acceptable level of accuracy. Reliable climatic/cyclostratigraphic records are needed to resolve these correlation uncertainties (e.g. Schneider et al. 2006), together with more magnetostratigraphic studies.

Carboniferous to Triassic rock sequences in the Central European Basin are up to 6,000 m thick. They comprise a unique and complete late Permian succession without gaps longer than 100 kyr. In northeast Germany, borehole Mirow 1/1a/74 cored 1,600 m of the 3,300 m Rotliegend succession and bottomed in volcanics of the Rotliegend Group (latest Carboniferous-Permian, 300–258 Ma). Here, we reinterpret the magnetostratigraphic results from the upper 1290 m thick part of the Rotliegend sediments. The sedimentary cycles observed in the perennial Rotliegend salt lake in northwest Germany by Gast (1995) can be correlated to northeast Germany (Gebhardt 1995) and thus to the magnetostratigraphy of borehole Mirow 1/1a/74. This allows calibration of the regional GPTS for the Late Permian based on cycle scaling.

The cycles of the Elbe Subgroup (latest Rotliegend) are interpreted as orbitally forced cycles (Gast 1995). They can only correspond to the long eccentricity cycle of ~ 400 kyr, because ~ 100 kyr eccentricity cycles cannot fill in the available time span. In the Elbe Subgroup, 14 such cycles were detected, corresponding to a total duration of ~ 5.6 Myr (Fig. 11). Unfortunately, the duration of the post-Illawarra magnetic zones can only be estimated roughly, because of intervals with uncertain polarity and without core material. Until now, the longest zone is the upper part of zone rny (cycles ro4.3 to ro4.5), which is estimated to have a minimum duration of 700 kyr (Fig. 11). Future work should be directed to study the 14 cycles of the Elbe Subgroups in detail to better determine the exact number of magnetic zones and their duration.

Part three – Discussion

Integrated stratigraphy and marine-continental correlations

Several examples are provided in the literature of good correlation of land-derived magnetostratigraphies with the polarity record retrieved from marine magnetic anomalies, which prove that geomagnetic polarity reversals are synchronous and global. This synchrony distinguishes magnetostratigraphy from biostratigraphy, bearing in mind that polarity reversals are fundamentally of a binary nature while biostratigrapic zones have a distinctive character. The first magnetic stratigraphies in sedimentary rocks (Creer et al. 1954; Irving and Runcorn 1957) documented normal and reverse polarities in the Proterozoic Torridonian Sandstones in Scotland, as well as in rocks of Devonian and Triassic age. These studies were conducted on poorly fossiliferous sediments that possessed however a magnetisation intensity measurable by the magnetometers available at that time, and as a consequence, correlations of polarity zones therein retrieved could not be supported by biostratigraphic data.

The modern era of magnetostratigraphy integrated with biostratigraphy started with the early studies on Plio-Pleistocene marine sediments and deep-sea cores (e.g., Opdyke 1972) and continued over the ensuing years with classic studies on e.g. the Cretaceous-Paleocene successions of the Central Apennines at Gubbio, Italy (e.g. Alvarez et al. 1977). This multidisciplinary approach has since been significantly refined and has extended the GPTS originally derived from palaeomagnetic studies on basaltic outcrops and marine magnetic anomalies. *Vice versa*, magnetostratigraphy may fundamentally help dating biostratigraphic zonations that have at best regional significance, like in the Paratethys where zonations based on ostracods or molluscs are primarily of environmental significance rather than being chronostratigraphic tools (Vasiliev et al. 2004).

In addition to the advent of astrochronology, another important stratigraphic tool comes from chemostratigraphy or isotope stratigraphy, in particular from stable isotopes (see Weissert et al. 2008). The integrated use of magnetostratigraphy, biostratigraphy, cyclostratigraphy, isotope stratigraphy, and radioisotopic dating from selected sections or cores contributes to refine the GPTS by continuously providing accurate age determinations of the constituent polarity reversals.

A major problem in correlating marine sequences with their time-equivalent continental sequences is

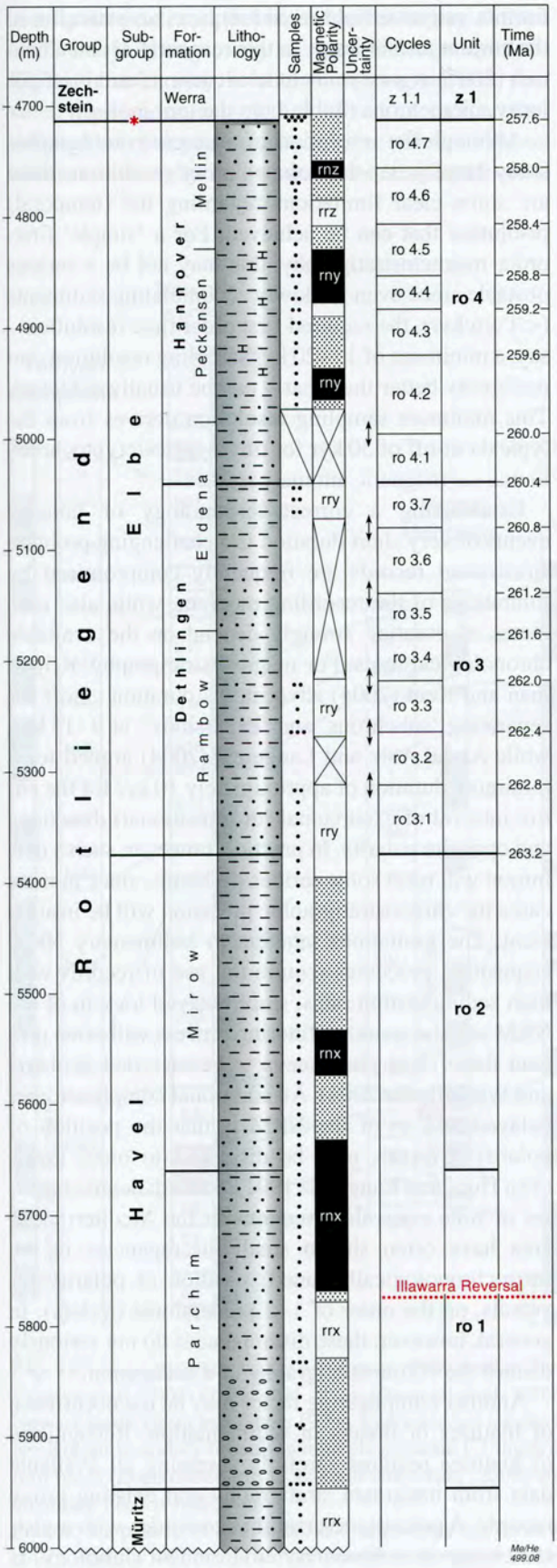

Fig. 11. Succession of the late Permian in northeast Germany, borehole Mirow 1/1a/74 cored 1,600 m of the 3,300 m Rotliegend succession and bottoms in volcanics of the Rotliegend Group. The Rotliegend succession was investigated with the purpose to detect the Illawarra reversal (Menning et al. 1988). Here, we reinterpret the magnetostratigraphic results from the upper 1,290 m thick part of the Rotliegend sediments; rnx, rrx, etc. refer to informally labeled polarity zones. The sedimentary cycles observed in the perennial Rotliegend salt lake in northwest Germany by Gast (1995) can be correlated to northeast Germany (Gebhardt 1995) using gamma-ray logs and thus to the magnetostratigraphy of bore hole Mirow 1/1a/74. This allows calibration of the regional GPTS for the Late Permian based on cycle scaling.

their fundamentally different fossil content. Marine transgressions within a continental sequence may give a first-order constraint, but such sequences are relatively rare. Here, magnetostratigraphy plays a crucial role, preferably aided by cyclostratigraphic constraints. A first example of a truly bed-to-bed correlation – at the precessional level – between the marine and continental realm was given by Van Vugt et al. (1998), who correlated early Pliocene lacustrine deposits in NW Greece with the marine Trubi formation in the central Mediterranean. Also the Miocene continental deposits of northern Spain have now been successfully correlated to time-equivalent marine successions in Italy (Abdul Aziz et al. 2004; Hüsing et al. 2007), and the ages of individual polarity reversals younger than 11 Ma are virtually indistinguishable within error resolution.

It must be noted that such detailed correlations are not – and can never be – based on magnetostratigraphic tie-points alone: positions of reversals may differ due to differential/delayed lock-in depth/time because of different environments and recording quality. Hence, although magnetostratigaphy may well serve as a first-order correlation, the final correlation is based on astronomical fine-tuning. This concept has also been applied on the Chinese loess sequences (Heslop et al. 2000), showing that recorded polarity reversals showed considerable delay because of a large lock-in depth in such aeolian/palaeosol deposits. This concept is still not widely accepted, however, and some studies have used magnetostratigraphic tie-points, which in some cases may cause the same reversal to occur both in a warm, interglacial stage in one locality, and in a cool stage in another place. This would make cyclostratigraphy a useless exercise and argues once again for an integrated stratigraphic approach in order to avoid such pitfalls.

Resolution: subchrons, cryptochrons, reversals, excursions, hiatuses

The International Commission on Stratigraphy has guided the use of magnetostratigraphic units (polarity zones), their time equivalents (polarity chrons), and chronostratigraphic units (polarity chronozones) (Anonymous 1977; Opdyke and Channell 1996). During the last two decades, the recognition of numerous short-lived polarity intervals or excursions (Langereis et al. 1997; Krijgsman and Kent 2004) as part of the Earth's magnetic field record requires an extension of the current terminology. In this respect, Laj and Channell (2007) argued to include excursions and brief polarity microchrons (Table 1) in the terminology.

Although the resolution of a magnetostratigraphic study largely depends on sampling resolution, there are some clear limitations regarding the (temporal) resolution that can be achieved. For a 'simple' first-order magnetostratigraphy, this may not be a serious obstacle since even in slowly accumulating sediments (< 1 cm/kyr), the required first order time resolution – say, a minimum of 15–20 kyr sampling resolution, but preferably better than that – can be usually achieved. This minimum sampling resolution derives from the typical cut-off of 30 kyr for tiny wiggles/cryptochrons in marine magnetic anomaly studies.

Establishing a correct terminology of polarity events of very short duration is a challenging problem since short records are frequently compromised by limitations of the recording medium, while also estimates of duration strongly depend on the available chronological tools. For magnetostratigraphy, Krijgsman and Kent (2004) advocated a duration cutoff for separating 'subchrons' and 'excursions', at 9–15 kyr, while Abdul Aziz and Langereis (2004) argued for a minimum duration of approximately 10 kyr for the entire interval of excursional (or transitional) directions and opposite polarity. In practice, however, such a definition will meet some serious problems, since in most cases the chronostratigraphic precision will be insufficient. The limitations inherent to sedimentary NRM acquisition processes require the use of records with high sedimentation rates, since delayed lock-in of the NRM and the resulting filtering process will often prevent these short phenomena to be recorded (Roberts and Winkelhofer 2004). An additional complication of delayed lock-in of the NRM is that the position of polarity reversals may be displaced to older levels (Van Hoof and Langereis 1991). Indeed, detailed studies of time equivalent sections in the Mediterranean area have often shown small discrepancies in the (astrochronologically tuned) position of polarity reversals, on the order of 1–2 precessional cycle(s). In general, however, these discrepancies do not seriously disturb the chronostratigraphy of a succession.

Another complicating factor may be the occurrence of hiatuses or breaks in sedimentation. Recognition of hiatuses requires carefully assessing all available data from integrated stratigraphy and existing proxy records. A polarity reversal that coincides with a visible change in sedimentary environment (lithology) is

usually suspect, and the same applies to any sudden and notable change, e.g. derived from proxy data. Biostratigraphy may help to recognise hiatuses provided they are large enough relative to zonation resolution. Also cyclostratigraphy may be of help to detect hiatuses: although small-scale cycles (e.g. precession) may seem continuous and undisrupted across a hiatus, the logic of cylostratigraphy dictates that all or most Milankovitch cycles (the eccentricity, obliquity, precession periods) can be recognised in their appropriate ratios. Recognition of hiatuses will likely remain an unavoidable obstacle in geology, which may be ad-

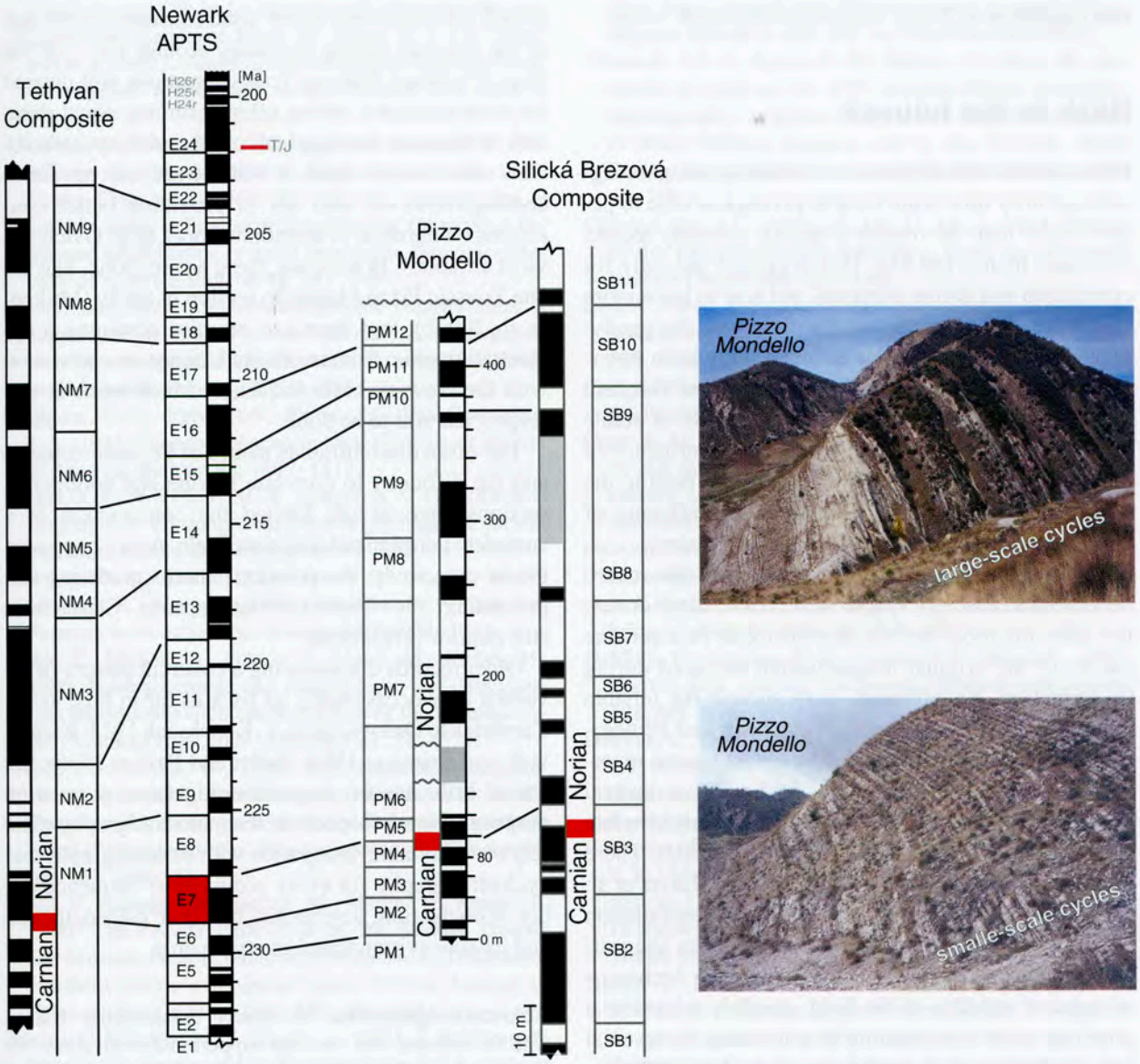

Fig. 12. Magnetostratigraphic correlation of the marine European sections of the Tethys region (Muttoni et al. 2001, 2004b; Krystyn et al. 2002; Gallet et al. 2003; Channell et al. 2003) to the astronomically tuned polarity time scale (APTS) of the Newark basin (Kent and Olsen 1999). Red intervals are the Carnian-Norian boundary intervals. Consensus places the Carnian-Norian boundary broadly within chronozone E7 implying an age between 227 and 229 Ma. The results from the Hartford basin (H-chronozones) from Kent and Olsen (2008) are shown, and the position of the palynological Triassic-Jurassic boundary (T/J) is indicated.
Photos: the pattern of both small and large scale cycles in the Sicilian Pizzo Mondello section seems promising to use cyclostratigraphy and obtain a more detailed correlation to the Newark reference section.

dressed by correlation of multiple sections over large areas. Because of its binary nature, magnetostratigraphy alone can hardly recognise the presence of hiatuses, but when embedded in an integrated stratigraphic approach, it may contribute to resolve them. Also strongly varying sedimentation rates, usually associated with lithology variations, may distort the observed polarity pattern; hence, providing a detailed lithostratigraphic log of the sampled sequence is an important requirement in any magnetostratigraphic study.

Back to the future?

Future efforts should focus on extending the geomagnetic polarity time scale back in geological time to periods older than the marine magnetic anomaly record, i.e. older than ~ 160 Ma. This is critical not only for correlation and dating purposes, but also to learn more about the characteristics of the field and the geodynamo that generates it. For example, long-term reversal frequency variations – long periods of frequent field reversals versus equally long periods of stable polarity (superchrons) – tell us about the influence of mantle processes on the generation of the field in the liquid outer core, and possibly about the influence of (nucleation and growth of) the solid inner core.

It is evident that by going back in time, the record becomes increasingly sparse while it also deteriorates: the older the rock, the less the chance to be a pristine carrier of the original magnetisation acquired during its formation. Nevertheless, very ancient but reliable records – although scarce – of Archean and Proterozoic age have been acquired. The oldest known reversal that is reliably documented – by a positive reversal test, fold test, and an intra-formational conglomerate test – has an age of ~ 2.8 Ga (Strik et al. 2003). There are reports of reversals as old as ~ 3.2 Ga (Layer et al. 1998), but their reliability still requires substantiation by a positive field test. Recently, it has been suggested that there is a very long trend – since the Archean – of reduced stability of the field, possibly related to a growing inner core, leading to a decrease in reversal frequency back in time (Biggin et al. 2008). Clearly, these rare observations of the ancient field are still far from being fit for correlation or dating purposes.

So, how far can we go back in time? One of the greatest achievements of early Mesozoic magnetostratigraphy is represented by the Late Triassic Newark astrochronological polarity time scale (APTS; Kent et al. 1995; Kent and Olsen 1999; Olsen and Kent 1999), which was constructed by anchoring magnetostratigraphy and Milankovitch chronostratigraphy to the radioisotopically dated Orange Mountain basalt (Fig. 12), and which was recently extended up to the Early Jurassic by including data from the Hartford Basin (Kent and Olsen 2008). The correlation of the Newark APTS to the Triassic sections of the Tethyan marine realm is still far from straightforward, as evidenced by the continuously changing interpretations as new results are acquired, although there is now good consensus on the age of the Carnian-Norian boundary around 227–228 Ma (Fig. 12). Many Tethyan Triassic sections still depend on biostratigraphic dating often assuming equal duration of biozones through lack of other dating methods. New radioisotopic dates of Triassic sections are forthcoming, however, and aid in providing better constraints on duration of ammonite zones (e.g. Ovtcharova et al. 2006). In addition, there are sections, like the late Triassic Pizzo Mondello section in Sicily (Muttoni et al. 2004b), that seems to promise obtaining a cyclostratigraphic framework and hence a correlation with the Newark basin sequence. Much work in this respect has still to be done.

The often discontinuous nature of Permian deposits and the difficulty to correlate marine and continental sections have as yet limited the construction of a complete Permian polarity time scale. As we have seen in our case study, the polarity patterns predating and postdating the Carboniferous-Permian Superchron still require verification.

Older records documenting a coherent pattern of reversals may occasionally go back as far in time as the Cambrian to Ordovician (e.g. Kirschvink 1978; Kirschvink and Rozanov 1984; Gallet and Pavlov 1996), but are of little use for magnetostratigraphic correlation purposes. New prospects in magnetostratigraphy must rely on 'automatic' integration with biostratigraphy and cyclostratigraphy for every sedimentary sequence under investigation, augmented by other palaeoclimatic and palaeoenvironmental proxy records.

Acknowledgements. We dearly thank Maria Bianca Cita for ongoing and constant support and motivation. We are grateful to Silja Hüsing who provided the details of figure 6 on the Monte dei Corvi results, while Andreas Hendrich did an excellent job on figures 10 and 11. Two reviewers (Valerian Bachtadse and an anonymous reviewer) provided useful comments. We thank those members of the International Subcommission on Stratigraphic Classification (ISSC) of the IUGS International Commission on Stratigraphy who provided useful and stimulating comments on an earlier version of the manuscript.

References

Abdul Aziz, H., Van Dam, J., Hilgen, F.J., Krijgsman, W., 2004. Astronomical forcing in Upper Miocene continental sequences: implications for the Geomagnetic Polarity Time Scale, Earth and Planetary Science Letters **222**, 243–258

Abdul Aziz, H., Langereis, C.G., 2004. Astronomical Tuning and Duration of Three new Subchrons (C5r.2r-1n, C5r.2r-2n and C5r.3r-1n) Recorded in a Middle Miocene Continental Sequence From NE Spain. In: J.T.E.Channell et al. (Eds.), Timescales of the Palaeomagnetic Field, Geophysical Monograph Series, Volume **145** (AGU), 328 pp.

Alvarez, W., Arthur, M.A., Fischer, A.G., Lowrie, W., Napoleone, G., Premoli-Silva, I., Roggenthen, W.M., 1977. Upper Cretaceous-Paleocene magnetic stratigraphy at Gubbio, Italy. V. Type section for the late Cretaceous-Paleocene geomagnetic reversal time scale. Geological Society of America Bulletin **88**, 383–389

Anonymous, 1977. Magnetostratigraphic polarity units. A supplementary chapter of the international subcommission on stratigraphic classification international stratigraphic guide. Geology **7**, 578–583.

Berggren, W.A., Kent, D.V., Flynn, J.J., Van Couvering, J.A., 1985. Cenozoic geochronology, Geological Society of America Bulletin **96**, 1407–1418.

Biggin, A.J., Strik, G.H.M.A., Langereis, C.G., 2008. Evidence for a very-long-term trend in geomagnetic secular variation, Nature Geosciences **1**, 395–398.

Bowring, S.A., Erwin, D.H., Jin, Y.G., Martin, M.W., Davidek, K., Wang, W., 1998. Geochronology of the end-Permian mass extinction. Science **280**, 1039–1045.

Brack, P., Mundil, R., Oberli, F., Meier, M., Rieber, H., 1996. Biostratigraphic and radioisotopic age data question the Milankovitch characteristics of the Latemar cycle (Southern Alps, Italy). Geology **24**, 371–375.

Brack, P., Muttoni, G., 2000. High-resolution magnetostratigraphic and lithostratigraphic correlations in Middle Triassic pelagic carbonates from the Dolomites (northern Italy). Palaeogeography, Palaeoclimatology, Palaeoecology **161**, 361–380.

Brack, P., Schlager, W., Stefani, M., Maurer, F., Kenter, J., 2000. The Seceda Drill Hole in the Middle Triassic Buchenstein beds (Livinallongo Formation, Dolomites, Northern Italy), a progress report. Rivista Italiana di Palaeontologia e Stratigrafia **106**, 283–292.

Brauns, C.M., Pätzold, T., Haack, U., 2003. A Re-Os study bearing on the age of the Kupferschiefer black shale at Sangerhausen (Germany). Abstracts XVth International Congress on Carboniferous and Permian Stratigraphy, Utrecht, Netherlands, p.66.

Brunhes, B., 1906. Recherches sur la direction d'aimantation des roches volcaniques. Journal of Physics IV **5**, 705–724.

Butler, R.F., 1992. Palaeomagnetism, magnetic domains to geologic terranes, Blackwell Scientific Publications (Boston), 319 pp.

Cande, S.C., Kent, D.V., 1992. A new geomagnetic polarity time-scale for the Late Cretaceous and Cenozoic. Journal of Geophysical Research **97**, 13917–13951.

Cande, S.C., Kent, D.V., 1995. Revised calibration of the Geomagnetic Polarity Time Scale for the Late Cretaceous and Cenozoic. Journal of Geophysical Research **100**, 6093–6095.

Channell, J.E.T., Mazaud, A., Sullivan, P., Turner, S., Raymo, M.E., 2002. Geomagnetic excursions and palaeointensities in the Matuyama Chron at Ocean Drilling Program Sites 983 and 984 (Iceland Basin), Journal of Geophysical Research **107**, doi: 10.1029/2001JB000491.

Channell, J.E.T., Kozur, H.W., Sievers, T., Mock, R., Aubrecht, R., Sykora, M., 2003. Carnian-Norian biomagnetostratigraphy at Silicka Brezova (Slovakia). Correlation to other Tethyan sections and to the Newark Basin, Palaeogeography, Palaeoclimatology, Palaeoecology **191**, 65–109.

Claoué-Long, J.C., Zhang, Z., Ma, G., Du, S., 1991. The age of the Permian-Triassic boundary, Earth and Planetary Science Letters **105**, 182–190.

Cox, A., Doell, R.R., Dalrymple, G.B., 1963. Geomagnetic polarity epochs and Pleistocene geochronometry, Nature **198**, 1049–1051.

Cox, A., Doell, R.R., Dalrymple, G.B., 1964. Reversals of the Earth's magnetic field, Science **144**, 1537–1543.

Creer, K.M., Irving, E., Runcorn, S.K., 1954. The direction of the geomagnetic field in remote epochs in Great Britain. Journal of Geomagnetism and Geoelectricity **6**, 164–168.

Davydov, V.I., Wardlaw, B.R., Gradstein, F.M., 2004. The Carboniferous Period, in: F.M.Gradstein, J.G.Ogg, A.G.Smith (Eds.), A Geologic Time Scale 2004, Cambridge University Press, pp.222–248.

DeMets, C., Gordon, R.G., Argus, D.F., Stein, S., 1990. Current plate motions, Geophysical Journal International **101**, 425–478.

DeMets, C., Gordon, R.G., Argus, D.F., Stein, S., 1994. Effect of recent revisions to the geomagnetic reversal time scale on estimates of current plate motions, Geophysical Research Letters **21**, 2191–2194.

Embleton, B.J.J., McElhinny, M.W., Ma, X.H., Zhang, Z.K., Li, X.L., 1996. Permo-Triassic magnetostratigraphy in China: the type section near Taiyuan, Shanxi Province, North China, Geophysical Journal International **126**, 382–388.

Gallet, Y., Pavlov, V., 1996. Magnetostratigraphy of the Moyero river section (north-western Siberia. Constraints on geomagnetic reversal frequency during the early Palaeozoic, Geophysical Journal International **125**, 95–105.

Gallet, Y., Krystyn, L., Besse, J., Marcoux, J., 2003. Improving the Upper Triassic numerical time scale from cross-correlation between Tethyan marine sections and the continental Newark basin sequence, Earth and Planetary Science Letters **212**, 255–261.

Gast, R.E., 1995. Sequenzstratigraphie. In: Deutsche Stratigraphische Kommission (Ed., coordination and editing

E. Plein), Stratigraphie von Deutschland I – Norddeutsches Rotliegendbecken. Courier Forschungsinstitut Senckenberg, Frankfurt a.M., **183**, 47–54.

Gebhardt, U., 1995. West-Ost Korrelationsprofil. In: Deutsche Stratigraphische Kommission (Ed., coordination and editing E. Plein), Stratigraphie von Deutschland I – Norddeutsches Rotliegendbecken. Courier Forschungsinstitut Senckenberg, Frankfurt a.M., **183**, 148–155.

Glenister, B.F., Wardlaw, B.R., Lambert, L.L., Spinosa, C., Bowring, S.A., Erwin, D.H., Menning, M., Wilde, G.L., 1999. Proposal of Guadalupian and component Roadian, Wordian, and Capitanian Stages as international standards for the Middle Permian Series. Permophiles, **34**, 3–11; IUGS Subcomm. Permian Stratigraphy (Boise State Univ., Iowa).

Gong, Z., Langereis, C.G., Mullender, T.A.T., 2008. The rotation of Iberia during the Aptian and the opening of the Bay of Biscay, Earth and Planetary Science Letters **273**, 80–93.

Gradinaru, E., Orchard, M.J., Nicora, A., Gallet, Y., Besse, J., Krystyn, L., 2007. The Global Boundary Stratotype Section and Point (GSSP) for the base of the Anisian Stage: Desli Caira Hill, North Dobrogea, Romania. Albertiana **36**, 54–71.

Gradstein, F.M., Ogg, J.G., Smith, A.G., Agterberg, F.P., Bleeker, W., Cooper, R.A., Davydov, V., Gibbard, P., Hinnov, L.A., House, M.R., Lourens, L., Luterbacher, H.P., McArthur, J., Melchin, M.J., Robb, L.J., Shergold, J., Villeneuve, M., Wardlaw, B.R., Ali, J., Brinkhuis, H., Hilgen, F.J., Hooker, J., Howarth, R.J., Knoll, A.H., Laskar, J., Monechi, S., Plumb, K.A., Powell, J., Raffi, I., Röhl, U., Sadler, P., Sanfilippo, A., Schmitz, B., Shackleton, N.J., Shields, G.A., Strauss, H., Van Dam, J., van Kolfschoten, T., Veizer, J., Wilson, D., 2004. A geologic time scale 2004. Cambridge University Press, Cambridge, pp.589.

Gubbins, D., 1999. The distinction between geomagnetic excursions and reversals, Geophysical Journal International **137**, F1–F3.

Guyodo, Y., Valet, J.P., 1999. Global changes in geomagnetic intensity during the past 800 thousand years. Nature **399**, 249–252.

Haag, M., Heller, F., 1991. Late Permian to Early Triassic magnetostratigraphy. Earth and Planetary Science Letters **107**, 42–54.

He, H., Pana, Y., Tauxe, L., Qina, H., Zhu, R., 2008. Toward age determination of the M0r (Barremian-Aptian boundary) of the Early Cretaceous, Physics of the Earth and Planetary Interiors **169**, 41–48.

Heirtzler, J.R., Dickson, G.O., Herron, E.M., Pitman III, W.C., Le Pichon, X., 1968. Marine Magnetic Anomalies, geomagnetic field reversals, and motions of the ocean floor and continents. Journal of Geophysical Research **73**, 2119–2136.

Heslop, D., Langereis, C.G., Dekkers, M.J., 2000. A new astronomical time scale for the loess deposits of Northern China, Earth and Planetary Science Letters **184**, 125–139.

Hilgen, F.J., 1991a. Astronomical calibration of Gauss to Matuyama sapropels in the Mediterranean and implication for the Geomagnetic Polarity Time Scale. Earth and Planetary Science Letters **104**, 226–244.

Hilgen, F.J., 1991b. Extension of the astronomically calibrated (polarity) time scale to the Miocene-Pliocene boundary. Earth and Planetary Science Letters **107**, 349–368.

Hilgen, F.J., Krijgsman, W., Langereis, C.G., Lourens, L.J., Santarelli, A., Zachariasse, W.J., 1995. Extending the astronomical (polarity) time scale into the Miocene, Earth and Planetary Science Letters **136**, 495–510.

Hilgen, F.J., Krijgsman, W., Langereis, C.G., Lourens, L.J., 1997. Breakthrough Made in Dating of the Geological Record, EOS, Transactions of the AGU **78**, 285 & 288.

Hilgen, F.J., Abdul Aziz, H., Krijgsman, W., Raffi, I., Turco, E., 2003. Integrated stratigraphy and astronomical tuning of the Serravallian and lower Tortonian at Monte dei Corvi (Middle-Upper Miocene, northern Italy), Palaeogeography Palaeoclimatology Palaeoecology **199**, 229–264.

Hilgen, F., Abdul Aziz, H., Bice, D., Iaccarino, S., Krijgsman, W., Kuiper, K., Montanari, A., Raffi, I., Turco, E., Zachariasse, W.J., 2005. The global boundary stratotype section and point (GSSP) of the Tortonian stage (Upper Miocene) at Monte Dei Corvi, Episodes, **28**, 6–17.

Hinnov, L.A., Goldhammer, R.K., 1991. Spectral analysis of the Middle Triassic Latemar Limestone. Journal of Sedimentary Petrology **61**, 1173–1193.

Hinnov, L., 2006. Discussion of "Magnetostratigraphic confirmation of a much faster tempo for sea-level change for the Middle Triassic Latemar platform carbonates" by D.V. Kent, G. Muttoni and P. Brack [Earth and Planetary Science Letters 228, 2004), 369–377]. Earth and Planetary Science Letters **243**, 841–846.

Hospers, J., 1951. Remanent magnetism of rocks and the history of the geomagnetic field, Nature **168**, 1111–1112.

Hounslow, M.W., McIntosh, G., 2003. Magnetostratigraphy of the Sherwood Sandstone Group (Lower and Middle Triassic), south Devon, UK: detailed correlation of the marine and non-marine Anisian. Palaeogeography Palaeoclimatology Palaeoecology **193**, 325–348.

Hounslow, M.W., Szurlies, M., Muttoni, G., Nawrocki, J., 2007. The magnetostratigraphy of the Olenekian-Anisian boundary and a proposal to define the base of the Anisian using a magnetozone datum. Albertiana **36**, 72–77.

Hüsing, S.K., Hilgen, F.J., Abdul Aziz, H., Krijgsman, W., 2007. Completing the Neogene geological time scale between 8.5 and 12.5 Ma, Earth and Planetary Science Letters **253**, 340–358.

Hüsing, S.K., Kuiper, K.F., Link, W., Hilgen, F.J., Krijgsman, W., 2009a. The upper Tortonian-lower Messinian at Monte dei Corvi (Northern Apennines, Italy): Completing a Mediterranean reference section for the Tortonian Stage, Earth and Planetary Science Letters **282**, 140–157.

Hüsing, S.K., Dekkers, M.J., Franke, C., Krijgsman, W., 2009b. The Tortonian reference section at Monte dei Corvi (Italy): evidence for early remanence acquisition in greigite-bearing sediments, Geophysical Journal International **179**, 125–143.

Irving, E., 1971. Nomenclature in magnetic stratigraphy. Geophysical Journal of the Royal Astronomical Society **24**, 529–531.

Irving, E., 1988. The palaeomagnetic confirmation of continental drift, EOS **69**, 994–999.

Irving, E., Parry, L.G., 1963. The magnetism of some Permian rocks from New South Wales. Geophysical Journal of the Royal Astronomical Society **7**, 395–411.

Irving, E., Runcorn, S.K., 1957. Analysis of the palaeomagnetism of the Torridonian sandstone series of north-west Scotland. Philosophical Transactions of the Royal Society of London **A 250**, 83–99.

Kent, D.V., Muttoni, G., Brack, P., 2004. Magnetostratigraphic confirmation of a much faster tempo for sea-level change for the Middle Triassic Latemar platform carbonates. Earth and Planetary Science Letters **228**, 369–377.

Kent, D.V., Muttoni, G., Brack, P., 2006. Reply to 'Discussion of "Magnetostratigraphic confirmation of a much faster tempo for sea-level change for the Middle Triassic Latemar platform carbonates" by D.V.Kent, G.Muttoni and P.Brack [Earth and Planetary Science Letters 228 (2004), 369–377] by L.Hinnov. Earth and Planetary Science Letters **243**, 847–850.

Kent, D.V., Olsen, P.E., 1999. Astronomically tuned geomagnetic polarity time scale for the Late Triassic. Journal of Geophysical Research **104**, 12831–12841.

Kent, D.V., Olsen, P.E., 2008. Early Jurassic magnetostratigraphy and palaeolatitudes from the Hartford continental rift basin (eastern North America. Testing for polarity bias and abrupt polar wander in association with the central Atlantic magmatic province. Journal of Geophysical Research **113**, B06105. doi: 10.1029/2007JB005407.

Kent, D.V., Olsen, P.E., Witte, W.K., 1995. Late Triassic-earliest Jurassic geomagnetic polarity sequence and palaeolatitudes from drill cores in the Newark rift basin, eastern North America. Journal of Geophysical Research **100**, 14965–14998.

Khramov, A.N., 1958. Palaeomagnetism and Stratigraphic Correlation (in Russian), Gostoptech, Leningrad, Russia, (English translation by A.J.Lojkine, Geophys. Dept., Australian Natl. Univ., Canberra, Australia).

Khramov, A.N., 1963. Palaeomagnetic investigations of Upper Permian and Lower Triassic sections on the northern and eastern Russian Platform. Trudy VNIGRI **204**, 145–174, Nedra, Leningrad. (in Russian)

Khramov, A.N., Goncharov, G.I., Komissarova, R.A., Osipova, E.P., Pogarskaya, I.A., Rodionov, V.P., Slautsitais, I.P., Smirnov, L.S., Forsh, N.N., 1974. Palaeozoic palaeomagnetism. Trudy VNIGRI **335**, 238 p., Nedra (Leningrad). (in Russian)

Kirschvink, J.L., 1978. The Precambrian-Cambrian boundary problem: paleomagnetic directions from the Amadeus Basin, Central Australia, Earth and Planetary Science Letters **40**, 91–100.

Kirschvink, J.L., 1980. The least-squares line and plane and the analysis of palaeomagnetic data, Geophys. Journal of the Royal Astronomical Society **62**, 699–718.

Kirschvink, J.L., Rozanov, A.Y., 1984. Magnetostratigraphy of lower Cambrian strata from the Siberian Platform: a palaeomagnetic pole and a preliminary polarity timescale (USSR), Geological Magazine **121**, 189–203.

Klitgord, K.D., Heustis, S.P., Mudie, J.D., Parker, R.L., 1975. An analysis of near-bottom magnetic anomalies: Sea floor spreading and the magnetized layer, Geophysical Journal of the Royal Astronomical Society **43**, 387–424

Krijgsman, W., Hilgren, F.J., Langereis, C.G., Santarelli, A., Zachariasse, W.J., 1995. Late Miocene magnetostratigraphy, biostratigraphy and cyclostratigraphy in the Mediterranean, Earth and Planetary Science Letters **136**, 475–494.

Krijgsman, W., Hilgen, F.J., Raffi, I., Sierro, F.J., Wilson, D.S., 1999. Chronology, causes and progression of the Messinian salinity crisis, Nature **400**, 652–655.

Krijgsman, W., Fortuin, A.R., Hilgen, F.J., Sierro, F.J., 2001. Astrochronology for the Messinian Sorbas basin (SE Spain) and orbital (precessional) forcing for evaporite cyclicity, Sedimentary Geology **140**, 43–60.

Krijgsman, W., Kent, D.V., 2004. Non-uniform occurrence of short-term polarity fluctuation in the geomagnetic field? New results from middle to late Miocene sediments of the north Atlantic (DSDP Site 608). In: Channell JET, et al. (Eds.) AGU Geophysical Monograph Series, **145:** Timescales of the Geomagnetic Field, pp.161–174. Washington, DC: AGU.

Krystyn, L., Gallet, Y., Besse, J., Marcoux, J., 2002. Integrated Upper Carnian to Lower Norian biochronology and implications for the Upper Triassic magnetic polarity time scale, Earth and Planetary Science Letters **203**, 343–351.

Kuiper, K.F., Deino, A., Hilgen, F.J., Krijgsman, W., Renne, P.R., Wijbrans, J.R., 2008. Synchronizing rock clocks of Earth history, Science **320**, 500–504.

LaBreque, J.L., Kent, D.V., Cande S.C., 1977. Revised magnetic polarity time scale for Late Cretaceous and Cenozoic time, Geology **5**, 330–335.

Laj, C., Channell, J.E.T., 2007. Geomagnetic excursions, In: Kono, M. (Ed.), Geomagnetism, Treatise on Geophysics **5**, 373–416

Langereis, C.G., Dekkers, M.J., De Lange, G.J., Paterne M., Van Santvoort, P., 1997. Magnetostratigraphy and astronomical calibration of the last 1.1 Myr from an eastern Mediterranean piston core and dating of short events in the Brunhes, Geophysical Journal International **129**, 75–94.

Langereis, C.G., Hilgen, F.J., 1991. The Rossello composite: a Mediterranean and global standard reference section for the Early to early Late Pliocene, Earth and Planetary Science Letters **104**, 211–225.

Langereis, C.G., Linssen, J.H., Mullender, T.A.T., Zijderveld, J.D.A., 1989. Demagnetisation. In: David E. James (editor), The Encyclopedia of Solid Earth Geophysics. Van Nostrand Reinhold Company, New York, 201–211.

Laskar, J., Robutel, P., Joutel, F., Gastineau, M., Correia, A.C.M., Levrard, B., 2004. A long term numerical solu-

tion for insolation quantities of the Earth, Astronomy and Astrophysics **428**, 261–285.

Layer, P.W., Lopez-Martinez, M., Kröner, A., York, D., McWilliams, M., 1998. Thermochronometry and palaeomagnetism of the Archaean Nelshoogte Pluton, South Africa, Geophysical Journal International **135**, 129–145.

Lourens, L.J., Hilgen, F.J., Laskar, J., Shackleton, N.J., Wilson, D., 2004. The Neogene Period, In: F.M.Gradstein, J.G.Ogg, A.G.Smith(Eds.), A Geologic Time Scale 2004, Cambridge University Press, pp.500.

Matuyama, M., 1929. On the direction of magnetisation of basalt in Japan, Tyosen and Manchuria, Japonese Academic Proceedings **5**, 203–205.

Menning, M., 1986. Zur Dauer des Zechsteins aus magnetostratigraphischer Sicht, Zeitschrift für geologische Wissenschaften **14**, 395–404.

Menning, M., 1995. A Numerical Time Scale for the Permian and Triassic Periods. An Integrated Time Analysis. In: Scholle, P., Peryt, T.M., Ulmer-Scholle, D.S. (Eds.), Permian of the Northern Continents. Springer-Verlag, Berlin 1, 77–97.???

Menning, M., 2001. A Permian Time Scale 2000 and correlation of marine and continental sequences using the Illawarra Reversal (265 Ma), Natura Bresciana, Ann. Mus. Civ. Sc. Nat., Monografia, **25**, 355–362.

Menning, M., Alekseev, A.S., Chuvashov, B.I., Davydov, V.I., Devuyst, F.-X., Forke, H.C., Grunt, T.A., Hance, L., Heckel, P.H., Izokh, N.G., Jin Y.-G., Jones, P., Kotlyar, G.V., Kozur, H.W., Nemyrovska, T.I., Schneider, J.W., Wang, X.-D., Weddige, K., Weyer, D., Work, D.M., 2006. Global time scale and regional stratigraphic reference scales of Central and West Europe, East Europe, Tethys, South China, and North America as used in the Devonian-Carboniferous-Permian Correlation Chart 2003 (DCP 2003). Palaeogeography Palaeoclimatology Palaeoecology **240**, 318–372.

Menning, M., Gast, R., Hagdorn, H., Käding, K.-C., Simon, T., Szurlies, M., Nitsch, E., 2005. Zeitskala für Perm und Trias in der stratigraphischen Tabelle von Deutschland 2002, zyklostratigraphische Kalibrierung von höherer Dyas und Germanischer Trias und das Alter der Stufen Roadium bis Rhaetium, Newsletters on Stratigraphy **41**, 173–210.

Menning, M., Jin, Y.-G., 1998. Comment on 'Permo-Triassic magnetostratigraphy in China: the type section near Taiyuan, Shanxi Province, North China' by B.J.J.Embleton, M.W.McElhinny, X.H.Ma, Z.K.Zhang, Z.X.Li, Geophysical Journal International **133**, 213–216.

Menning, M., Katzung, G., Lützner, H., 1988. Magnetostratigraphic investigations in the Rotliegendes (300–252 Ma) of Central Europe. Zeitschrift für geologische Wissenschaften **16**, 1045–1063.

Merrill, R.T., McFadden, P.L., 1994. Geomagnetic field stability: reversal events and excursions, Earth and Planetary Science Letters **121**, 57–69.

Merrill, R.T., McElhinny, M.W., McFadden, P.L., 1996. The magnetic field of the Earth: palaeomagnetism, the core, and the deep mantle. International Geophysics Series, vol. **63**, 531 pp. Academic Press, San Diego.

Mundil, R., Brack, P., Meier, M., Rieber, H., Oberli, F., 1996. High-resolution U-Pb dating of Middle Triassic volcaniclastics: time-scale calibration and verification of tuning parameters for carbonate sedimentation. Earth and Planetary Science Letters **141**, 137–151.

Mundil, R. et al., 2003. Cyclicities in Triassic platform carbonates: synchronizing radio-isotopic and orbital clocks. Terra Nova **15**, 81–87.

Mundil, R., Ludwig, K.R., Metcalfe, I., Renne, P.R., 2004. Age and timing of the end Permian mass extinctions: U/Pb geochronology on closed-system zircons, Science **305**, 1760–1763.

Muttoni, G., Kent, D.V., Meço, S., Nicora, A., Gaetani, M., Balini, M., Germani, D., Rettori, R., 1996. Magneto-biostratigraphy of the Spathian to Anisian (Lower to Middle Triassic) Kçira Section, Albania. Geophysical Journal International **127**, 503–514.

Muttoni, G., Kent D.V., Brack, P., Nicora, A., Balini, M., 1997. Middle Triassic Magneto-Biostratigraphy from the Dolomites and Greece, Earth and Planetary Science Letters **146**, 107–120.

Muttoni, G., Gaetani, M., Budurov, K., Zagorchev, I., Trifonova, E., Ivanova, D., Petrounova, L., Lowrie, W., 2000. Middle Triassic palaeomagnetic data from northern Bulgaria: constraints on Tethyan magnetostratigraphy and palaeogeography. Palaeogeography, Palaeoclimatology, Palaeoecology **160**, 223–237.

Muttoni, G., Kent, D.V., Di Stefano, P., Gullo, M., Nicora, A., Tait, J., Lowrie, W., 2001. Magnetostratigraphy and biostratigraphy of the Carnian/Norian boundary interval from the Pizzo Mondello section (Sicani Mountains, Sicily), Palaeogeography Palaeoclimatology Palaeoecology **166**, 383–399.

Muttoni, G., Nicora, A., Brack, P., Kent, D.V., 2004a. Integrated Anisian-Ladinian boundary chronology. Palaeogeography Palaeoclimatology Palaeoecology **208**, 85–102.

Muttoni, G. Kent, D.V., Olsen, P.E., Di Stefano, P., Lowrie, W., Bernasconi, S., Martín Hernández, F., 2004b. Tethyan magnetostratigraphy from Pizzo Mondello (Sicily) and correlation to the Late Triassic Newark astrochronological polarity time scale. Geological Society of America Bullettin **116**, 1043–1058.

Nawrocki, J., Szulc, J., 2000. The Middle Triassic magnetostratigraphy from the Peri-Tethys basin in Poland. Earth and Planetary Science Letters **182**, 77–92.

Ogg, J.G., Agterberg, F.P., Gradstein, F.M., 2004. The Cretaceous Period. In: GTS 2004 (Gradstein, F.M., Ogg, J.G., Smith, A.G., Eds.), A geologic time scale 2004, Cambridge Univ. Press, Cambridge, p.344–383.

Ogg, J.G., Ogg, G., Gradstein, F.M., 2008. The Concise Geologic Time Scale, Cambridge University Press, pp.184.

Olsen, P.E., Kent, D.V., 1999. Long-period Milankovitch cycles from the Late Triassic and Early Jurassic of eastern North America and their implications for the calibration of the Early Mesozoic time-scale and the long-term behaviour of the planets. Philosophical Transactions of the Royal Society of London **A 357**, 1761–1786.

Opdyke, N.D., 1972. Palaeomagnetism of deep-sea cores, Reviews of Geophysics and Space Physics **10**, 213–249.

Opdyke, N.D., Channell, J.E.T., 1996. Magnetic stratigraphy. San Diego, USA: Academic Press, 346pp.

Opdyke, N.D., Roberts, J., Claoué-Long, J., Irving, E., Jones, P.J., 2000. Base of the Kiaman: Its definition and global stratigraphic significance. Geologocal Society of America Bulletin **112**, 1315–1341.

Ovtcharova, M., Bucher, H., Schaltegger, U., Galfetti, T., Brayard, A., Guex, J., 2006. New Early to Middle Triassic U-Pb ages from South China: Calibration with ammonoid biochronozones and implications for the timing of the Triassic biotic recovery, Earth and Planetary Science Letters **243**, 463–475.

Peterson, D.N., Nairn, A.E.M., 1971. Palaeomagnetism of Permian red beds from the South-western United States. Geophysical Journal of the Royal Astronomical Society **23**, 191–207.

Preto, N., Hinnov, L.A., Hardie, L.A., De Zanche, V., 2001. Middle Triassic orbital signature recorded in the shallow-marine Latemar carbonate buildup (Dolomites, Italy). Geology **29**, 1123–1126.

Rea, D.K., Blakely, R.J., 1975. Short-wavelength magnetic anomalies in a region of rapid seafloor spreading, Nature **255**, 126–128.

Roberts, A.P., Winkelhofer, M., 2004. Why are geomagnetic excursions not always recorded in sediments? Constraints from post-depositional remanent magnetisation lock-in modelling, Earth and Planetary Science Letters **227**, 345–359

Schneider, J.W., Korner, F., Roscher, M., Kroner, U., 2006. Permian climate development in the northern peri-Tethys area – The Lodeve basin, French Massif Central, compared in a European and global context, Palaeogeography Palaeoclimatology Palaeoecology **240**, 161–183.

Shackleton, N.J., Berger, A., Peltier, W.R., 1990. An alternative astronomical calibration of the lower Pleistocene time scale based on ODP Site 677, Transactions of the Royal Society of Edinburgh: Earth Sciences **81**, 251–261.

Singer, B.S., Relle, M.K., Hoffman, K.A., Battle, A., Laj, C., Guillou, H., Carracedo, J.C., 2002. Ar/Ar ages from transitionally magnetized lavas on La Palma, Canary Islands, and the geomagnetic instability timescale, Journal of Geophysical Research **107**, 2307, doi: 10.1029/2001JB001613.

Steiner, M.B., 2006. The magnetic polarity time scale across the Permian-Triassic boundary, In: Lucas, S.G., Cassinis, G., Sschneider, J.W. (Eds.), Non-Marine Permian Biostratigraphy and Biochronology. Geological Society, London, Special Publications **265**, 15–38.

Stern, D.P., 2002. A millennium of geomagnetism, Reviews of. Geophysics **40**, 1007, doi: 10.1029/2000RG000097.

Strasser, A., Hilgen, F.J., Heckel, P.H., 2006. Cyclostratigraphy – concepts, definitions, and applications, Newsletters on Stratigraphy **42**, 75–114.

Strik, G., Blake, T.S., Zegers, T.E., White, S.H., Langereis, C.G., 2003. Palaeomagnetism of flood basalts in the Pilbara Craton, Western Australia: Late Archaean continental drift and the oldest known reversal of the geomagnetic field, Journal of Geophysical Research **108**, 2551, doi: 10.1029/2003JB002475.

Szurlies, M., Bachmann, G.H., Menning, M., Nowaczyk, N.R., Käding, K.-C., 2003. Magnetostratigraphy and high-resolution lithostratigraphy of the Permian-Triassic boundary interval in Central Germany. Earth and Planetary Science Letters **212**, 263–278.

Szurlies, M., 2007. Latest Permian to Middle Triassic cyclomagnetostratigraphy from the Central European Basin, Germany: Implications for the geomagnetic polarity timescale. Earth and Planetary Science Letters **261**, 602–619.

Tauxe, L., 1998. Palaeomagnetic Principles and Practice, 299 pp., Kluwer Academic Publishers.

Van Hoof, A.A.M., Langereis, C.G., 1991. Reversal records in marine marls and delayed acquisition of remanent magnetisation. Nature **351**, 223–224.

Van Couvering, J.A., Castradori, D., Cita, M.B., Hilgen, F.J., 2000. The base of the Zanclean Stage and of the Pliocene Series, Episodes **23**, 172–178.

Van Vugt, N., Steenbrink, J., Langereis, C.G., Hilgen, F.J., Meulenkamp, J.E., 1998. Magnetostratigraphy-based astronomical tuning of the early Pliocene lacustrine sediments of Ptolemais (NW Greece) and bed-to-bed correlation with the marine record, Earth and Planetary Science Letters **164**, 535–551.

Varadi, F., Runnegar, B., Mitchum, R.M., 2003. Successive refinements in long-term integrations of planetary orbits, Astrophysical Journal **592**, 620–630.

Vasiliev, I., Krijgsman, W., Langereis, C.G., Panaiotu, C.E., Matenco, L., Bertotti, G., 2004. Towards an astrochronological framework for the eastern Paratethys Mio-Pliocene sedimentary sequences of the Focsani basin (Romania), Earth and Planetary Science Letters **227**, 231–247.

Vasiliev, I., Franke, C., Meeldijk, J.D., Dekkers, M.J., Langereis, C.G., Krijgsman, W., 2008. Putative greigite magnetofossils from the Pliocene epoch, Nature Geoscience **1**, 782–786

Verosub, K.L., Banerjee, S.K., 1977. Geomagnetic excursions and their palaeomagnetic record, Reviews of Geophysics and Space Physics **15**, 145–155.

Weissert, H., Joachimski, M., Sarnthein, M., 2008. Chemostratigraphy, Newsletters on Stratigraphy **42**, 145–179.

Wilson, D.S., 1993. Confirmation of the astronomical calibration of the magnetic polarity time scale from sea-floor spreading rates. Nature **364**, 788–790.

Wilson, D.S., Hey, R.N., 1981. The Galapagos axial magnetic anomaly: Evidence for the Emperor event within the Brunhes and for a two-layer magnetic scource, Geophysical Research Letters **8**, 1051–1054.

Zijderveld, J.D.A., 1967. Demagnetisation of rocks: Analysis of results. In Collinson, D., Creer, K., Runcorn, S. (Eds.), Methods in Palaeomagnetism, New York, USA: Elsevier, pp. 254–286.

Manuscript received: January 21, 2009, rev. version received: November 27, 2009, accepted for print: December 8, 2009.

Newsletter on Stratigraphy
Vol. **43/3:** 235–250, April 2010

Acritarch biostratigraphy of the Lower-Middle Ordovician boundary (Dapingian) at the Global Stratotype Section and Point (GSSP), Huanghuachang, South China

Li Jun*[1,2], Thomas Servais[2] and Yan Kui[1,2,3]

With 7 figures

Abstract. The Lower to Middle Ordovician Dawan Formation has been investigated palynologically at Huanghuachang, South China (Global Stratotype Section and Point of the base of the Dapingian, first Global Stage of the Middle Ordovician Series) with the aim of identifying the biostratigraphical potential of acritarch assemblages for the recognition of the Lower-Middle Ordovician boundary, recently defined by the first appearance of the conodont *Baltoniodus*? *triangularis*. For comparison, the nearby Daping section has also been sampled. Based on their first appearances, some of the taxa recorded may be useful for recognition of the Lower-Middle Ordovician boundary in sections where conodonts, graptolites or other fossils are absent. While the genera *Barakella* and *Liliosphaeridium* are indicators of the base of the Dapingian, *Stelomorpha* is a diagnostic genus present in the boundary interval because species of this genus first appear both below and above the GSSP. Other diagnostic taxa useful for long-distance correlation, which include *Orthosphaeridium* and *Dicrodiacrodium*, first appear higher in the Dapingian. Several of the stratigraphically significant taxa are typical of the peri-Gondwanan palaeobioprovince, while others also occur outside of the Gondwana palaeocontinent. The acritarch successions recovered from the South China Plate at Huanghuachang and Daping can therefore be correlated with sequences known from other peri-Gondwanan areas. In addition, correlations are also possible with other palaeocontinents, in particular with Baltica.

Key words. Acritarch, biostratigraphy, Lower-Middle Ordovician boundary, South China

1. Introduction

The Global Stratotype Section and Point (GSSP) for the base of the Middle Ordovician Series (i.e., the base of the Dapingian Stage, Fig. 1) has been defined based on the First Appearance Datum (FAD) of the conodont *Baltoniodus*? *triangularis* in the Huanghuachang section near Yichang City, Hubei Province, South China (Wang et al. 2005). This level approximately correlates with the boundary between the lower and upper intervals of the *Azygograptus suecicus* graptolite Biozone and nearly coincides with the base of the *Belonechtina*

Author's address:
[1] Nanjing Institute of Geology and Palaeontology, Chinese Academy of Sciences, Nanjing 210008, China
[2] FRE 3298 du CNRS, Géosystèmes, Université de Lille 1, F-59655 Villeneuve d'Ascq, France
[3] LPS, Nanjing Institute of Geology and Palaeontology, Chinese Academy of Sciences, Nanjing 210008, China
* **Corresponding author:** Tel. +86 2583282153; fax: +86 2583357026; E-Mail address: junli@nigpas.ac.cn

DOI: 10.1127/0078-0421/2010/0043-0235
0078-0421/10/0043-0235 $ 4.00

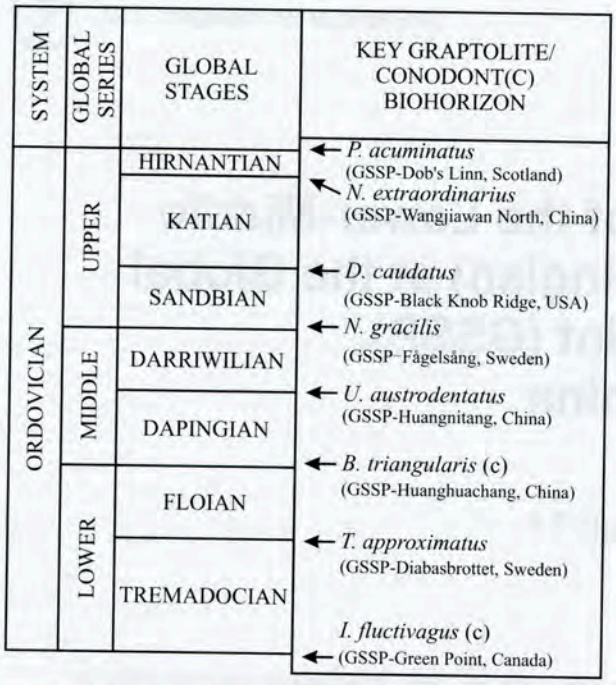

Fig. 1. Stratigraphical subdivision of the Ordovician, including Global Series and Global Stages, and key graptolite/conodont (c) taxa used for the definition of series and stage boundaries.

henryi chitinozoan Biozone (Wang et al. 2005). One of the issues this raises is how to correlate the base of the Dapingian Stage at the GSSP with areas and successions that do not contain correlative conodont, graptolite or chitinozoan faunas.

As Molyneux et al. (2007) pointed out, "acritarch biostratigraphy has not figured prominently in the development of Ordovician chronostratigraphy at a global scale, unlike graptolite, conodont and latterly chitinozoan biostratigraphical schemes". After proving to be useful for long-distance correlations and having potential for the definition of Ordovician boundaries, such as the base of the second stage of the Lower Ordovician Series (i.e., the Tremadocian-Floian boundary; Servais and Molyneux 1997, Servais and Mette 2000; Molyneux et al. 2007), acritarchs may thus also have a role to play in the correlation of the base of the Middle Ordovician Series (i.e., the Floian-Dapingian boundary) and of other recently defined boundaries.

Brocke et al. (2000) and Li et al. (2002) have already indicated the importance of the acritarchs from the South Chinese *Azygograptus suecicus* graptolite Biozone for recognising the Lower-Middle Ordovician boundary and the potential of acritarchs for international correlations. Now that the boundary has been defined in the Huanghuachang section in South China, it is important to analyse the acritarchs from this and the neighbouring sections in detail.

In light of the above, the aims of the present paper are: (1) to present new results on acritarch biostratigraphy from the GSSP for the Lower-Middle Ordovician at Huanghuachang and from the nearby Daping section; (2) to review the acritarch assemblages from other South Chinese sections crossing this boundary; (3) to compare the South Chinese acritarch assemblages at the boundary with those from peri-Gondwanan sections; and (4) to propose selected acritarch morphotypes with First Appearance Data (FAD) that might be used to correlate time slices within the Floian and Dapingian Stages around the margin of Gondwana, as well as between Gondwana and other palaeocontinents.

2. Previous studies

Studies on acritarch assemblages from the Dapingian Stage of the Huanghuachang and Daping sections have been carried out since the early 1980s, with the first publication by Zhong (1981), who presented a short report on the microphytoplankton from Huanghuachang. Subsequently, Lu (1987) described acritarchs from a single sample in the *suecicus* zone of the same section. Since the early 1990s, acritarchs from both the Huanghuachang and the Daping sections have been investigated with foci on taxonomy, biostratigraphy, palaeogeography and palaeoenviroment.

Acritarch biostratigraphy formed an important part of the investigations of Yin et al. (1998) and Tongiorgi et al. (2003) from the Huanghuachang and Daping sections. Brocke and other authors presented preliminary results from the two sections in several publications (Brocke 1997a, b; Brocke et al. 1999, 2000). As indicated above, Li et al. (2002) discussed the potential of acritarchs from the South Chinese *Azygograptus suecicus* graptolite Biozone of the Yichang area for the definition of the Lower-Middle Ordovician boundary.

In addition to biostratigraphical applications, Tongiorgi et al. (1998, 2003) interpreted the varying composition of the acritarch assemblages with regard to palaeoenvironmental changes. Subsequently, Li et al. (2004) presented a nearshore-offshore trend of Ordovician acritarchs from South China, indicating that the material from the Yichang area, being located in the central part of the carbonate platform, yielded a higher

diversity of species and genera. The acritarchs from the Yichang area are usually also better preserved, which explains why most studies have been published from this area, and in particular from the two sections of Huanghuachang and Daping (Li et al. 2004).

It is important to note that comparisons between the different biostratigraphical schemes used by the different teams of acritarch workers remain difficult. Acritarch workers have usually correlated their palynological samples with graptolite or conodont biozones. However, problems arise because the names of these biozones have been used inconsistently. According to Tongiorgi et al. (2003), the base of the *suecicus* Biozone in the Daping section is 1.48 m above the base of the Dawan Formation. More recent investigations of the graptolite stratigraphy in the section, however, indicate that the base of the *suecicus* graptolite Biozone is about 19 metres above the base of the Dawan Formation (Fig. 4). The stratigraphical position of acritarch samples and their attribution to graptolite biozones in previous works must therefore be considered with some caution.

3. Material and Methods

The material investigated in the present study comes from the GSSP for the base of the Middle Ordovician at Huanghuachang and from the nearby Daping section (Fig. 2). The Huanghuachang section is located near the town of Huanghuachang, about 22 km northeast of Yichang City, Hubei Province, South China (for precise locations of the two sections, see Tongiorgi et al. 2003). In this area, the Dawan Formation is divided into three members (Fig. 3). The lower member (20 m in thickness) consists of grey, thinly bedded nodular limestones intercalated with yellowish-green shales; the middle member (12 m in thickness) consists of medium to thinly bedded purplish limestones interbedded with few calcareous mudstones; and the upper member (12 m in thickness) consists of greenish-grey mudstones and calcareous mudstones interbedded with thinly bedded or nodular limestones.

The Dawan Formation can be differentiated from the underlying, thinly bedded to massive bioclastic limestones of the Honghuayuan Formation by the occurrence of limestones containing glauconite at the base, and from the overlying Kuniutan Formation by the disappearance of shales and occurrence of nodular limestones in the latter (Fig. 3).

Biostratigraphical investigations in the Dawan Formation are mostly based on conodonts and graptolites. Here, we follow the most recent graptolite biozonation, established by a group of specialists from the Nanjing Institute of Geology and Palaeontology (Zhang pers. comm. 2004; Chen and Zhan 2006).

A total of 34 palynological samples was collected from the shales or calcareous shales in the Huanghua-

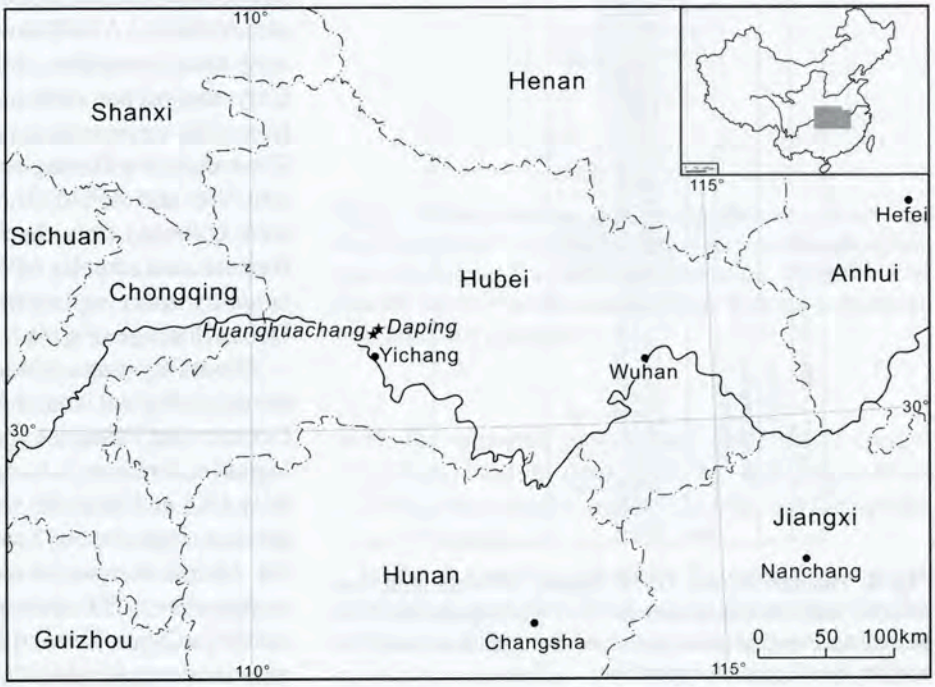

Fig. 2. Location of the Huanghuachang and Daping sections north of Yichang City, Hubei Province.

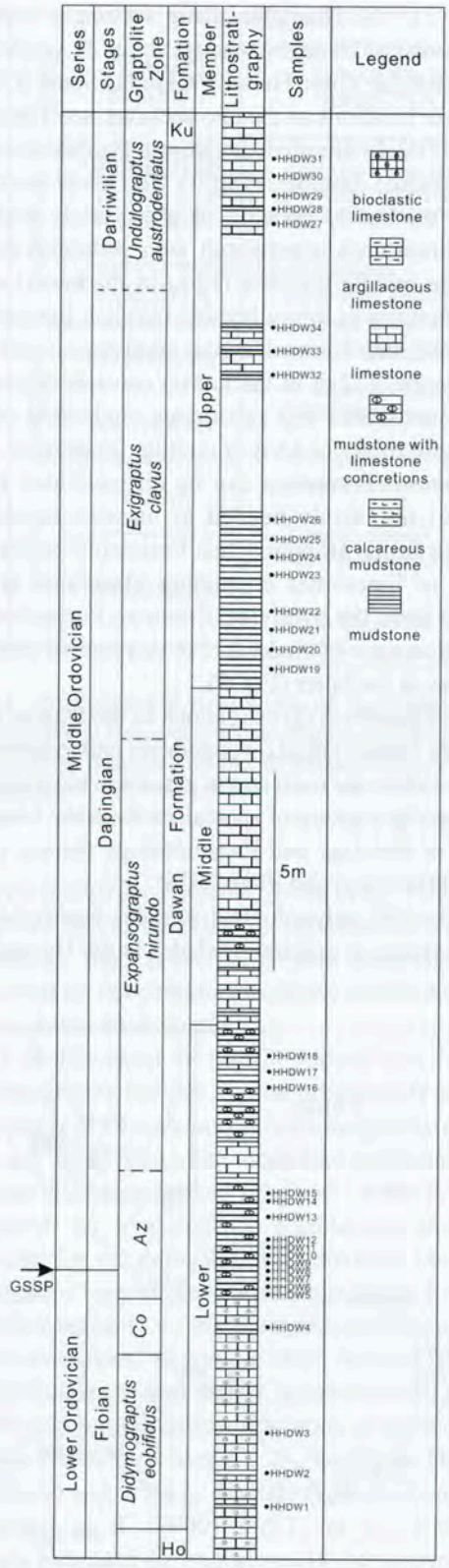

Fig. 3. Huanghuachang GSSP section: lithostratigraphical column and sample positions. *Co*: *Corymbograptus deflexus*; *Az*: *Azygograptus suecicus*; Ho: Honghuayuan Formation; Ku: Kuniutan Formation.

chang section for this study. Samples HHDW1–HHDW3 come from the interval attributed to the *Didymograptus eobifidus* graptolite Biozone of the Dawan Formation. Recently, *Didymograptellus bifidus* was discovered in the original *Corymbograptus deflexus* graptolite Biozone and occurs earlier than *C. deflexus* in the Huanghuachang section (Wang et al. 2005). According to Zhang and Chen (2006), the *D. bifidus* graptolite Biozone in Huanghuachang can be correlated to the *Didymograptus eobifidus* graptolite Biozone and the *Corymbograptus deflexus* graptolite Biozone in the Upper Yangtze platform.

HHDW4 is from the *Corymbograptus deflexus* graptolite Biozone, and HHDW5–HHDW15 come from the *Azygograptus suecicus* graptolite Biozone. The GSSP of the Dapingian is located within the *Azygograptus suecicus* graptolite Biozone, between samples HHDW7 and HHDW8. The overlying samples HHDW16–HHDW18 are from the *Expansograptus hirundo* graptolite Biozone, HHDW19–HHDW26 and HHDW32–HHDW34 are from the *Exigraptus clavus* graptolite Biozone, and HHDW27–HHDW31 are from the *Undulograptus austrodentatus* graptolite Biozone and are thus of Darriwilian age (Fig. 3).

A total of 21 samples was collected from the shales or calcareous shales in the Daping section. The Daping section is located about 5 km northeast of the Huanghuachang section, between the towns of Huanghuachang and Fenxiang at the Chengjiahe village. The lithostratigraphical description and the position of palynological samples is indicated in Figure 4. The samples AFI4001–AFI4004 were collected from the *Didymograptus eobifidus*, AFI4005–AFI4007 from the *Corymbograptus deflexus*, and AFI4008–AFI4010 from the *Azygograptus suecicus* graptolite Biozones. The base of the Dapingian is located between samples AFI4009 and AFI4010. Samples AFI4011–AFI4015 were collected from the *Exigraptus clavus* graptolite Biozone, and samples AFI4016–AFI4020 are from the *Undulograptus austrodentatus* graptolite Biozone of Darriwilian age (Fig. 4).

About fifty grams of each sample were processed in the palynological laboratory of the Nanjing Institute of Geology and Palaeontology following standard palynological techniques, which included a treatment with 37% HCl and 40% HF to remove the carbonates and silicates, respectively. Samples were not oxidized, and the sample residues were sieved through a 15 μm screen. About 300 specimen were counted for each sample using a Zeiss Axioskop 2 Plus light microscope and identified to the species level. All slides and

residues are housed in the collections of the Nanjing Institute of Geology and Palaeontology, Chinese Academy of Sciences, Nanjing, China.

4. Results

Figures 5 and 6 illustrate the results from the two sections. In the acritarch assemblages from the Dawan Formation of the Huanghuachang section, 94 species have been recorded and attributed to 35 genera (Figure 5). From the base to the top, the acritarch assemblage in the *D. eobifidus* graptolite Biozone, based on three samples, contains 17 genera and 47 species, and is dominated by the genera *Baltisphaeridium* (33.6–36.4%), *Leiosphaeridia* (18.6–30.5%) and *Peteinosphaeridium* (7.5–34.0%). The acritarch assemblage from the *C. deflexus* graptolite Biozone, which is represented in one sample, comprises 32 species attributed to 18 genera, with two of the same three genera being dominant: *Stelliferidium* (51.6%), *Baltisphaeridium* (19.7%) and *Peteinosphaeridium* (10.3%). As already recognised by Li et al. (2007), the acritarch assemblages from the *A. suecicus* graptolite Biozone are the most diverse, containing 33 genera and 81 species in eleven samples. These assemblages are dominated by *Baltisphaeridium* (3.3–67.0%), *Leiosphaeridia* (7.0–43.9%), *Polygonium* (2.3–39.6%), and *Stelliferidium* (0–26.1%). Within the *E. hirundo* graptolite Biozone (as represented in three samples), the acritarch assemblage is composed of 44 species assigned to 22 genera and is dominated by *Baltisphaeridium* (43.4–60.8%), *Leiosphaeridia* (12.9–20.2%) and *Peteinosphaeridium* (6.1–13.8%). The acritarch assemblage based on ten samples from the *E. clavus* graptolite Biozone comprises 45 species assigned to 23 genera. It is dominated by *Stelliferidium* (0–74.3%), *Baltisphaeridium* (5–50.0%), *Cymatiogalea* (0–46.6%), and *Leiosphaeridia* (11.3–33.0%). The acritarch assemblage from the *U. austrodentatus* graptolite Biozone of Darriwilian age contains 26 genera and 59 species from a total of six samples. These assemblages are dominated by *Baltisphaeridium* (28.3–58.9%), *Cymatiogalea* (0.3–31.0%), *Polygonium* (3.1–28.3%), and *Leiosphaeridia* (10.2–25.7%).

The acritarch assemblages from the Dawan Formation in the Daping section are comparable to those from the Huanghuachang section. Figure 6 illustrates the stratigraphical distribution of the taxa identified. Diversity trends are similar to those of the Huanghuachang section, as are the relative abundances of the most frequent genera. In the *C. deflexus* graptolite Biozone, the acritarch assemblage contains 31 species (17 genera) and is dominated by *Baltisphaeridium* (27.4%), *Peteinosphaeridium* (22.6%) and *Leiosphaeridia* (15.3%).

In the *A. suecicus* graptolite Biozone, the acritarch assemblage recorded from a single sample contains 34 species attributed to 13 genera, and is dominated by *Baltisphaeridium* (46.7%), *Peteinosphaeridium*

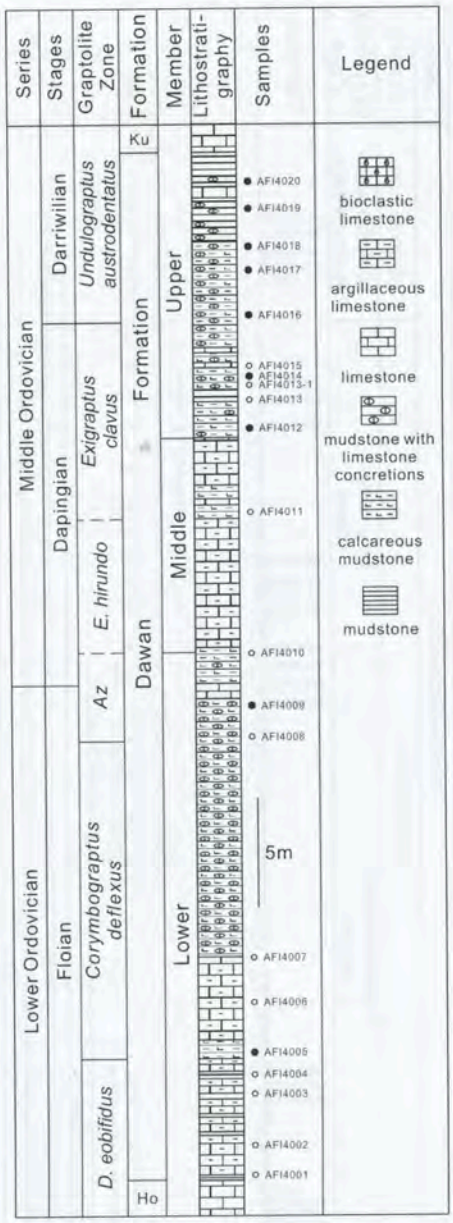

Fig. 4. Daping section: lithostratigraphical column and sample positions. *Az*: *Azygograptus suecicus*; Ho: Honghuayuan Formation; Ku: Kuniutan Formation. Hollow circles indicate barren samples, solid circles indicate palynologically productive samples.

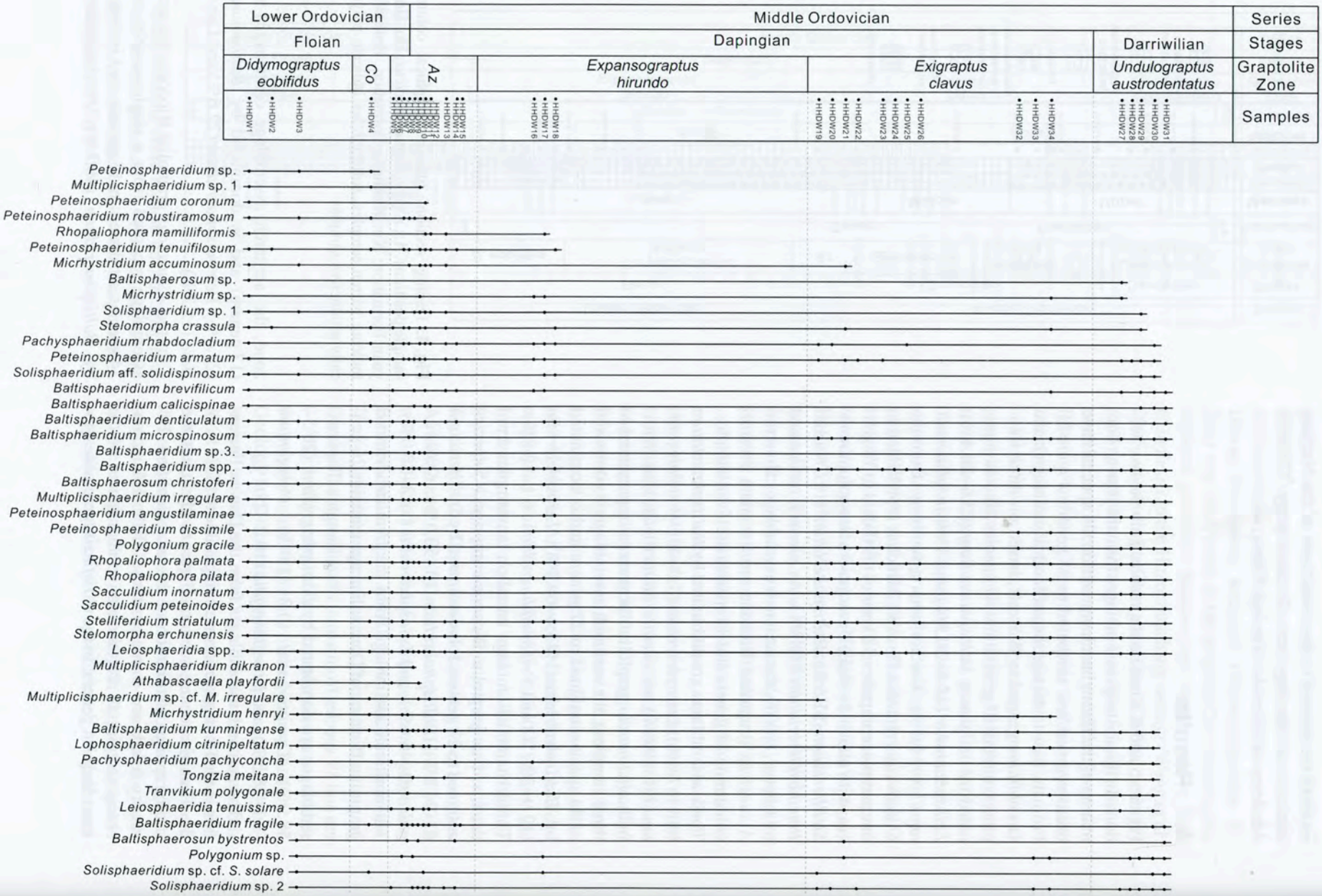
Lower Ordovician
Middle Ordovician
Series
Floian
Dapingian
Darriwilian
Stages
Didymograptus eobifidus
Co
Az
Expansograptus hirundo
Exigraptus clavus
Undulograptus austrodentatus
Graptolite Zone
HHDW1
HHDW2
HHDW3
HHDW4
HHDW12
HHDW13
HHDW14
HHDW15
HHDW16
HHDW17
HHDW18
HHDW19
HHDW20
HHDW21
HHDW22
HHDW23
HHDW24
HHDW25
HHDW26
HHDW32
HHDW33
HHDW34
HHDW27
HHDW28
HHDW29
HHDW30
HHDW31
Samples
Peteinosphaeridium sp.
Multiplicisphaeridium sp. 1
Peteinosphaeridium coronum
Peteinosphaeridium robustiramosum
Rhopaliophora mamilliformis
Peteinosphaeridium tenuifilosum
Micrhystridium accuminosum
Baltisphaerosum sp.
Micrhystridium sp.
Solisphaeridium sp. 1
Stelomorpha crassula
Pachysphaeridium rhabdocladium
Peteinosphaeridium armatum
Solisphaeridium aff. solidispinosum
Baltisphaeridium brevifilicum
Baltisphaeridium calicispinae
Baltisphaeridium denticulatum
Baltisphaeridium microspinosum
Baltisphaeridium sp.3.
Baltisphaeridium spp.
Baltisphaerosum christoferi
Multiplicisphaeridium irregulare
Peteinosphaeridium angustilaminae
Peteinosphaeridium dissimile
Polygonium gracile
Rhopaliophora palmata
Rhopaliophora pilata
Sacculidium inornatum
Sacculidium peteinoides
Stelliferidium striatulum
Stelomorpha erchunensis
Leiosphaeridia spp.
Multiplicisphaeridium dikranon
Athabascaella playfordii
Multiplicisphaeridium sp. cf. M. irregulare
Micrhystridium henryi
Baltisphaeridium kunmingense
Lophosphaeridium citrinipeltatum
Pachysphaeridium pachyconcha
Tongzia meitana
Tranvikium polygonale
Leiosphaeridia tenuissima
Baltisphaeridium fragile
Baltisphaerosun bystrentos
Polygonium sp.
Solisphaeridium sp. cf. S. solare
Solisphaeridium sp. 2

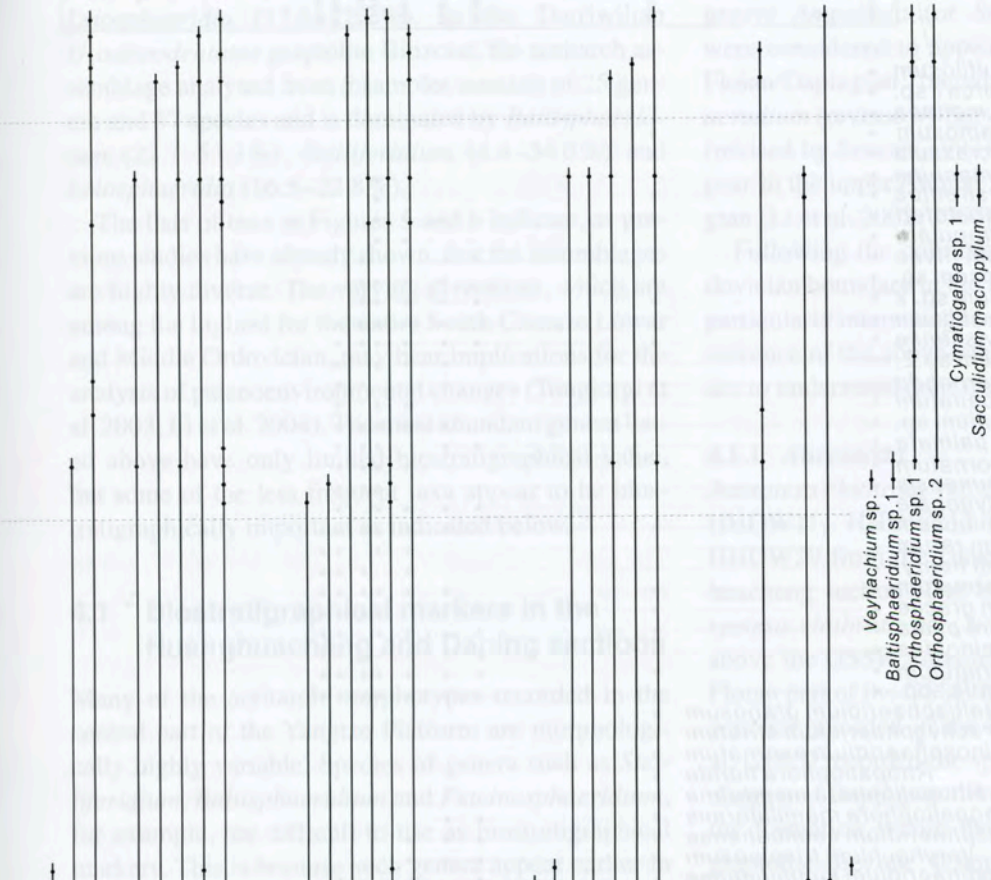

Fig. 5. Distribution of acritarch species in the Huanghuachang section. *Co: Corymbograptus deflexus*; *Az: Azygograptus suecicus*.

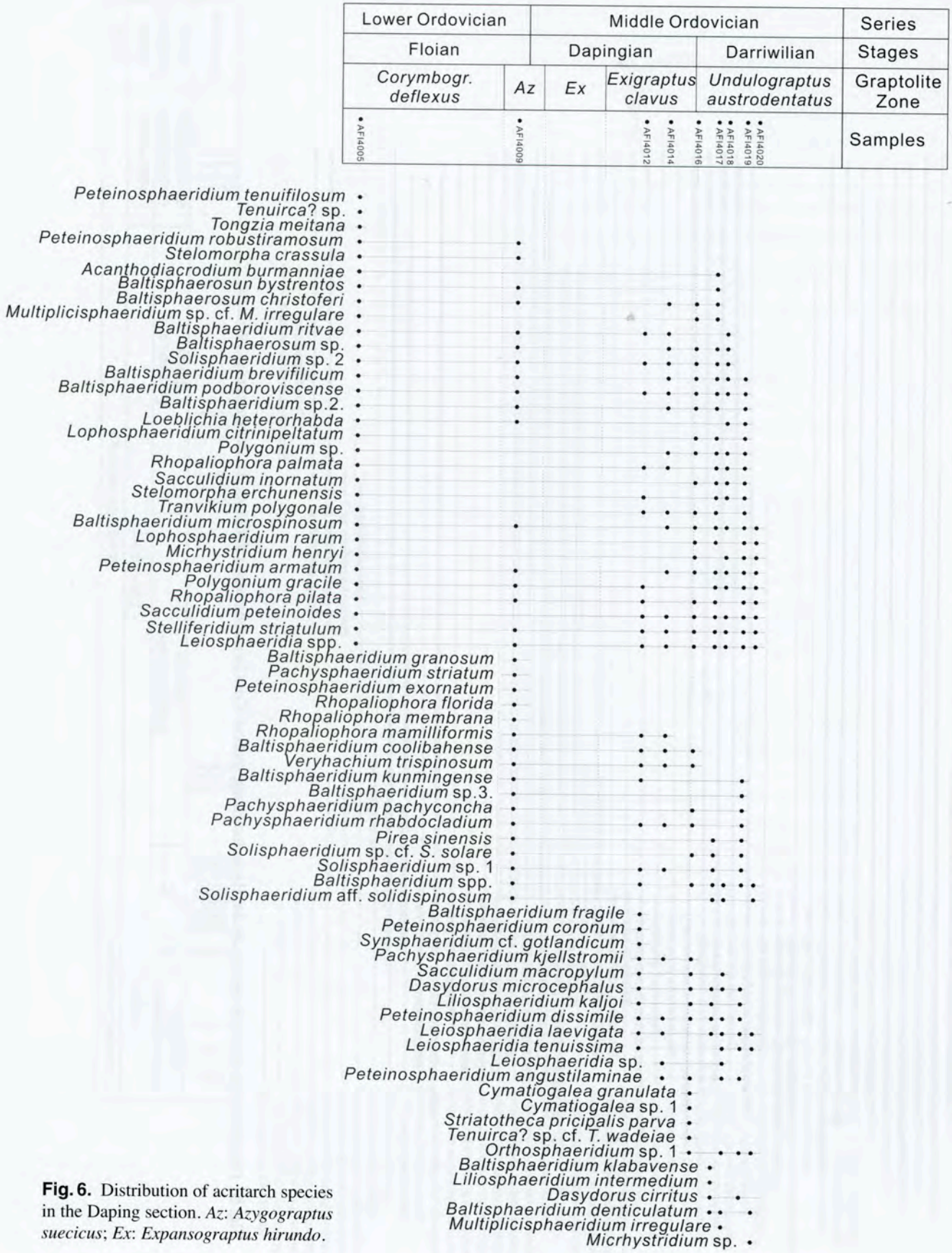

Fig. 6. Distribution of acritarch species in the Daping section. *Az*: *Azygograptus suecicus*; *Ex*: *Expansograptus hirundo*.

(14.0%) and *Rhopaliophora* (12.5%). A slightly higher diversity has been recorded in the acritarch assemblage from the *E. clavus* graptolite Biozone, which contains 15 genera and 35 species (based on 2 samples). This assemblage is dominated by *Stelliferidium* (2.5–70.5%), *Baltisphaeridium* (7.0–65.4%) and *Leiosphaeridia* (17.8–22.2%). In the Darriwilian *U. austrodentatus* graptolite Biozone, the acritarch assemblage analysed from 5 samples consists of 25 genera and 57 species and is dominated by *Baltisphaeridium* (22.7–53.3%), *Stelliferidium* (4.4–34.0%) and *Leiosphaeridia* (16.5–22.8%).

The lists of taxa in Figures 5 and 6 indicate, as previous studies have already shown, that the assemblages are highly diverse. The varying diversities, which are among the highest for the entire South Chinese Lower and Middle Ordovician, may bear implications for the analysis of palaeoenvironmental changes (Tongiorgi et al. 2003; Li et al. 2004). The most abundant genera listed above have only limited biostratigraphical value, but some of the less frequent taxa appear to be biostratigraphically important as indicated below.

4.1 Biostratigraphical markers in the Huanghuachang and Daping sections

Many of the acritarch morphotypes recorded in the central part of the Yangtze Platform are morphologically highly variable. Species of genera such as *Stelliferidium*, *Baltisphaeridium* and *Peteinosphaeridium*, for example, are difficult to use as biostratigraphical markers. This is because such genera appear earlier in the Cambrian to Tremadocian, and individual species can be difficult to distinguish from comparable morphotypes, similarly to the species of the galeate acritarch plexus, for example (Servais et al. 2004). In the present study, we do not concentrate on systematic palaeontology, but only discuss the biostratigraphical potential of selected taxa that are easily distinguishable from other species and genera.

Brocke et al. (1995, 2000), Brocke (1998), and Li et al. (2002, 2003) selected several Early-Middle Ordovician taxa that can easily be recognised and, based on their FADs, are biostratigraphically useful. Easily distinguishable taxa present in the Floian are the genera *Coryphidium* and *Striatotheca*, the first species of which appear in the Tremadocian as shown in the reviews by Servais (1997) and Servais et al. (2008). Among taxa that are useful for the recently defined Lower-Middle Ordovician boundary, *Arbusculidum filamentosum* and *Aureotesta clathrata* were considered to appear below the boundary in the *deflexus* graptolite Biozone in South China. A recent study shows earlier occurrences for the two taxa, *Arbusculidum filamentosum* being recorded from the *eobifidus* graptolite Biozone, while *Aureotesta* is found as early as in the *approximatus* graptolite Biozone (Yan 2007). The genera *Ampullula* (or *Stelomorpha*) and *Barakella* were considered to appear close to or just above the Floian/Dapingian boundary. The genera *Dicrodiacrodium* (revised by Servais et al. 1996) and *Frankea* (revised by Servais 1993), on the other hand, first appear in the upper Arenig, now attributed to the Dapingian (Li et al. 2002, 2003).

Following the definition of the Lower-Middle Ordovician boundary in the Huanghuachang section, it is particularly interesting to review the stratigraphical occurrence of the above-mentioned and other taxa in order to understand their usefulness for biostratigraphy.

4.1.1 *Aureotesta*

Aureotesa clathrata var. *simplex* occurs in the samples HHDW11, HHDW21, HHDW23, HHDW27, and HHDW29 from the Dawan Formation of the Huanghuachang section. The lowermost occurrence of *Aureotesa clathrata* var. *simplex* in HHDW11 is 0.6 m above the GSSP. *Aureotesta* is thus not present in the Floian part of the GSSP. In the present study, the genus was not recorded in the Daping section. Tongiorgi et al. (2003) recorded the species in both the Huanghuachang and Daping sections in the lower part (unit 2) of the formation within the upper part of the *suecicus* graptolite Biozone. It appears thus from all studies in the Yichang sections that *Aureotesta* is not present below the base of the Middle Ordovician.

However, as indicated in the revision of the genus by Brocke et al. (1997, 2000), the genus has been recorded from other South Chinese sections in the *deflexus* graptolite Biozone, i.e., clearly below the base of the Middle Ordovician. An even earlier occurrence of the genus has been reported from another section: *Aureotesta* is present in the *approximatus* graptolite Biozone of the Dacao Formation from the Chengkou section, Chongqing City (Yan 2007).

4.1.2 *Arbusculidium filamentosum*

The second species considered to have its FAD slightly below the Lower-Middle Ordovician boundary is *Arbusculidium filamentosum*. At Huanghuachang, this species first appears in sample HHDW8, just above the GSSP. The species has not been recovered from the Daping section during the new investigations. As with

A. clathrata, the stratigraphical distribution of *A. filamentosum* observed here confirms that of Tongiorgi et al. (2003), who recorded the species very rarely in 'unit 2' of the Dawan Formation, but not below the *suecicus* graptolite Biozone. The species thus appears in the Yichang sections above the boundary. However, in their revision of the genus *Arbusculidium*, Fatka and Brocke (1999) indicated a FAD of the genus in the *deflexus* graptolite Biozone, with a first occurrence in South China in this biozone by Li (1987). In a recent study, *Arbusculidium filamentosum* has been found in the *eobifidus* graptolite Biozone in the Meitan Formation of Guizhou Province (Yan 2007).

4.1.3 *Barakella*

Li et al. (2002, 2003) considered the genus *Barakella* as a potential marker for the Lower-Middle Ordovician boundary. This genus has never been recorded below the boundary so far. In the Huanghuachang section *Barakella rara* occurs in samples HHDW9 and HHDW12, i.e., in the *suecicus* graptolite Biozone. Interestingly, the first occurrence of *Barakella* in sample HHDW9 is located just 22 cm above the GSSP. As indicated by Li et al. (2003) and confirmed by Tongiorgi et al. (2003), the genus *Barakella* has never been found below the *suecicus* graptolite Biozone, and the genus has not yet been recorded in the Floian (Yan 2007). The genus is thus potentially a marker for the base of the Dapingian in South China.

4.1.4 *Liliosphaeridium*

Another taxon that might be useful for biostratigraphical applications is the genus *Liliosphaeridium*. The species *Liliosphaeridium intermedium* occurs rarely in samples HHDW17 and HHDW31 from the Dawan Formation of the Huanghuachang section, respectively from the *hirundo* and the *austrodentatus* graptolite Biozones. *L. intermedium* also occurs in the Daping section in levels attributed to the *clavus* and *austrodentatus* graptolite Biozones. These occurrences confirm the observations of Tongiorgi et al. (2003), who also recorded the genus only in the upper part of the Daping section (*austrodentatus* graptolite Biozone). Tongiorgi et al. (2003) noted that the oldest occurrence of the genus is at the base of the upper member of the Dawan Formation in the Daping section, which would indicate that the genus is not present in the Lower Ordovician. Interestingly, the species *L. kaljoi* has also been recorded from the Huanghuachang section. This species is present, although very rare, in sample HHDW9, located just 22 cm above the GSSP. Like *Barakella*, the genus *Liliosphaeridium* may thus be an excellent marker for the base of the Dapingian.

4.1.5 *Orthosphaeridium*

Orthosphaeridium is another very easily recognisable taxon. It is common in Middle and Upper Ordovician rocks, but its FAD has never been clearly established. The species of *Orthosphaedidium* in the Chinese sections (*O.* sp. 1 and *O.* sp. 2) occur in samples HHDW21, HHDW26, HHDW32–33, HHDW27–29, and HHDW31 of the Dawan Formation at Huanghuachang, i.e. in the *clavus* and *austrodentatus* graptolite Biozones. *Orthosphaedidium* sp. 1 is also found in samples AFI4016 and AFI4018–4020 from the *austrodentatus* graptolite Biozone of the Daping section, notably from intervals where Tongiorgi et al. (2003) also recovered the genus. *Orthosphaeridium* thus appears to be an indicator for the Middle Ordovician in South China. It is clearly absent from the Lower Ordovician (Yan 2007).

4.1.6 *Sacculidium*

The genus *Sacculidium*, like *Liliosphaeridium*, has so far only been recorded from the upper part of the Arenig, corresponding to the Dapingian. In their revisions of the genus, Ribecai et al. (2002) and Tongiorgi et al. (2003) indicated that its oldest occurrences are in the upper part of the Dawan Formation. *Sacculidium* could thus be an indicator for the Dapingian. In the present study, we recovered rare *Sacculidium macropylum* from samples HHDW33 and HHDW34 of the Dawan Formation at Huanghuachang, within the *clavus* graptolite Biozone. The species is also found in samples AFI4012, AFI4016 and AFI4018 at Daping, in the *clavus* and *austrodentatus* graptolite Biozones, thus confirming a first appearance in the Dapingian. However, the species *Sacculidium inornatum* is present in the upper Floian (AFI4005) of the Daping section (Figure 6). The genus therefore appears slightly below the Floian-Dapingian boundary.

4.1.7 *Stelomorpha*

Li et al. (2002) considered the genus *Ampullula* (most of its species have been attributed to *Stelomorpha*, see discussion in Tongiorgi et al. 2003) to be a possible marker for the base of the Middle Ordovician, as the species *S. princeps* has its FAD in the *suecicus* Biozone and the genus had not been recorded below that biozone (Brocke 1997b).

In the present study, the four species of *Stelomorpha* found by Tongiorgi et al. (2003) have also been record-

ed. While the latter authors encountered the first specimens in the lower (but not lowest) part of the *suecicus* zone, the new investigations from samples that are located below those of Tongiorgi et al. (2003) now clearly show older occurrences in the two sections.

Stelomorpha composta occurs in samples HHDW9–10 and HHDW17 of the Dawan Formation at Huanghuachang, from both the *suecicus* and *hirundo* graptolite biozones, while *S. princeps* occurs rarely in sample HHDW9, just 22 cm above GSSP and in the *suecicus* graptolite Biozone. Thus, neither species has been found in the Floian so far. However, the two other species of *Stelomorpha*, *S. crassula* and *S. erchunensis*, are present below the boundary interval in both sections, in the *eobifidus* and *deflexus* graptolite Biozones.

5. Regional and international correlation of the Lower-Middle Ordovician boundary using acritarchs

5.1 Correlations within South China

As indicated above, problems arise when comparing the correlations of acritarch samples with graptolite biozones in South China, as both the names of the graptolite biozones and their exact position in the sections have changed. Nevertheless, most of the biostratigraphically significant taxa selected above confirm the stratigraphical distribution of acritarchs indicated in the previous study of the two sections by Tongiorgi et al. (2003).

A literature review shows that most of the taxa recorded from the Dawan Formation at Huanghuachang and Daping have similar occurrences in other sections from the Yangtze Platform. *Aureotesa clathrata* var. *simplex* and *Arbusculidium filamentosum* have been found by Brocke (1998) in the *suecicus* Zone of the Dawan Formation in the Datianba and Wangjiazai sections, but these taxa are also present in samples from the *deflexus* Biozone. Both taxa are thus present in the Floian of South China. *Barakella* has been considered a marker for the base of the Middle Ordovician because it has been described from the *suecicus* graptolite Biozone of the Huanghuachang and Daping sections by different authors (Lu 1987; Yin 1995; Tongiorgi et al. 1995, 2003), and also from the *suecicus* graptolite Biozone of the Meitan Formation in Honghuayuan section, North Guizhou Province (Yan and Li 2005; Yan 2007). As yet, the genus has not been recorded from the Floian. *Barakella felix* has also been recorded from Hubei Province (Jianyangping section, *A. suecicus* Biozone) and Sichuan Province (Datianba section, *A. suecicus* Biozone, Wangjiazei, *U. sinodentatus* Biozone) by Brocke (1998) and Brocke et al. (2000).

Liliosphaeridium intermedium was recorded from the Arenig and Llanvirn of Sichuan and Guizhou by Brocke (1998) and Brocke et al. (2000) and from the *suecicus* graptolite Biozone of the Dawan Formation in the Huanghuachang and Daping sections, Yichang City (Tongiorgi and Di Milia 1999; Tongiorgi et al. 2003), but never below this graptolite biozone. Although the genus *Sacculidium* is now clearly present in the upper part of the Lower Ordovician, the species *Sacculidium macropylum* may be a marker for the Middle Ordovician because, as with the present study, the species has been recorded from the *clavus*, *austrodentatus* and *intersitus* graptolite Biozones of the Honghuayuan section, northern Guizhou Province, South China (Yan 2004; Yan and Li 2005; Yan 2007).

Stelomorpha composta, a species with the potential to mark the base of the Middle Ordovician in South China, has so far only been reported from the Huanghuachang and Daping sections, where other occurrences in the *suecicus* Zone have been described (Yin 1995; Yin et al. 1998; Tongiorgi et al. 1995, 2003). *S. princeps* has not only been described from the *suecicus* Zone in the Huanghuachang and Daping sections, but also from the same zone in the Wangjiazai section of Sichuan Province (Brocke 1997a) and from the *sinodentatus* graptolite Biozone (from levels equivalent to the *clavus* graptolite Biozone) in the Datianba section in Sichuan Province (Brocke 1998).

5.2 Correlations with peri-Gondwanan areas

Correlations of the biostratigraphical markers of the South Chinese sections with other localities of the margin of Gondwana are partly possible. *Aureotesa clathrata* var. *simplex* is a stratigraphical marker, reported from many 'Arenig-Llanvirn' sections of the following localities: eastern Newfoundland, Canada (Martin in Dean and Martin 1978); northwestern Argentina (Ottone in Ottone et al. 1992; Rubinstein et al. 1999; Rubinstein and Toro 1999, 2001); Central Bohemia (Vavrdová 1979, 1990); the English Lake District, UK (Turner and Wadge 1979; and as *M.* cf. *simplex* by Molyneux 1990); Chitral, Central Pakistan (Quintavalle et al. 2000); Central Sardinia (Albani 1989; Di Milia and Tongiorgi 1992); northeastern Iran (Ghavidel-Syooki

dle and Upper Ordovician rocks, has its FAD higher in the Dapingian. The genus *Stelomorpha* (also named *Ampullula*) appears below the boundary, but species such as *Stelomorpha composta* and *S. princeps*, which appear just above the GSSP (Fig. 7), have the potential for stratigraphical index fossils.

Correlations are possible not only within the Gondwanan areas, but also with Baltica, which like South China was located at intermediate palaeolatitudes. *Barakella* is possibly also an excellent correlative element with sections in peri-Gondwana, in particular with regard to sequences from North Africa. On the other hand, the first occurrence of *Liliosphaeridium* possibly enables a correlation of the base of the Middle Ordovician in peri-Gondwana and Baltica.

Detailed revisions of some of these key taxa are needed in order to clarify their precise stratigraphical ranges.

Acknowledgements. This paper is part of a result of a Chinese-French collaboration project (CAS – CNRS). L.J. and Y.K. are grateful for several Chinese projects (NSFC 40672014, 40802006, and LPS 083108). L.J. also acknowledges the University of Lille 1 for providing a position as invited professor. Yan Kui acknowledges the Chinese Academy of Sciences for providing financial support for a postdoctoral visit at the University of Lille 1. The authors gratefully acknowledge the detailed revisions of the manuscript by Rainer Brocke (Frankfurt) and Stewart Molyneux (Keyworth-Nottingham), and the editorial help of Jörg Pross (Frankfurt). This is a contribution to the International Geoscience Programme 'Ordovician Palaeogeography and Palaeoclimate' (IGCP 503).

References

Achab, A., Rubinstein, C.V., Astini, R.A., 2006. Chitinozoans and acritarchs from the Ordovician peri-Gondwana volcanic arc of the Famatina System, northwestern Argentina. Review of Palaeobotany and Palynology **139**, 129–149.

Albani, R., 1989. Ordovician (Arenig) acritarchs from the Solanas Sandstone Formation, central Sardinia, Italy. Bollettino della Società Paleontologica Italiana **28**, 3–37.

Bagnoli, G., Ribecai, C., 2001. On the biostratigraphic significance of the Ordovician acritarch genus *Liliosphaeridium* on Öland, Sweden. Review of Palaeobotany and Palynology **117**, 195–215.

Brocke, R., 1997a. First results of palynological investigations of the Lower Arenig acritarchs from the Yangtze Platform, southwest China. In: Fatka, O., Servais, T. (Eds.), Acritarcha in Praha. Acta Universitatis Carolina, Geologica **40**, 337–355.

Brocke, R., 1997b. Evaluation of the Ordovician acritarch genus *Ampullula* Righi. Annales de la Société Géologique de Belgique **120**, 73–97.

Brocke, R., 1998. Palynomorpha (Acritarchen, Prasinophyceae, Chlorophyceae) aus dem Ordovizium der Yangtze-Plattform, Südwest China. Ph.D. Thesis, Technische Universität Berlin, Berlin, Germany, 225p.

Brocke, R., Fatka, O., Servais, T., 1997. A review of the Ordovician acritarchs *Aureotesta* and *Marrocanium*. Annales de la Société Géologique de Belgique **120**, 1–21.

Brocke, R., Fatka, O., Molyneux, S., Servais, T., 1995. First appearance of selected Early Ordovician acritarch taxa from peri-Gondwana. In: Cooper, J.D., Droser, M.L., Finney, S.C. (Eds.), Ordovician Odyssey: short papers for the Seventh International Symposium on the Ordovician System, SEPM Volume **77**, Las Vegas, Nevada, USA, p.473–476.

Brocke, R., Li, J., Wang, Y., 1999. Preliminary results on upper "Arenigian" to lower "Llanvirnian" acritarchs from South China. In: Kraft, P., Fatka, O. (Eds.), Quo vadis Ordovician? Short papers of the 8th international Symposium on the Ordovician System (Prague, June 20–25, 1999). Acta Universitatis Carolina, Geologica **43**, 259–261.

Brocke, R., Li, J., Wang, Y., 2000. Upper Arenigian to lower Llanvirnian acritarch assemblages from South China: a preliminary evaluation. Review of Palaeobotany and Palynology **113**, 27–40.

Burmann, G., 1976. Übersicht über das ordovizische Mikroplankton im Südteil der DDR (Vogtland, Wildenfelser Zwischengebirge). Jahrbuch für Geologie **7/8**, 47–62.

Chen, P., Zhan, R., 2006. The Lower to Middle Ordovician Dawan Formation and its coeval rocks in the Yangtze region. Journal of Stratigraphy **30**, 11–20 (in Chinese with English abstract).

Cooper, A.H., Rushton, A.W.A., Molyneux, S.G., Hughes, R.A., Moore, R.M., Webb, B.C., 1995. The stratigraphy, correlation, provenance and palaeogeography of the Skiddaw Group (Ordovician) in the English Lake District. Geological Magazine **132**, 185–211.

Cramer, F.H., Kanes, W.H., Díez R., M.D.C., Christopher, R.A., 1974. Early Ordovician acritarchs from the Tadla Basin of Morocco. Palaeontographica, Abt. **B 146**, 57–61.

Dean, W.T., Martin, F., 1978. Lower Ordovician acritarchs and trilobites from Bell Island, eastern Newfoundland. Bulletin of the Geological Survey of Canada **284**, 1–35.

Di Milia, A., Tongiorgi, M., 1992. Reworked palynomorphs in the Solanas Sandstone (Central Sardinia) and their significance for the basin anaysis. In: Carmignani, L., Sassi, F.P. (Eds.), Contribution to the geology of Italy with special regard to the Paleozoic basements. A volume dedicated to Tommaso Cocozza. IGCP 276 Newsletters **5**, 461–463.

Eisenack, A., 1959. Neotypen baltischer Silur – Hystrichosphären und neue Arten. Palaeontographica, Abt. **A 112**, 193–211.

Fatka, O., Brocke, R., 1999. Morphologic variability in two populations of *Arbusculidium filamentosum* (Vavrdová 1965) Vavrdová 1972. Palynology **23**, 153–180.

Fournier-Vinas, C., 1985. Acritarches ordoviciens des Zeddara (Maroc Oriental). Géobios **18**, 807–813.

Ghavidel-Syooki, M., 2000. Palynostratigraphy and palaeogeography of Lower Palaeozoic strata in the Ghelli area,

Northeastern Alborz Range, of Iran (Kopet-Dagh Region). Journal of Sciences (Islamic Republic of Iran) **11**, 305–318.

Ghavidel-Syooki, M., 2001. Palynostratigraphy and paleobiogeography of the Lower Paleozoic sequence in the northeastern Alborz Range (Kopet- Dagh region) of Iran. In: Goodman, D.K., Clarke, R.T. (Eds.), Proceedings IX International Palynological Congress, Houston, Texas, U.S.A., 1996, AASP Foundation, Houston, p. 17–35.

Górka, H., 1969. Microorganismes de l'Ordovicien de Pologne. Acta Palaeontologia Polonica **22**, 1–102.

Li, J., 1987. Ordovician acritarchs from the Meitan Formation of Guizhou Province, South-west China. Palaeontology **30**, 613–634.

Li, J., 1989. Early Ordovician Mediterranean province acritarchs for Upper Yangtze Region, China. In: Chinese Academy of Science (Ed.), Developments in Geoscience: Contribution to the 28th Geological Congress 1989, Washington, D.C., U.S.A. Science Press, Beijing, p. 231–234.

Li, J., Brocke, R., Servais, T., 2002. The acritarchs of the South Chinese *Azygograptus suecicus* graptolite Biozone and their bearing on the definition of the Lower-Middle Ordovician boundary. Comptes Rendus Paleovol **1**, 75–81.

Li, J., Servais, T., 2002. Ordovician acritarchs of China and their utility for global palaeobiogeography. Bulletin de la Société Géologique de France **173**, 399–406.

Li, J., Molyneux, S.G., Rubinstein, C.V., Servais, T., 2003. Acritarchs from peri-Gondwana at the Lower and Middle Ordovician Stage boundaries. In: Albanesi, G.L., Beresi, M.S., Peralta, S.H. (Eds.), INSUGEO, Serie Correlación Geológica **17**, 95–99.

Li, J., Servais, T., Yan, K., Zhu, H., 2004. A nearshore-offshore trend in the acritarch distribution of the Early-Middle Ordovician of the Yangtze Platform, S-China. Review of Palaeobotany and Palynology **130**, 141–161.

Li, J., Servais, T., Yan, K., Su, W., 2007. Microphytoplankton diversity curves of the Chinese Ordovician. Bulletin de la Société Géologique de France **178**, 399–409.

Lu, L., 1987. Acritarchs from the Dawan Formation (Arenigian) of Huanghuachang in Yichang, western Hubei. Acta Micropalaeontologica Sinica **4**, 87–102 (in Chinese with English abstract).

Martin, F., Rickards, B., 1979. Acritarches, chitinozoaires et graptolites ordoviciens et siluriens de la Vallée de la Sennette (Massif du Brabant, Belgique). Annales de la Société Geologique de Belgique **102**, 189–197.

Molyneux, S.G., 1990. Advances and problems in Ordovician palynology of England and Wales. Journal of the Geological Society **147**, 615–618.

Molyneux, S.G., Raevskaya, E., Servais, T., 2007. The *messaoudensis-trifidum* acritarch assemblage and correlation of the base of Ordovician Stage 2 (Floian). Geological Magazine **144**, 143–156.

Ottone, E.G., Toro, B.A., Waisfield, B.G., 1992. Lower Ordovician palynomorphs from the Acoite formation, northwestern Argentina. Palynology **16**, 93–116.

Quintavalle, M., Tongiorgi, M., Gaetani, M., 2000. Lower to Middle Ordovician acritarchs and chitinozoans from Northern Karakorum mountains, Pakistan. Rivista Italiana di Paleontologia e Stratigrafia **106**, 3–18.

Raevskaya, E., Vecoli, M., Bednarczyk, W., Tongiorgi, M., 2004. Billingen (Lower Arenig/Lower Ordovician) acritarchs from the East European Platform and their palaeobiogeographic significance. Lethaia **37**, 97–111.

Ribecai, C., Bruton, D.L., Tongiorgi, M., 2000. Acritarchs from the Ordovician of the Oslo Region, Norway. Norsk Geologisk Tidsskrift **80**, 251–258.

Ribecai, C., Raevskaya, E., Tongiorgi, M., 2002. *Sacculidium* gen. nov. (Acritarcha), a new representative of the Ordovician *Stelomorpha-Tranvikium* plexus. Review of Palaeobotany and Palynology **121**, 163–203.

Righi, E., 1991. *Ampullula*, a new acritarch genus from the Ordovician (Arenig-Llanvirn) of Öland, Sweden. Review of Palaeobotany and Palynology **68**, 119–126.

Rubinstein, C.V., Toro, B., 1999. Acritarch and graptolite biostratigraphy in the lower Arenig of the peri-Gondwana related Eastern Cordillera, Argentina. In: Kraft, P., Fatka, O. (Eds.), Quo vadis Ordovician? Short papers of the 8th International Symposium on the Ordovician System (Prague, June 20–25,1999). Acta Universitatis Carolina, Geologica **43**, 255–258.

Rubinstein, C.V., Toro, B., 2001. Review of acritarch biostratigraphy in the Arenig of the Eastern Cordillera, Northwestern Argentina: new data and calibration with the graptolite zonation. Contributions to geology and palaeontology of Gondwana in honour of Helmut Wopfner, Cologne, 421–439.

Rubinstein, C.V., Toro, B.A., Waisfeld, G., 1999. Acritarch biostratigraphy of the upper Tremadoc-Arenig of the Eastern Cordillera, northwestern Argentina: relationships with graptolite and trilobite faunas. In: Tongiorgi, M., Playford, G. (Eds.), Studies in Palaeozoic palynology, Selected papers from the CIMP Symposium at Pisa, 1998. Bollettino della Società Paleontologica Italiana **38**, 267–286.

Servais, T., 1991. Contribution to the stratigraphy of the Ordovician Rigenée Formation (Brabant Massif, Belgium) with a preliminary study on acritarchs. Annales de la Société Geologique de Belgique **114**, 233–245.

Servais, T., 1993. The Ordovician acritarch *Frankea*. In: Molyneux, S.G., Dorning, K.J. (Eds.), Contributions to acritarch and chitinozoan research. Special Papers in Palaeontology **48**, 79–95.

Servais, T., 1997. The Ordovician *Arkonia-Striatotheca* acritarch plexus. Review of Palaeobotany and Palynology **98**, 47–79.

Servais, T., Maletz, J., 1992. Lower Llanvirn (Ordovician) graptolites and acritarchs from the "assise de Huy", Bande de Sambre-et-Meuse, Belgium. Annales de la Société Geologique de Belgique **115**, 265–285.

Servais, T., Molyneux, S.G., 1997. The *messaoudensis-trifidum* acritarch assemblage (Ordovician: late Tremadoc-early Arenig) from the subsurface of Rügen (Baltic Sea, NE-Germany). Palaeontographica Italica **84**, 113–161.

Servais, T., Mette, W., 2000. The *messaoudensis-trifidum* acritarch assemblage (Ordovician: late Tremadoc-early

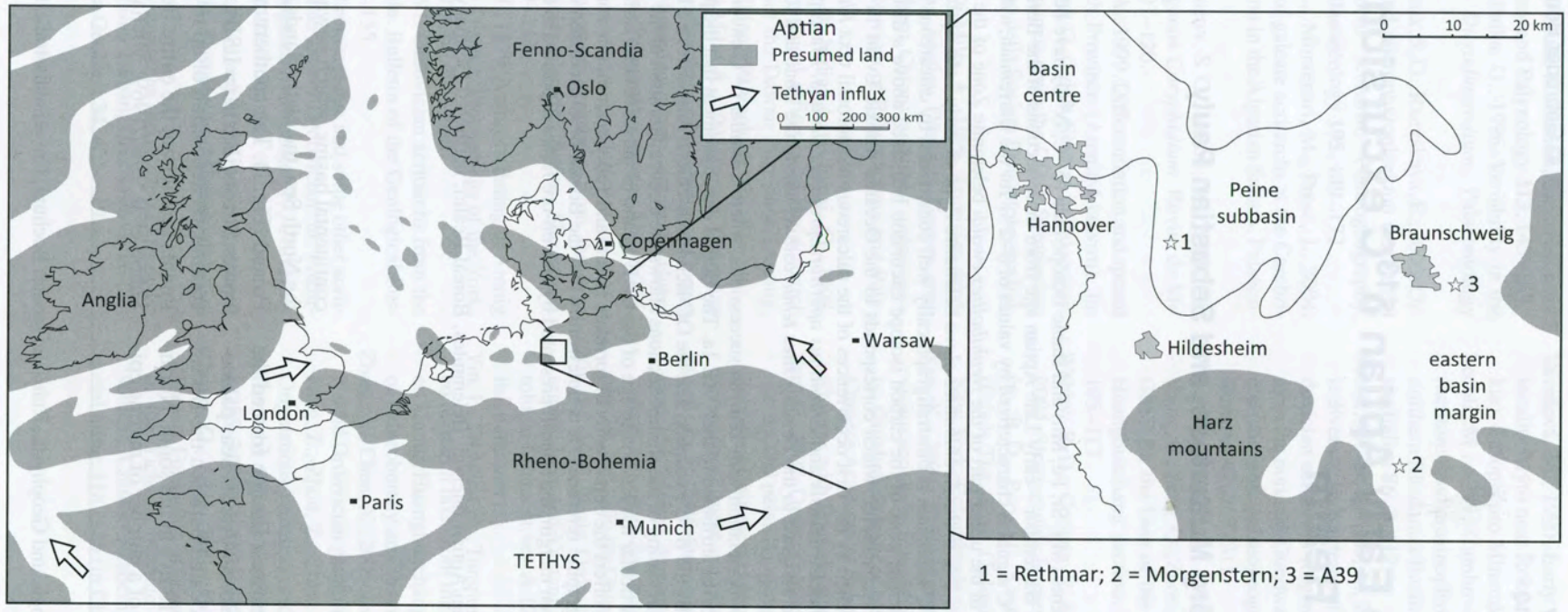

Fig. 1. Palaeogeographic map of the Aptian of northwest Europe showing the sections studied here.

1979; Mutterlose 1992; Mutterlose and Bornemann 2000). This includes the Barremian – Aptian interval, which has been exposed in recent years in various quarries, clay pits and temporary exposures, both in the basin centre and basin margin. Detailed biostratigraphic schemes are readily available for the Barremian – Aptian including calcareous nannofossils (Bischoff and Mutterlose 1998), planktonic foraminifera (Rückheim and Mutterlose 2002), and ammonites (Kemper 1971, 1995). These in turn allow the integration of new stable isotope data ($\delta^{13}C$, $\delta^{18}O$) into the existing biostratigraphic schemes.

The Barremian/Aptian boundary interval is characterized by significant palaeoceanographic and palaeobiological changes caused by increased seafloor-spreading rates and submarine volcanism (Larson 1991a, b). The pulse of oceanic crust production began at 120–125 Ma (Larson 1991a, b). A first peak of crust production occurred at 125 Ma (Barremian-Aptian boundary interval according to the time-scale of Harland et al. 1990; Gradstein et al. 2004; Ogg et al. 2008), a second peak is placed at 120 Ma (Early Aptian). These processes increased CO_2 emissions, which in turn are believed to have caused the onset of the mid-Cretaceous greenhouse climate (e. g., Arthur et al. 1985; Larson and Erba 1999; Mehay et al. 2009). This greenhouse world, which was accompanied by a high eustatic level (Haq et al. 1987), lasted throughout the Aptian – Turonian (e. g., Abreu et al. 1998; Wilson et al. 2002). The palaeoceanographic conditions favoured the deposition of organic-rich black shales resulting in the Oceanic Anoxic Events (OAEs). The earliest OAE, of Early Aptian age, the OAE 1a, is known from various Tethyan sections and is characterized by relative light $\delta^{13}C$ values at its base. This negative shift is followed by a positive $\delta^{13}C$ excursion of up to +4‰ (e. g., Weissert and Erba 2004; Weissert et al. 2008). This C-isotope pattern is interpreted to record a global perturbation of the carbon cycle that has been observed from various sections in northern Italy (Menegatti et al. 1998; Erba et al. 1999), Switzerland (Menegatti et al. 1998; Wissler et al. 2003), France (e. g., Moullade et al. 1998a; Heimhofer et al. 2004; Herrle et al. 2004), the middle East (Vahrenkamp 1996), the central Atlantic (Herrle et al. 2004), the Pacific (Jenkyns 1995) and elsewhere (e. g., Bralower et al. 1999; Price 2003; Ando et al. 2008).

The current paper shows data of trace elements (Mg, Sr, Fe, Mn) and stable isotope data ($\delta^{13}C$, $\delta^{18}O$) obtained from 136 belemnite rostra of Barremian – early Late Aptian age from three biostratigraphically well dated sections of the Boreal Realm (northwest Germany). The aim of the study is a) to record the $\delta^{13}C$ and $\delta^{18}O$ signals from the Barremian/Aptian interval of the Boreal Realm with respect to the carbon isotope anomaly, b) to date this record biostratigraphically, c) to link this dataset to well documented black shale sequences of the Boreal Realm (Fischschiefer), d) to test to what extent the $\delta^{13}C$ excursion is also reflected in the extremely shallow water settings of the Boreal Realm, e) to correlate Boreal and Tethyan sections.

2. Geological setting

The marginal sea, which covered northwest Europe during the Barremian was connected to the Boreal-Arctic Sea in the north by an open seaway, allowing for an exchange of water masses and the immigration of Boreal biota. The Barremian was characterized by an overall regressive trend (Rawson and Riley 1982; Ruffell 1991) causing a sea-level lowstand. The limited exchange of seawater to the north caused a stratification of the water column in the southernmost basins of the northwest European sea, including the LSB, the Polish-Danish Basin and the south Netherland Basin (Fig. 1). These restricted conditions resulted in the deposition of finely laminated sediments. These "Blätterton" layers (= paper shales), are characterized by high organic matter contents (TOC 6–8 %; Mutterlose et al. 2009) and were deposited under anoxic bottom water conditions. The most distinctive of these laminated horizons, known as the "Hauptblätterton", is of late Early Barremian age and is interpreted to reflect a short-term warming episode (*Aulacoteuthis* spp. belemnite Zone) (Mutterlose et al. 2009; Malkoč and Mutterlose 2010). Various subordinate Blätterton horizons and intercalated dark clays with impoverished, commonly endemic, floras and faunas are typical of the remainder of the Late Barremian. These endemic elements include calcareous nannofossils, ammonites and belemnites.

The earliest Aptian was characterized by a continuation of these sedimentary patterns, dominated by black clays and laminated shales. A final distinctive laminated horizon, the Fischschiefer of mid Early Aptian age, marks the end of this long-lasting episode of black shale deposition. A subsequent transgression during the Aptian gave way to the flooding of the northwest European Basin, resulting in the deposition of hemi-pelagic marls (*Hedbergella* Marls). This flooding event allowed an exchange of marine floras and faunas, resulting in a more cosmopolitan composition of the assemblages (Mutterlose and Böckel 1998).

The southern basin margin of the LSB, situated directly north of the Harz Mountains (Fig. 1), is characterized by shallow-water deposits throughout the Barremian – Aptian. In contrast to the clays and mudstones of the basin facies, these shallow-water sediments are mainly composed of coarse siliciclastics (sandstones, siltstones), iron ooliths and clastic ironstones, which are derived from reworked Lower Jurassic sideritic nodules (Neuss 1979). This marginal marine iron ore facies reflects an extreme setting of the Barremian – Aptian interval including the Fischschiefer. Despite the extremely shallow-water setting, probably less than 100 m, the sediments yield fully marine faunas (foraminifera, ammonites, belemnites).

3. Material and Methods

3.1 Material

Belemnite rostra from three different localities were analyzed in order to obtain $\delta^{13}C$ and $\delta^{18}O$ data from the Barremian/Aptian boundary interval of the Boreal Realm. The three sections are located east and southeast of Hannover (northern Germany) and span the complete Barremian to early Late Aptian interval.

Rethmar: Rethmar is located 20 km southeast of Hannover (52° 18.37′ N; 10° 01.21′ E). A section of 197 m thick Barremian – Aptian sediments was described in detail by Mutterlose and Wiedenroth (1995). The suc-

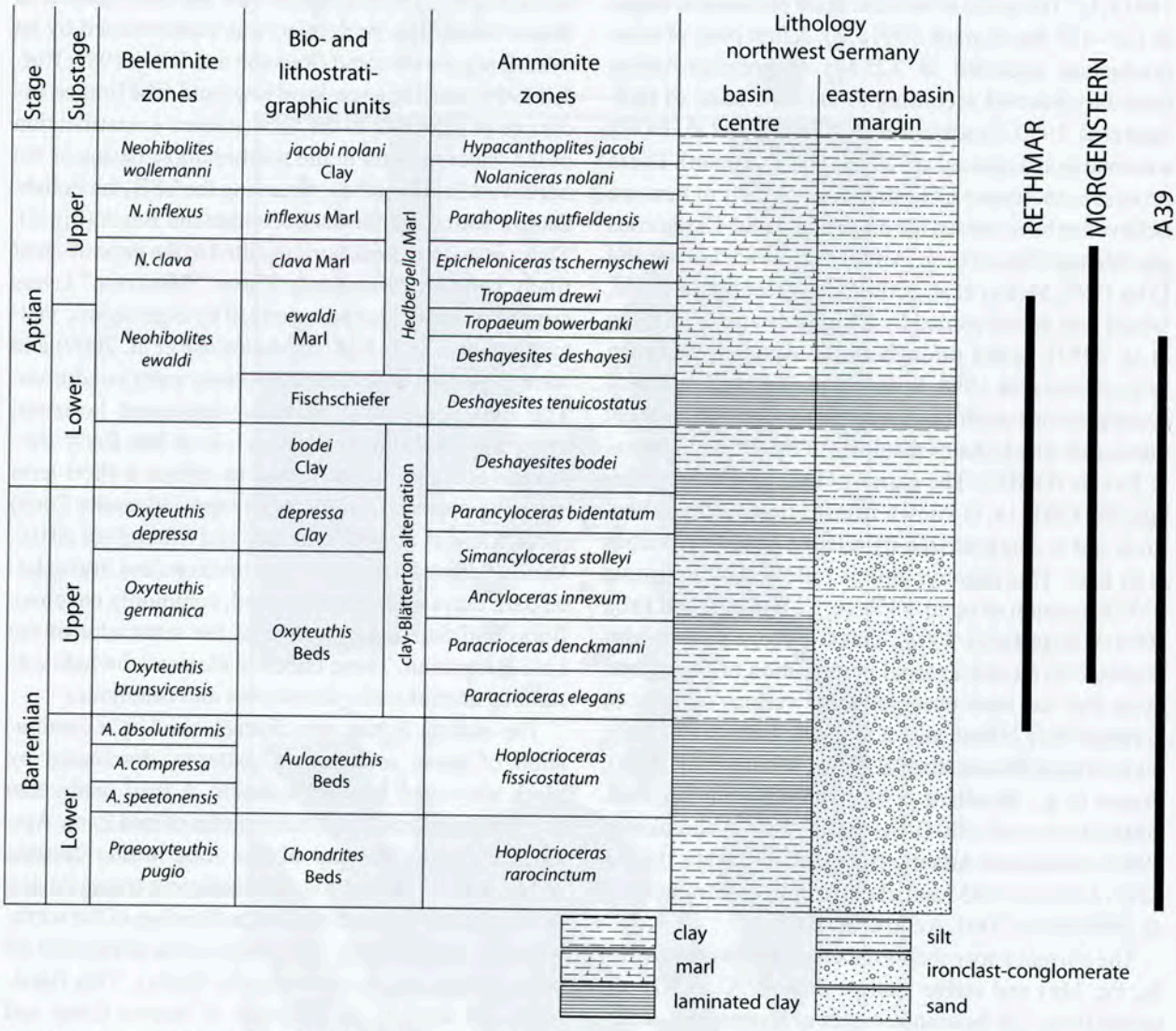

Fig. 2. Bio- and lithostratigraphy of the Barremian and Aptian in northwest Europe. Stratigraphic ranges of the sections are indicated.

cession consists of 144 m of Barremian and 50 m of Lower Aptian mudstones, including a gap of three m covering the Barremian/Aptian boundary interval. The Barremian and lowermost Aptian is characterized by an alternation of finely laminated TOC-rich black shales and dark claystones followed by pale marls in the middle Aptian. Palaeogeographically the Rethmar section occupied a rather distal basin position, the coastline being situated about 20 km further south (Fig. 1). Biostratigraphically the exposed beds can be assigned to the Late Barremian *Oxyteuthis germanica* and *Oxyteuthis depressa* belemnite zones and the Early Aptian *Neohibolites ewaldi* belemnite Zone (Fig. 2). Twenty-four belemnites (Barremian: 20 belemnite rostra; Aptian: 4 belemnite rostra) were analyzed geochemically.

Morgenstern: The Morgenstern section, located 10 km northeast of Goslar (51° 58.15′ N; 10° 27.17′ E), is characterized by 58 m of sediments of Late Barremian to early Late Aptian age. The 41 m thick Barremian succession consists of coarse clastics including sandstones, siltstones and reworked ironclasts forming iron ore seams; for details see Neuss (1979). This reworked material is of lower Jurassic origin, as is indicated by reworked early Jurassic ammonites. The overlying 17 m of siliciclastics and iron ores include a 4 m thick laminated silty claystone horizon, the Fischschiefer. This interval is of Aptian age. The coarse sediments clearly reflect the shallow water position of this section, the coastline being about 5 km further to the southwest. A total of 46 belemnites were analyzed from this section, including four belemnites from the *Oxyteuthis brunsvicensis* belemnite Zone, 15 from the *O. germanica* Zone and five from the *O. depressa* Zone. Fifteen belemnites from the *N. ewaldi* Zone and seven belemnites from the *Neohibolites clava* belemnite Zone span the Aptian part of the successsion.

A39: The road cutting of the motorway "A39" located three km east of Braunschweig (52° 14.819′ N, 10° 36.657′ E to 52° 14.845 N, 10° 36.322′ E) gave access to a 103 m thick sequence of Barremian – Early Aptian sediments (Mutterlose et al. 2009). The Lower Barremian consists of 12.5 m of mudstones and laminated marls (*Praeoxyteuthis pugio* and *Aulacoteuthis* spp. belemnite zones). The Upper Barremian is represented by an approximately 78 m thick sequence of dark clays and laminated mudstones. The Lower Aptian (12.5 m) is characterized by dark clays, laminated mudstones (Fischschiefer), three tuff horizons followed by pale marls. Palaeogeographically the section can be attributed to the basin facies. A total of 66 belemnites (8 from the *P. pugio* Zone; 4 from the *Aulacoteuthis* spp. Zone; 14 from the *O. brunsvicensis* Zone; 21 from the *O. germanica* Zone; 15 from the *O. depressa Zone*; 4 from the *N. ewaldi* Zone) were analyzed for their stable isotope signatures and 60 samples were studied for their calcareous nannofossils (*P. pugio Zone:* 7; *Aulacoteuthis* spp. Zone: 12; *O. brunsvicensis* Zone: 11; *O. germanica* Zone: 1; *O. depressa Zone*: 11; *N. ewaldi* Zone: 18).

3.2 Methods

A total of 136 belemnite rostra (24 from Rethmar; 46 from Morgenstern; 66 from the A39 section) were analyzed for their trace element content (Mg, Sr, Fe, Mn) and stable isotopes ($\delta^{13}C$, $\delta^{18}O$). The solid belemnite rostra were split with a chisel and from each rostrum one sample was taken halfway between the apical line and the outer rim to avoid any potentially altered areas. The samples were drilled with a hand-held driller (0.4 mm tungsten drillbit). The powdered samples were stored in cleaned glass containers to avoid any further contamination.

The trace elements were studied by using an ICP-OES (Rethmar and Morgenstern sections) and an ICP-AES (A39 section) respectively. Almost 1.5 mg (± 10 %) of the powdered sample were weighed and dissolved in 2 ml of HNO_3 (3 %) and 1 ml of pure water for the ICP-OES; the samples for the ICP-AES were dissolved in HCl suprapur and pure water. Internal standards certified the analyzed element content.

The stable isotopes of samples from the Rethmar and Morgenstern sections ($\delta^{13}C$ and $\delta^{18}O$) were analyzed with a Gasbench II coupled with a Finnigan Delta S mass spectrometer in Bochum; samples from the A39 section were measured using a Finnigan MAT 251 mass spectrometer combined with a Carbo Kiel device in Kiel (see for details Mutterlose et al. 2009). The low-Mg-calcite (LMC) samples of the belemnite rostra (0.46 mg ± 0.04 mg) were dissolved in H_3PO_4 to measure the ratio of carbon and oxygen isotopes. Internal standards verified the analyzed isotope ratio (see Appendices 1–3 for standard deviation of the singles localities) and all δ values are reported relative to the V-PDB standard.

The LMC of the rostra is believed to have been precipitated in equilibrium with Cretaceous seawater (Lowenstam and Epstein 1954). LMC is defined as having a "low" Mg content (< 5,000 ppm). Sr contents in marine calcites decrease during diagenesis, because

of a "high" Sr content in seawater and a low Sr content in diagenetic and meteoric waters (Veizer 1974, 1983; Brand and Veizer 1980; Marshall 1992; Wierzbowski and Joachimski 2009). In this study, all samples with Sr contents less than 1,000 ppm are thought to reflect a potentially altered signal. A relative high concentration of Fe and Mn indicates a diagenetic alteration of the belemnite rostra. Fe concentrations of > 200 ppm and Mn concentrations of > 50 ppm are here thought to indicate a potential diagenetic alteration. Various authors, using LMC samples like belemnite rostra, have chosen different thresholds for identifying diagenetic alteration (e.g., van de Schootbrugge et al. 2000: Fe > 300 ppm and Mn > 30 ppm; Price et al. 2000: Fe > 250 ppm and Mn > 100 ppm; Rosales et al. 2004: Fe > 250 ppm and Mn > 150 ppm).

Due to these individually defined thresholds for Sr, Fe and Mn it is difficult to define an accurate limit for potentially altered samples. Data for all samples are shown in Figs. 3–5 and Appendices 1–3. Those samples which have values below/above the thresholds are marked with an open symbol in Figs. 3, 4, 5 and 8.

For the investigation of the calcareous nannofossils 60 samples from the A39 section were used. The random settling technique following Williams and Bralower (1995) and Geisen et al. (1999) was applied for slide preparation. For the preparation of the settling slides 15 to 27 mg of the dried samples were used. The cover slide was fixed with Norland Optical Adhesive to an object slide. To estimate the required weight of content and to detect preservation changes caused by preparation, common smear slides were prepared and compared to

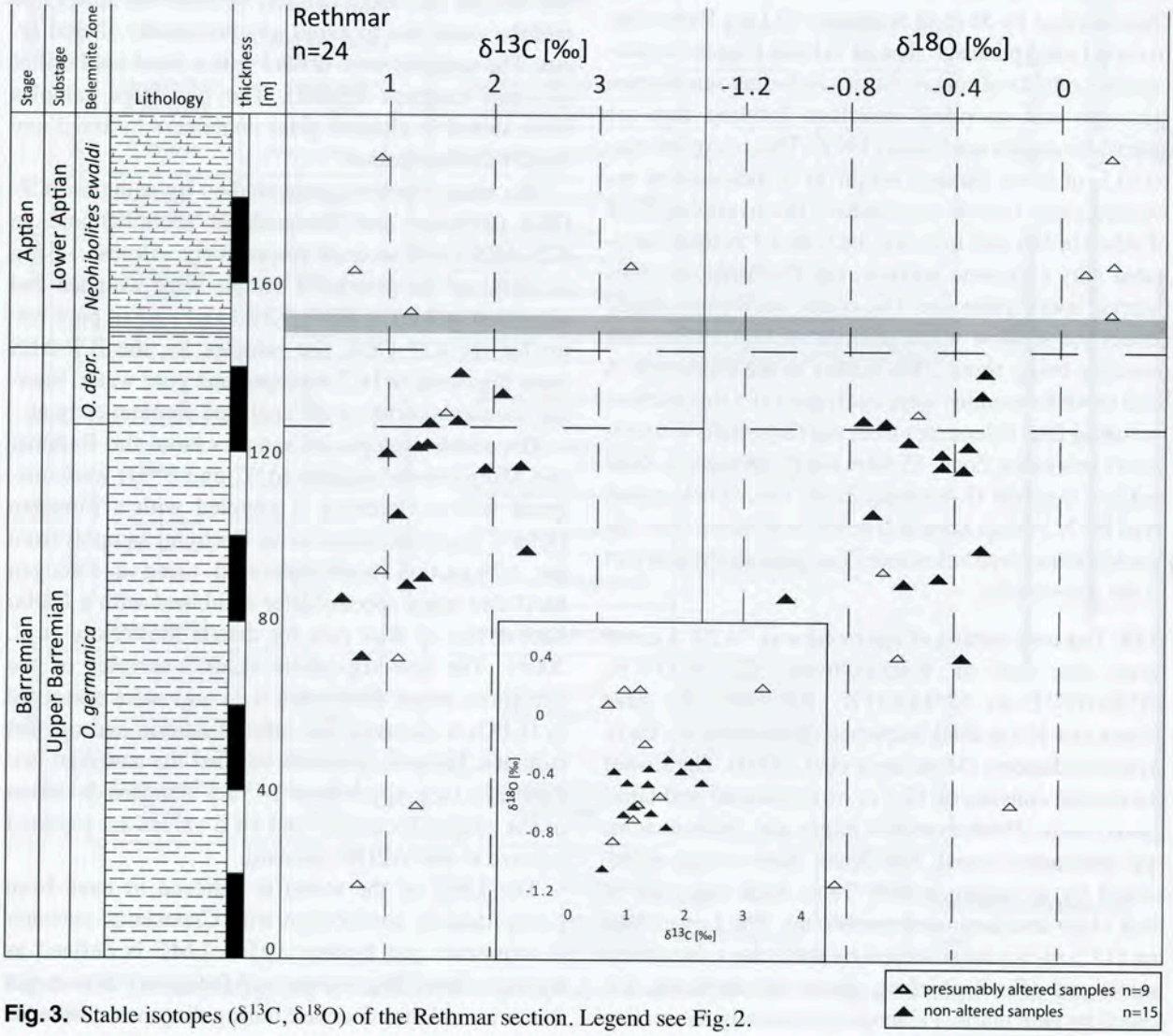

Fig. 3. Stable isotopes ($\delta^{13}C$, $\delta^{18}O$) of the Rethmar section. Legend see Fig. 2.

the settling slides. Counts of calcareous nannofossils were performed by using an OLYMPUS BH-2 light microscope with cross-polarized-light at a magnification of × 1,500. Two traverses of the slides were studied for each sample. The quality of preservation of the nannofossils was based on the degree of etching and overgrowth. Identification of taxa follows the taxonomic concepts of Perch-Nielsen (1985) and Bown (1998).

4. Results

4.1 Trace elements, $\delta^{18}O$ and $\delta^{13}C$

Rethmar (Appendix 1; Fig. 3: 24 rostra): The Mg content varies from 972 to 2,499 ppm and the Sr content from 804 to 1,415 ppm. Fe and Mn concentrations range from 9 to 1,432 ppm and 1 to 100 ppm respectively. Low Sr and/or high Fe-Mn values are indicative of potential diagenetic alteration. Potential alteration is shown by 9 samples, resulting in 15 non-altered samples.

The carbon isotopes show values ranging between +0.8‰ and +2.3‰ in the *O. germanica* Zone, being less noisy in the *O. depressa* Zone (+1.6‰ to +2.1‰). An increase marks the *N. ewaldi* Zone, with highest values (+3.3‰) directly above the Fischschiefer, and lower values thereafter (+0.9‰).

The stable oxygen isotopes show a trend from negative values (−1.0‰ to −0.2‰) in the *O. germanica* and *O. depressa zones* to more positive values in the *N. ewaldi* Zone (+0.2‰).

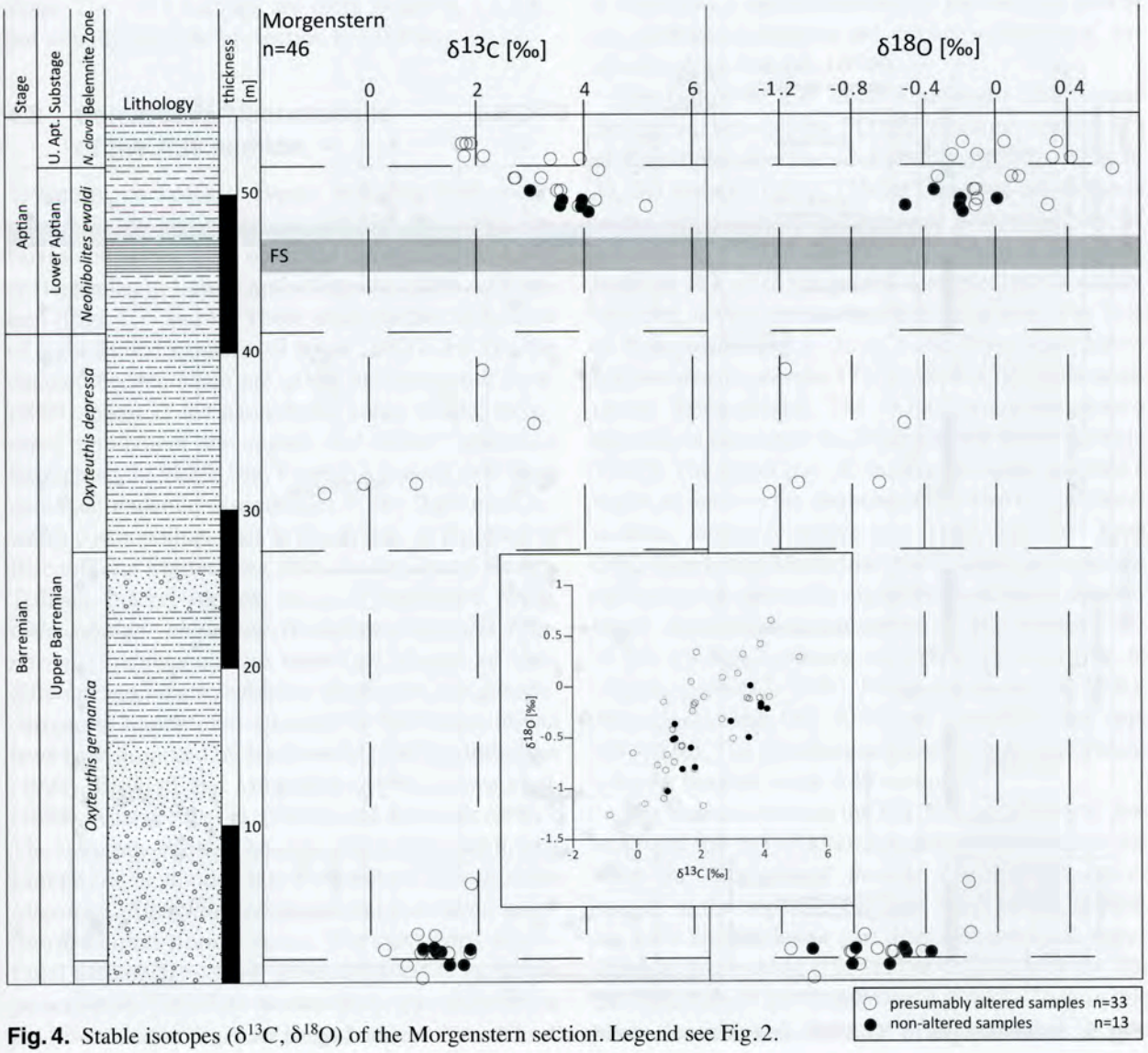

Fig. 4. Stable isotopes ($\delta^{13}C$, $\delta^{18}O$) of the Morgenstern section. Legend see Fig. 2.

Morgenstern (Appendix 2; Fig. 4: 46 rostra): The Mg content varies from 942 to 2,594 ppm, the Sr content from 809 to 1,293 ppm; the lowest values below 1,000 ppm are located in the Aptian *N. ewaldi* and *N. clava* zones. The Fe content varies from 30 to 1,595 ppm and the Mn values show a pattern of 6 to 1,225 ppm. Out of the 46 belemnites analyzed from this section, 33 rostra show a potential alteration, indicated by low Sr contents and high Fe-Mn contents respectively.

$\delta^{13}C$ values of 0.0‰ to +2.0‰ are typical of the *O. brunsvicensis* and *O. germanica* zones, showing the highest values approximately 6 m above the Fischschiefer (+3.5‰ to +5.2‰). After this interval, the $\delta^{13}C$ values decrease to lighter values around +2.7‰ to +3.2‰. Near the top of the *N. ewaldi* Zone, and at the bottom of the overlying *N. clava* Zone, the $\delta^{13}C$ values increase again to high values around +3.4‰ to +4.3‰. After this short peak, the results decrease again to values around +2‰ (+1.7‰ to +2.1‰).

The $\delta^{18}O$ data show a clear trend from negative values (–1.2‰ to –0.2‰) in the Upper Barremian. The isotopic composition above the Early Aptian Fischschiefer is more positive (–0.5‰ to +0.7‰). The most negative values occur in the *O. germanica* Zone, those of the underlying and overlying zones are more positive.

A39 (Appendix 3; Fig. 5: 66 rostra): The Mg data vary from 885 to 4,898 ppm, Sr from 1,064 to 2,435 ppm, Fe from 7 to 3,343 ppm, and Mn from 1 to 135 ppm. Diagenetic alteration is thus indicated for 18 rostra. Mutterlose et al. (2009) considered only three samples to have been altered diagenetically because of a higher threshold for Fe in that study.

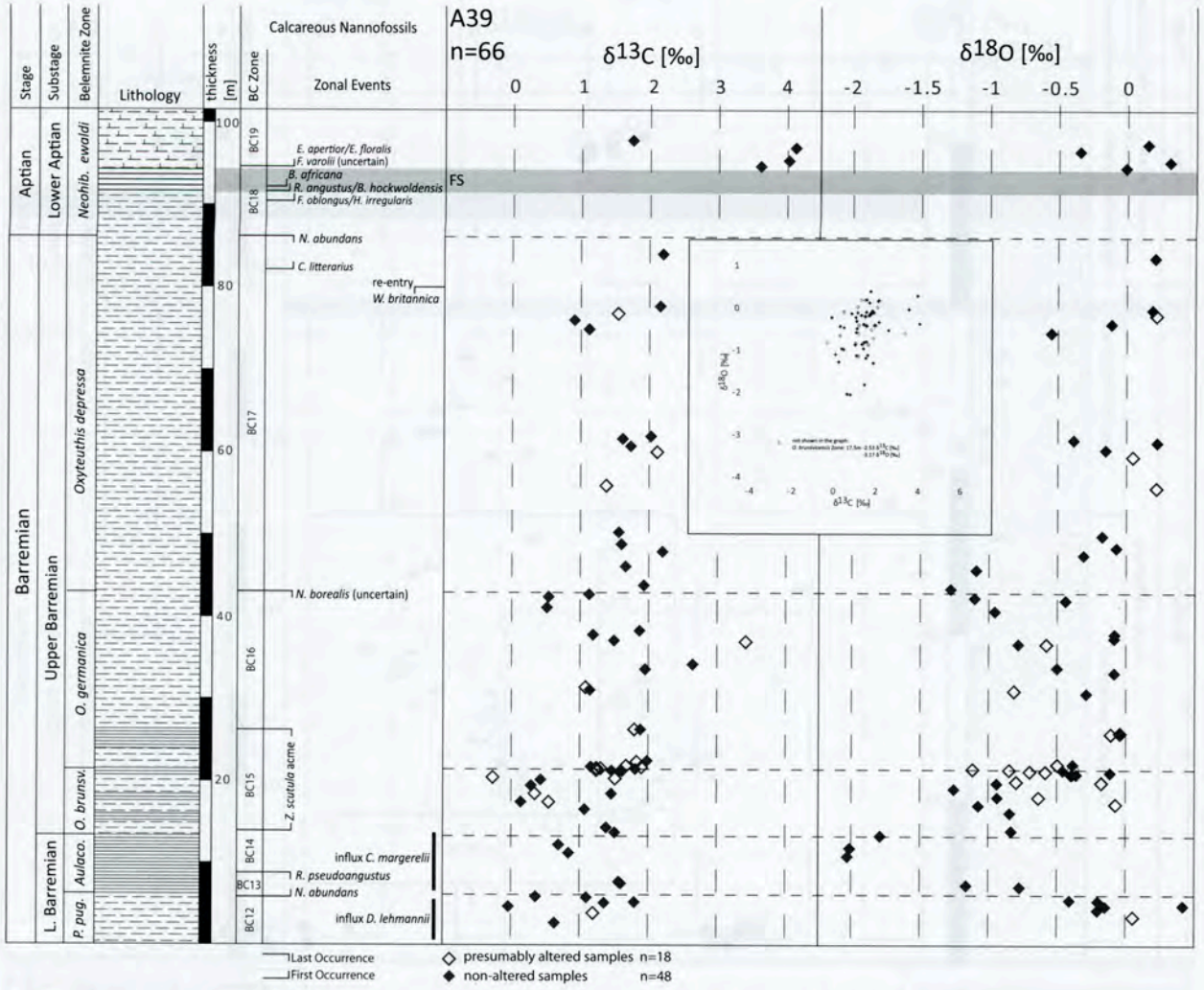

Fig. 5. Stable isotopes ($\delta^{13}C$, $\delta^{18}O$) and calcareous nannofossils of the A39 section. Legend see Fig. 2.

The carbon isotope composition reflects more or less the same conditions as in the Morgenstern section and show constant values of 0‰ and +2‰ for the Barremian. The values for the *P. pugio* and *Aulacoteuthis* spp. zones range from 0‰ to +1.5‰, whereas the Upper Barremian values are slightly higher, around +1‰ to +2‰. The highest values of $\delta^{13}C$ are visible directly above the Fischschiefer, with values around +3.5‰ to +4‰ in the Early Aptian.

The lower *P. pugio* Zone shows positive $\delta^{18}O$ values of +0.4‰, with a decrease to −1.2‰ in the upper part of this zone, after which values decrease further to −2‰ in the *Aulacoteuthis* Zone. The *O. brunsvicensis* and the *O. germanica* zones show $\delta^{18}O$ values from −1.3‰ to −0.1‰, which indicate a cooling trend after the *Aulacoteuthis* Zone. A short-term warming period can be observed at the beginning of the *O. depressa* Zone. The $\delta^{18}O$ findings are more negative, −1.3‰, but steadily increase up-section to +0.2‰.

4.2 Calcareous Nannofossils of the A39 section

Seventeen nannofossil events including first occurrences (FOs), last occurrences (LOs), re-entries, influxes and acmes were observed throughout the Lower Barremian to Lower Aptian interval of the A39 section (Figs. 5, 6 and 8). These allowed the recognition of eight Boreal nannofossil zones (BC12–BC19), the detailed bed numbers are given by Mutterlose et al. (2009). Most of the nannofossil zones can be recognized throughout the region and allow correlation throughout the North Sea. There is a general shift from dominant endemic assemblages in the Barremian towards cosmopolitan ones in the Aptian, as reported by Bischoff and Mutterlose (1998). In the Boreal Realm, Tethyan marker-species (e.g., *Litraphidites bollii*, *Calcicalathina oblongata*, *Hayesites irregularis*, *Nannoconus steinmannii*) are often rare, absent, or have different age-ranges, based on the sequence of first occurrences. Nannofossil schemes for the Boreal region have been proposed by Jakubowski (1987), Mutterlose (1992), Bischoff and Mutterlose (1998), Bown et al. (1998), Ainsworth et al. (2000), and Jeremiah (2001). The Barremian/Aptian boundary interval in northwest Europe can be divided into three zones: *Chiastozygus litterarius*, *Flabellites oblongus* and *Eprolithus apertior/Eprolithus floralis* zones. The calcareous nannofossil assemblages show generally good to moderate preservation. Excellent preservation was observed in the Fischschiefer.

The FOs of *Chiastozygus litterarius* (Fig. 6; 6, 7) and *Flabellites oblongus* (Fig. 6; 13, 14) define the base of the *C. litterarius* Zone. In the A39 section this zone extends from sample 165/4 to 169/1 (dark mudstones, highest *O. depressa* Zone), having a thickness of about 7 m. The *C. litterarius* Zone spans the latest Barremian to earliest Aptian interval and corresponds to the lower part of the *Lithraphidites moray-firthensis* Zone of Jakubowski (1987). The LO of *Nannoconus abundans* (sample 165/8) approximates the Barremian/Aptian boundary (Jakubowski 1987; Mutterlose 1991, 1992; Bown et al. 1998). Within the *C. litterarius* Zone, acmes were recognized for *Biscutum constans* (5–10%) (Fig. 6; 1, 2), *Discorhabdus ignotus* (2–7%) (Fig. 6; 4), *Rhagodiscus* spp. (9–12%), *Watznaueria* spp. (39–55%) (Fig. 6; 20–22) and *Zeugrhabdotus* spp. (5–16%) (Fig. 6; 10–12). The LO of *N. abundans*, a species endemic to the southern part of the northwest European sea, occurs within the *C. litterarius* Zone (sample 165/8).

The following 4 m thick *F. oblongus* Zone spans the interval between the FO of *F. oblongus* and the FO of *Eprolithus apertior* or *Eprolithus floralis* (Fig. 6; 23, 24) (sample 169/3–176/3). This zone corresponds to the upper part of the *L. moray-firthensis* Zone of Jakubowski (1987). The FO of *F. oblongus* coincides with the FO of *H. irregularis* (sample 169/3) which, however, is very rare in the studied samples. The FOs of *R. angustus* (Fig. 6; 16, 17) and *Braarudosphaera hockwoldensis* (sample 172/1) coincide with the onset of the Fischschiefer. The FO of *Braarudosphaera africana* is located in the Fischschiefer facies (sample 173/2). The upper part of the Fischschiefer exhibits a slight increase in the abundance and size of rare *Rucinolithus terebrodentarius* (see Tremolada and Erba 2002; Herrle and Mutterlose 2003), whereas *Assipetra infracretacea* shows no significant variation. Assemblage characteristics are acmes of *B. constans* (12–21%), *Cyclagelosphaera margerelii* (1–4%) (Fig. 6; 19), *D. ignotus* (2–13%), *Rhagodiscus* spp. (4–10%), *Watznaueria* spp. (16–50%) and *Zeugrhabdotus* spp. (11–26%). The *F. oblongus* Zone includes the Fischschiefer horizon in the A39 section.

The interval between the FO of *E. apertior* or *E. floralis* and the LO of *Micrantholithus hochschulzii* defines the *E. apertior/E. floralis* Zone, which corresponds to the uppermost part of the *L. moray-firthensis* Zone and the lower part of the *Rhagodiscus asper* Zone of Jakubowski (1987). The definition of the upper boundary of the *E. apertior/E. floralis* Zone in this study is arbitrary, because *M. hochschulzii* is rare

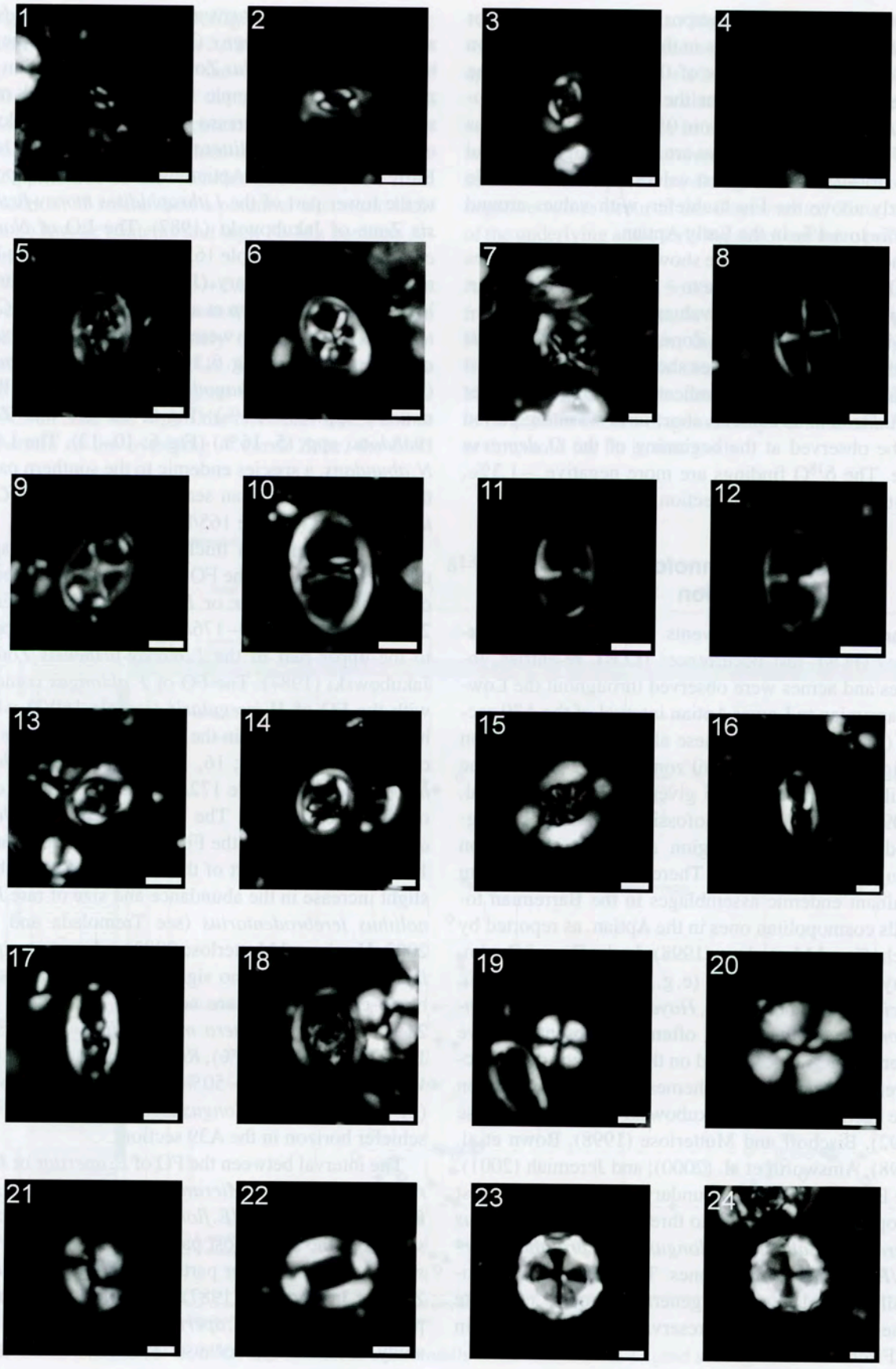
1
2
3
4
5
6
7
8
9
10
11
12
13
14
15
16
17
18
19
20
21
22
23
24

throughout the section. *E.apertior* and *E.floralis* are dissolution resistant species which are ideal for a biostratigraphical zonation. Based on the FO of *Eprolithus* directly above the Fischschiefer in bed 176/1, the marlstones and pale mudstones (beds 176–184) have been assigned a mid Early Aptian age. The calcareous nannofossil assemblages show higher diversities than the Barremian ones and yield well preserved nannofossils. The following acmes occur within this zone: *B.constans* (17–32%), *Crucibiscutum hayi* (1–7%), *D.ignotus* (3–11%), *Repagulum parvidentatum* (1–6%), *Rhagodiscus* spp. (6–12%), *Zeugrhabdotus* spp. (9–23%), and *Watznaueria* spp. (13–37%).

4.3 Ammonites

The first occurrence of the ammonite genus *Deshayesites*, which includes here the genus *Prodeshayesites* sensu Casey (1960), is an ideal bio-horizon for defining the base of the Aptian. Internationally the Barremian/Aptian boundary is therefore defined by the FO of the ammonite genus *Deshayesites* which evolved from the Barremian *Colchidites-Turkmeniceras* group, probably in Turkmenistan. The Tethyan standard zonation of the Early Aptian is based on three ammonite zones, the *Deshayesites oglanlensis*, the *Deshayesites weissi* and the *Deshayesites deshayesi* zones, in ascending order (see Reboulet et al. 2006). The Boreal Realm supplied Early Aptian zonation schemes for southern England (Casey 1961a, b) and northwest Germany (Kemper 1967, 1971, 1995) which differ from the Tethyan schemes. In southern England the lowermost Aptian is represented by non-marine Wealden sediments and hence the earliest *Deshayesites* are not covered by the monographic study of Casey (1960, 1961a, b) of the marine (Lower Greensand) sediments. The northwest German sections supplied specimens of *Deshayesites bodei* from the lowermost Aptian, followed by *Deshayesites tenuicostatus* (Fig. 7; B, C, D) and *Deshayesites deshayesi*.

Bed 170 of the A39 section yielded a rich ammonite assemblage consisting of *D.tenuicostatus*, *Deshayesites lestrangei* (Fig. 7; A), *Aconeceras nisoides* and *Ancyloceras urbani* (Fig. 7; E, F). Following Kemper (1967, 1995), the species *Deshayesites fissicostatus*, described in detail by Casey (1963), is here seen as a junior synonym of *D.tenuicostatus*, erected by Koenen (1902). *D.tenuicostatus*, in contrast to *D.deshayesi*, is an evolute form with a dense ribbing pattern assigning the material from bed 170 to the early stock of *Deshayesites*. Following the Boreal zonation scheme, the Fischschiefer is included in the *D.tenuicostatus* Zone. This age assignment is confirmed by findings from the Timmern clay pit about 15 km southeast of the A39 section. This pit, which exposed the Fischschiefer, yielded a rich *D.tenuicostatus* ammonite fauna (Kemper 1971).

4.4 Belemnites

The Barremian/Aptian boundary interval is marked by a distinctive turnover of belemnite faunas. *Oxyteuthis*, which is endemic to the Boreal Barremian, is the last genus of the suborder Belemnitina. It becomes extinct near the Barremian-Aptian boundary. Stolley (1925) mentions rare *Oxyteuthis senilis* from the lowermost Aptian but no oxyteuthid belemnites were found in any our bed-by-bed collecting from the Lower Aptian. The Early Aptian belemnites can be attributed to the genus *Neohibolites* (suborder Belemnopseina) which forms the stock group for the Aptian – Maastrichtian belemnites. The Aptian *Neohibolites* form an evolutionary lineage consisting of *Neohibolites ewaldi-Neohibolites clava-Neohibolites inflexus*. *N.ewaldi* is typical of the Early Aptian; in the A39 section its FO has been observed below the Fischschiefer. The grad-

Fig. 6. Calcareous nannofossil micrographs (XPL, cross-polarised light; scale-bar represents 2 μm). 1, 2, *Biscutum constans* (Górka 1957) Black in Black and Barnes 1959, Samples 176/3 and 176/5. 3, *Crucibiscutum hayi* (Black 1973) Jakubowski 1986, Sample 180/1. 4, *Discorhabdus ignotus* (Górka 1957) Perch-Nielsen 1968, Sample 172/1. 5, *Bukrilithus ambiguus* Black 1971a, Sample 176/5. 6, 7, *Chiastozygus litterarius* (Górka 1957) Manivit 1971, Samples 171/1 and 176/3. 8, *Staurolitithes crux* (Deflandre and Fert 1954) Caratini 1963, Sample 176/5. 9, *Tegumentum octiformis* (Köthe 1981) Crux 1981, Sample 174/1. 10, *Zeugrhabdotus diplogrammus* (Deflandre in Deflandre and Fert 1954) Burnett in Gale et al. 1996, Sample 176/5. 11, 12, *Zeugrhabdotus erectus* (Deflandre in Deflandre and Fert 1954) Reinhardt 1956, Samples 176/5 and 174/4. 13, 14, *Flabellites oblongus* (Bukry 1969) Crux in Crux et al. 1982, Samples 174/4 and 171/2. 15, *Retecapsa angustiforata* Black 1971a, Sample 172/1. 16, 17, *Rhagodiscus angustus* (Stradner 1963) Reinhardt 1971, Samples 176/3 and 176/5. 18, *Rhagodiscus asper* (Stradner 1963) Reinhardt 1967, Sample 176/3. 19, *Cyclagelosphaera margerelii* Noël 1965, Sample 172/1. 20, *Watznaueria barnesiae* (Black 1959) Perch-Nielsen 1968, Sample 176/3. 21, *Watznaueria fossacincta* (Black 1971) Bown in Bown and Cooper 1989, Sample 172/1. 22, *Watznaueria ovata* Bukry 1969, 176/5. 23, 24, *Eprolithus floralis* (Stradner 1962) Stover 1966, Samples 176/5 and 176/7.

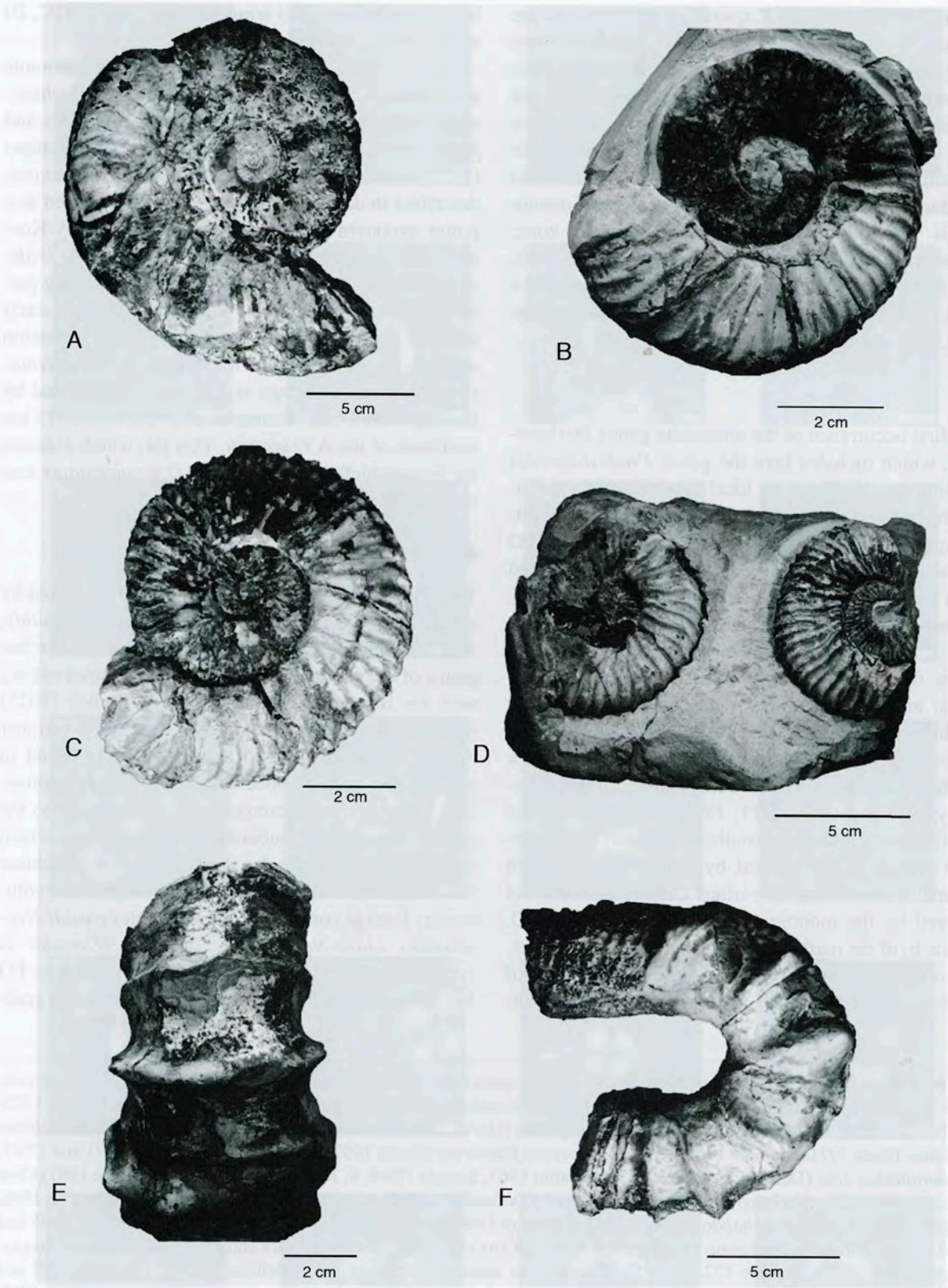

Fig. 7. Ammonites from section A39; *Neohibolites ewaldi* belemnite Zone (Lower Aptian). All ammonites from bed 170. A: *Deshayesites lestrangei* Casey 1963. B, C, D: *Deshayesites tenuicostatus* (Koenen 1902). E (extern), F (lateral): *Ancyloceras urbani* (Neumayr and Uhlig 1881).

ual change from *N. ewaldi* to the rather club-shaped *N. clava* marks the beds which contain the ammonite genus *Tropaeum*, approximating the Lower/Upper Aptian boundary interval.

5. Discussion

Various species of *Deshayesites* are the basis for standard zonation scheme of the early Aptian successions both in the Tethys (France: Moullade et al. 1998a, b; Renard et al. 2005; Iran: Raisossadat 2004; Spain: Moreno-Bedmar et al. 2009) and in the Boreal Realm (southern England: Casey 1961a, b, 1963; northwest Germany: Kemper 1967, 1971, 1995). This includes the interval of the Oceanic Anoxic Event 1a, which is located somewhere above the Barremian/Aptian boundary and below the $\delta^{13}C$ positive excursion. Unfortunately, the genus *Deshayesites* is, however, unknown from the shallow-water successions of the northern Tethys (Switzerland: Menegatti et al. 1998) and the pelagic successions of northern Italy (Erba 1996, Erba et al. 1999), which serve as the reference records for the OAE 1a and the associated $\delta^{13}C$ excursion (Gradstein et al. 2004). In these sections the OAE 1a and the $\delta^{13}C$ excursion were therefore dated using calcareous nannofossils and planktonic foraminifera, correlating the OAE 1a with the upper part of the *C. litterarius*-NC 6 nannofossil Zone and the lower part of the *Leupoldina cabri* planktonic foraminiferal Zone.

In correlating the OAE 1a and the $\delta^{13}C$ excursion throughout the Tethyan Realm, and with successions of the Boreal Realm, several problems arose for various reasons: I) *Deshayesites* is absent in the pelagic black shale sections of the Tethys, II) the ammonites in the French sections are poorly preserved and therefore have perhaps been misinterpreted (see discussion by Moreno-Bedmar et al. 2009), III) another problem is the fact that the succession of the deshayesitids in the earliest Aptian of the Boreal Realm differs from the Tethys succession at the species level. The most recent standard biozonation scheme suggested for the Tethys (Reboulet et al. 2006; Moreno-Bedmar et al. 2009) recognizes three ammonite zones based on *Deshayesites*, of which the lower *D. oglanlensis* and *D. weissi* zones equate with the *D. bodei* and *Deshayesites tenuicostatus* zones of the Boreal succession. Moreno-Bedmar et al. (2009) gave the most recent overview and assigned the OAE 1a in the Spanish sections to the *D. weissi* Zone, while the $\delta^{13}C$ positive excursion was attributed to the lower part of the overlying *D. deshayesi* Zone. This age assignment of the OAE 1a in the Tethys differs from earlier proposals by Moullade et al. (1998a, b) and Renard et al. (2005), who suggested a *D. deshayesi* age for the OAE 1a.

The ammonite findings from the A39 section support the age assignment and stratigraphic re-interpretations by Moreno-Bedmar et al. (2009). The beds directly below the Fischschiefer horizon (= OAE 1a) yielded a rich ammonite association consisting of *D. tenuicostatus* and *D. lestrangei*. This fauna and the Fischschiefer can thus be assigned to the *D. tenuicostatus* Zone of the Boreal zonal scheme, and the succeeding $\delta^{13}C$ excursion to the *D. tenuicostatus* Zone or, more probably, to the younger *D. deshayesi* Zone (Fig. 8).

The sequence of calcareous nannofossil events (LOs, FOs, acmes) observed in the A39 section allows a detailed zonation of the Barremian/Aptian boundary interval, including the Fischschiefer and the positive $\delta^{13}C$ excursion. The FO of *C. litterarius* predates the Barremian/Aptian boundary, while the LO of *N. abundans*, a taxon endemic to the northwest European sea, approximates the boundary. The FOs of *F. oblongus* and *H. irregularis* directly below, and the FOs of *E. apertior* and *E. floralis* directly above the Fischschiefer give an accurate biostratigraphic assignment of this anoxic event in the Boreal Realm. *R. angustus*, another important index species, has its FO in the Fischschiefer. In Italy, the OAE 1a (= Selli Level) is sandwiched by the FO of *H. irregularis* below and the FO of *E. floralis* above this black shale horizon (Erba 1994; Erba 2004). Bischoff and Mutterlose (1998) and Herrle and Mutterlose (2003) observed similar calcareous nannofossil events (FOs of *E. apertior* and *E. floralis* above the OAE 1a), whereas secondary events (e.g., FOs of *B. africana* and *B. hockwoldensis* occur primary after the OAE 1a). The calcareous nannofossil events of the Boreal Realm and the Tethys are thus in good accordance and show both black shale horizons to be of the same age. The deposition of the Fischschiefer therefore correlates well with the OAE 1a event of the Tethys (Fig. 8), where black shales are widespread on the marine shelf and continental margin successions of Europe (Cismon section in Italy – pelagic conditions: Menegatti et al. 1998; Serre Chaitieu section: Heimhofer et al. 2004).

In the Tethys, the deposition of the organic-rich sediments discussed here correlates with the lower part of the *Leupoldina cabri* planktonic foraminiferal Zone (e.g., Magniez-Janin et al. 1997; Moullade et al. 1998a, b; Aguado et al. 1999; Erba et al. 1999; Bellanca et al. 2002; Ogg et al. 2004). Planktonic for-

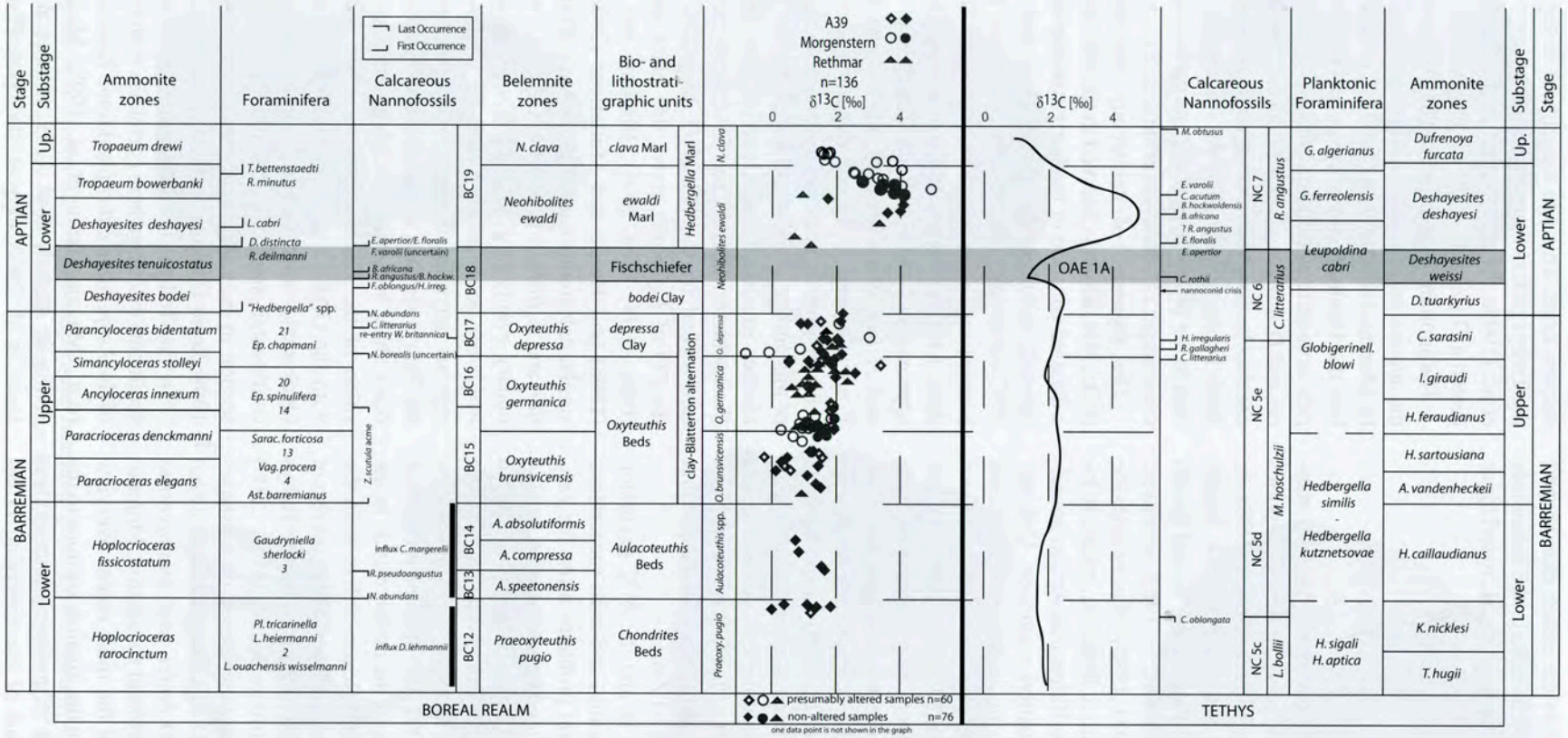

Fig. 8. Correlation of the Boreal Realm of the investigated sections and the Tethys.
Boreal Realm: Ammonite, Foraminifera, Belemnite zones and Bio- and lithostratigraphic units modified after: Mutterlose 2000a, b and Rückheim and Mutterlose 2002; Calcareous Nannofossils and Boreal $\delta^{13}C$: this study.
Tethys: $\delta^{13}C$, Planktonic Foraminifera and Ammonite zones: after Weissert et al. 2008 and Moreno-Bedmar et al. 2009. Tethyan calcareous nannofossils are modified after Bown et al. 1998, Tremolada and Erba (2002), and Herrle and Mutterlose (2003).

aminifera are, however, extremely rare in the Hauterivian and Barremian of the Boreal Realm; they only become more common from the mid Aptian onwards. The age assignment of the Boreal Fischschiefer using planktonic foraminifera is thus rather difficult and the record is probably related to sea-level induced immigration waves (Weiss 1995; Rückheim and Mutterlose 2002). Rückheim and Mutterlose (2002) identified rare specimens of *L. cabri* from well above the Fischschiefer, giving the $\delta^{13}C$ excursion a *L. cabri* Zone age. Various horizons within the Fischschiefer yield the planktonic foraminiferal genera *Clavihedbergella*, *Blowiella* and *Globigerinelloides*, indicating a first short-term Tethyan influx. According to these findings, the Fischschiefer and the basal part of the overlying *Hedbergella* Marl have to be assigned to the *Blowiella blowi* Zone.

The positive $\delta^{13}C$ excursion of +4‰ directly above the Fischschiefer has been observed in all three Boreal sections studied here, including the extremely shallow-water section of Morgenstern, where iron ores were deposited. This excursion can be correlated with segment C6 and the lower part of C7 (sensu Menegatti et al. 1998) observed in the Italian Cismon section. There, the $\delta^{13}C_{carb}$ data (bulk rock) increase up to +4‰ in limestones overlying the OAE 1a, predated by the FO of the nannofossil *E. floralis* (Weissert et al. 1998; Hochuli et al. 1999). These findings are biostratigraphically in good agreement and allow a correlation of the excursion with the *D. deshayesi* ammonite Zone (Fig. 8).

The carbon isotope excursion following the OAE 1a therefore records a synchronous shift of the carbon budget not only for the Tethys but also for the Boreal seas caused by a major perturbation of the carbon cycle. This study confirms that the positive carbon isotope shift is not only present in northern Italy (Menegatti et al. 1998; Erba et al. 1999), Switzerland (Menegatti et al. 1998; Wissler et al. 2003), France (Moullade et al. 1998a, b; Heimhofer et al. 2004), the Middle East (Vahrenkamp 1996), the central Atlantic (Herrle et al. 2004), and the Pacific (Jenkyns 1995), but also in the Boreal Realm. This implies a major change in the carbon cycle, which in turn suggests that the $\delta^{13}C$ excursion was not related to a significant temperature change but rather reflects an independent global signal related to the carbon budget of the oceans. Previous studies of the $\delta^{13}C$ values of Barremian belemnites from the Boreal Realm resulted in a rather noisy signature (Malkoč and Mutterlose 2010), which documents that the incorporation of the carbon isotopes into the belemnite skeleton was at least partly controlled by metabolic effects.

6. Conclusions

The $\delta^{13}C$ signal of the analyzed belemnite rostra shows values of 0–2‰ for the Barremian. A shift towards more positive data of 4–5‰ is to be observed in the upper part of the Early Aptian *Neohibolites ewaldi* belemnite Zone. A subsequent decrease to 2‰ is placed in the early Late Aptian *Neohibolites clava* belemnite Zone. This positive $\delta^{13}C$ excursion in the Boreal Realm is biostratigraphically well constrained by calcareous nannofossils, ammonites and belemnites. The highest positive carbon isotope values has been observed above a distinctive black shale layer, the Fischschiefer (= OAE 1a). The latter is sandwiched by the first occurrences of the calcareous nannofossil taxa *Rhagodiscus angustus*, *Braarudosphaera hockwoldensis* and *Eprolithus apertior/Eprolithus floralis*. Macropalaeontologically the Fischschiefer can be assigned to the *Deshayesites tenuicostatus* ammonite Zone, the subsequent onset of the positive excursion can be assigned to the *Deshayesites deshayesi* ammonite Zone or mid *N. ewaldi* Zone. The Boreal $\delta^{13}C$ excursion occurs both in the basin centre and the basin margin, the latter represented by an iron-ore facies deposited in extremely shallow coastal waters.

The good biostratigraphic dating of the studied sections allows the direct calibration of the $\delta^{13}C$ excursion in the Boreal Realm. In particular the ammonite age of the OAE 1a and of the associated carbon isotope anomaly is documented. This offers the opportunity to correlate Boreal and Tethyan ammonite zones using the $\delta^{13}C$ curve as a chemostratigraphic reference. All these findings from well dated successions of the Boreal Realm also shed light on the age of the Tethyan $\delta^{13}C$ excursion, which has been assigned to different Early Aptian ammonite zones over the last few years. These findings also prove that the perturbation of the carbon cycle, reflected by the $\delta^{13}C$ excursion, affected the Boreal Realm.

Acknowledgements. We are grateful to D. Buhl and B. Gehnen for support during the analysis of the stable isotopes and trace elements and U. Heimhofer for some critical comments. E. Erba, J. O. Herrle and G. D. Price improved the manuscript by useful discussions. Financial support by DFG (MU 667/28-1, 2) is acknowledged. C. J. Wood improved the English of this contribution.

7. Taxonomic Index

A full list of all taxa cited in the text, figures and tables is given below.

Ammonites:
Aconeceras Hyatt 1903
Aconeceras nisoides (Sarasin 1893)
Ancyloceras urbani (Neumayr and Uhlig 1881)
Deshayesites bodei Koenen 1902
Deshayesites deshayesi (Leymerie 1840)
Deshayesites fissicostatus (Casey 1964)
Deshayesites Kazansky 1941
Deshayesites lestrangei (Casey 1963)
Deshayesites tenuicostatus (Koenen 1902)
Prodeshayesites Casey 1960
Tropaeum Casey 1960

Belemnites:
Oxyteuthis Stolley 1911
Oxyteuthis senilis Stolley 1925
Neohibolites Stolley 1911
Neohibolites clava Stolley 1911
Neohibolites ewaldi (Strombeck 1861)
Neohibolites inflexus Stolley 1911

Calcareous nannofossils:
Assipetra Roth 1973
Assipetra infracretacea (Thierstein 1973) Roth 1973
Biscutum Black in Black and Barnes 1959
Biscutum constans (Górka 1957) Black in Black and Barnes 1959
Braarudosphaera Deflandre 1947a
Braarudosphaera africana Stradner 1961
Braarudosphaera hockwoldensis Black 1992
Bukrylithus Black 1971a
Bukrylithus ambiguus Black 1971a
Calcicalathina Thierstein 1971
Calcicalathina oblongata (Worsley 1971) Thierstein 1971
Chiastozygus Gartner 1968
Chiastozygus litterarius (Górka 1957) Manivit 1971
Crucibiscutum Jakuboski 1986
Crucibiscutum hayi (Black 1973) Jakubowski 1986
Cyclagelosphaera Noël 1965
Cyclagelosphaera margerelii Noël 1965
Discorhabdus Noël 1965
Discorhabdus ignotus (Górka 1957) Perch-Nielsen 1968
Eprolithus Stover 1966
Eprolithus apertior Black 1973
Eprolithus floralis (Stradner 1962) Stover 1966
Flabellites Thierstein 1973
Flabellites oblongus (Bukry 1969) Crux in Crux et al. 1982
Hayesites Manivit 1971
Hayesites irregularis (Thierstein in Roth and Thierstein 1972) Applegate et al. in Covington and Wise 1987
Litraphidites Deflandre 1963
Litraphidites bollii (Thierstein 1971) Thierstein 1973
Nannoconus Kamptner 1931
Nannoconus abundans Stradner and Grün 1963
Nannoconus steinmannii Kamptner 1931
Repagulum Forchheimer 1972
Repagulum parvidentatum (Deflandre and Fert 1954) Forchheimer 1972
Retecapsa Black 1971a
Retecapsa angustiforata Black 1971
Rhagodiscus Reinhardt 1967
Rhagodiscus angustus (Stradner 1963) Reinhardt 1971
Rhagodiscus asper (Stradner 1963) Reinhardt 1967
Rhagodiscus pseudoangustus Crux 1987
Rucinolithus Stover 1966
Rucinolithus terebrodentarius Applegate, Brawlower, Covington and Wise 1987
Staurolithites Caratini 1963
Staurolithites crux (Deflandre and Fert 1954) Caratini 1963
Tegumentum Thierstein in Roth and Thierstein 1972
Tegumentum octiformis (Köthe 1981) Crux 1989
Watznaueria Reinhardt 1964
Watznaueria barnesiae (Black 1959) Perch-Nielsen 1968
Watznaueria britannica (Stradner 1963) Reinhardt 1964
Watznaueria fossacincta (Black 1971) Bown in Bown and Cooper 1989
Watznaueria ovata Bukry 1969
Zeugrhabdotus Reinhardt 1965
Zeugrhabdotus diplogrammus (Deflandre in Deflandre and Fert 1954) Burnett in Gale et al. 1996
Zeugrhabdotus erectus (Deflandre in Deflandre and Fert 1954) Reinhardt 1965

References

Abreu, V.S., Hardenbol, J., Haddad, G.A., Baum, G.R., Droxler, A.W., Vail, P.R., 1998. Oxygen isotope synthesis: A Cretaceous Ice-House? SEPM Special Publication **54**, 75–80.

Aguado, R., Castro, J.M., Company, M., Gea, G.A. de, 1999. Aptian bio-events and integrated biostratigraphic analysis of the Almadich Formation, Inner Prebetic Domain, SE Spain. Cretaceous Research **20**, 663–683.

Ainsworth, N.R., Riley, L.A., Gallagher, L.T., 2000. An Early Cretaceous lithostratigraphic and biostratigraphic framework for the Britannia Field reservoir (Late Barremian-Late Aptian), UK North Sea. Petroleum Geoscience **6**, 345–367.

Ando, A., Kaiho, K., Kawahata, H., Kakegawa, T., 2008. Timing and magnitude of early Aptian extreme warming: Unraveling primary δ18O variation in indurated carbonates at Deep Sea Drilling Project Site 463, central Pacific Ocean. Palaeogeography, Palaeoclimatology, Palaeoecology **260**, 463–476.

Arthur, M.A., Dean, W.E., Schlanger, S.O., 1985. Variations in global carbon cycling during the Cretaceous related to climate, volcanism and change of atmospheric CO_2. Geophysical Monograph **32**, 504–529.

Bellanca, A., Erba, E., Neri, R., Premoli-Silva, I., Sprovieri, M., Tremolada, F., Verga, D., 2002. Palaeoceanographic significance of the Tethyan Livello Selli (early Aptian) from the Hybla Formation, northwestern Sicily: biostratigraphy and high-resolution chemostratigraphic records. Palaeogeography, Palaeoclimatology, Palaeoecology **185**, 175–196.

Bischoff, G., Mutterlose, J., 1998. Calcareous nannofossils of the Barremian/Aptian boundary interval in NW Europe: biostratigraphic and palaeoecologic implications of a high resolution study. Cretaceous Research **19**, 635–661.

Bown, P.R., 1998. Calcareous nannofossil biostratigraphy, 314pp. (Chapman & Hall, London).

Bown, P.R., Rutledge, D.C., Crux, J.A., Gallagher, L.T., 1998. Lower Cretaceous. In: Bown, P.R. (Ed.), Calcareous Nannofossil Biostratigraphy. Chapman and Hall, London, p.86–102.

Bralower, T.J., CoBabe, E., Clement, B., Sliter, W.V., Osburn, C.L., Longoria, J., 1999. The record of global change in Mid-Cretaceous (Barremian-Albian) sections from the Sierra Madre, northeastern Mexico. *The Journal of Foraminiferal Research* **29**, 418–437.

Brand, U., Veizer, J., 1980. Chemical diagenesis of a multicomponent carbonate system-1: Trace elements. Journal of Sedimentary Petrology **50**, 1219–1236.

Casey, R., 1960. A Monograph of the Ammonoidea of the Lower Greensand. Pt.I. Palaeontographical Society, Jg. 1959, S.I–XXXXVI, p.1–44.

Casey, R., 1961a. The stratigraphical Palaeontology of the Lower Greensand. Palaeontology **3**, 487–621, London.

Casey, R., 1961b. A monograph of the Ammonoidea of the Lower Greensand, part III. Palaeontographical Society, London, p.119–216.

Casey, R., 1963. A monograph of the Ammonoidea of the Lower Greensand, part V. Palaeontographical Society Monographs **117**, 289–398.

Erba, E., 1994. Nannofossils and superplumes: the early Aptian "nannoconid crisis". Paleoceanography **9**, 483–501.

Erba, E., 1996. The Aptian stage. Bulletin de l'Institut Royal des Sciences Naturelles de Belgique **66** supplement, p.31–43.

Erba, E., Chanell, J.E.T., Claps, M., Jones, C., Larson, R., Opdyke, B., Premoli Silva, I., Riva, A., Salvini, G., Torricelli, S., 1999. Integrated stratigraphy of the Cismon Apticore (southern Alps, Italy). A "reference section" for the Barremian-Aptian interval at low latitudes. Journal of Foraminiferal Research **29**, 371–391.

Erba, E., 2004. Calcareous nannofossils and Mesozoic oceanic anoxic events. Marine Micropaleontology **52**, 85–106.

Geisen, M., Bollmann, J., Herrle, J., Mutterlose, J., Young, J., 1999. Calibration of the random settling technique for calculation of absolute abundances of calcareous nannoplankton. Micropaleontology **45**, 437–442.

Gradstein, F.M., Ogg, J.G., Smith, A.G., 2004. Geologic Time Scale 2004. Cambridge University Press, 640 pp.

Haq, B.U., Hardenbol, J., Vail, P.R., 1987. Chronology of fluctuating sea levels since the Triassic. Science **235**, 1156–1167.

Harland, W.B., Armstrong, R.L., Cox, A.V., Craig, L.E., Smith, A.G., Smith, D.G., 1990. A Geologic Time Scale 1989 (Cambridge University Press, Cambridge), 236 pp.

Heimhofer, U., Hochuli, P.A., Herrle, J.O., Andersen, N., Weissert, H., 2004. Absence of major vegetation and palaeoatmospheric pCO_2 changes associated with oceanic anoxic event 1a (Early Aptian, SE France). Earth and Planetary Science Letters **223**, 303–318.

Herrle, J.O., Mutterlose, J., 2003: Calcareous nannofossils from the Aptian – Lower Albian of southeast France: palaeoecological and biostratigraphic implications. Cretaceous Research **24**, 1–22.

Herrle, J.O., Kössler, P., Friedrich, O., Erlenkeuser, H., Hemleben, C., 2004. High resolution carbon isotope records of the Aptian to lower Albian from SE France and the Mazagan Plateau (DSDP Site 545). A stratigraphic tool for paleoceanographic and paleobiologic reconstruction. Earth and Planetary Science Letters **218**, 149–161.

Hochuli, P.A., Menegatti, A.P., Weissert, H., Riva, A., Erba, E., Premoli Silva, I., 1999. Episodes of high productivity and cooling in the early Aptian Alpine Tethys. Geology **27**, 657–660.

Jakubowski, M., 1987. A proposed Lower Cretaceous calcareous nannofossil zonation scheme for the Moray Firth area of the North Sea. Abhandlungen der Geologischen Bundesanstalt (Wien) **39**, 99–119.

Jenkyns, H.C., 1995. Carbon-isotope stratigraphy and palaeoceanographic significance of the lower Cretaceous shallow water carbonates of Resolution Guyot, Mid-Pacific mountains. Proceedings of the Ocean Drilling Program, Scientific Results **143**, 99–104.

Jeremiah, J., 2001. A Lower Cretaceous nannofossil zonation for the North Sea Basin. Journal of Micropalaeontology **20**, 45–80.

Kemper, E., 1967. Die älteste Ammoniten-Fauna im Aptium Nordwest-Deutschlands. Paläontologische Zeitschrift **41**, 119–131.

Kemper, E., 1971. Zur Gliederung und Abgrenzung des norddeutschen Aptium mit Ammoniten. Geologisches Jahrbuch **89**, 359–390.

Kemper, E., 1979. Die Unterkreide Nordwestdeutschlands. Ein Überblick. In: Wiedmann, J. (Ed.), Aspekte der Kreide Europas, IUGS Series **A 6**: Schweizerbart, Stuttgart, p. 1–9.

Kemper, E., 1995. Die Entfaltung der Ammoniten und die Meeresverbindungen im borealen Unter- und Mittel-Apt. Geologisches Jahrbuch A **141**, 171–199.

Koenen, A. v., 1902. Die Ammonitiden des norddeutschen Neocom. Abhandlungen der Preussischen Geologischen Landesanstalt, Neue Folge **24**, 451 pp.

Larson, R.L., 1991a. Latest pulse of earth: evidence for a mid-cretaceous superplume. Geology **19**, 547–550.

Larson, R.L., 1991b. Geological consequences of superplumes. Geology **19**, 963–966.

Larson, R.L., Erba, E., 1999. Onset of the mid-Cretaceous greenhouse in the Barremian-Aptian: Igneous events and the biological, sedimentary, and geochemical responses. Paleoceanography **14**, 663–678.

Lowenstam, H.A., Epstein, S., 1954. Palaeotemperatures of the post-Albian Cretaceous as determined by the oxygen isotope method. Journal of Geology **62**, 207–248.

Malkoč, M., Mutterlose, J., 2010. The early Barremian warm pulse and the late Barremian cooling: a high-resolution geochemical record of the Boreal Realm. Palaios **25**, 13–22.

Magniez-Janin, F., Bréhéret, J.G., Delanoy, G., 1997. Un example de spéciation lié à l'eustatisme: l'apparition précoce de *Schakoina cabri* (foraminifere planctonique mésogéen). Comptes Rendus de l'Académie des Sciences de Paris, Sciences de la Terre et des Planètes **325**, 225–230.

Marshall, J.D., 1992.Climatic and oceanographic isotopic signals from the carbonate rock record and their preservation. Geological Magazine **129**, 143–160.

Méhay, S., Keller, C.E., Bernasconi, S.M., Weissert, H., Erba, E., Bottini, C., Hochuli, P.A., 2009. A volcanic CO_2 pulse triggered the Cretaceous Oceanic Anoxic Event 1a and a biocalcification crisis. Geological Society of America **37**, 819–822.

Menegatti, A.P., Weissert, H., Brown, R.S., Tyson, R.V., Farrimond, P., Strasser, A., Caron, M., 1998. High-resolution $\delta^{13}C$ stratigraphy through the early Aptian "Livello Selli" of the Alpine Tethys. Paleoceanography **13**, 530–545.

Michael, E., 1974. Zur Palökologie und Faunenführung des norddeutschen Unterkreide-Meeres. Geologisches Jahrbuch **A 19**, 1–68.

Michael, E., 1979. Mediterrane Fauneneinflüsse in den borealen Unterkreide-Becken Europas, besonders Nordwestdeutschlands. In: Wiedmann, J. (Ed.), Aspekte der Kreide Europas, IUGS Series A **vol.6**, Schweizerbart, Stuttgart, p. 305–321.

Moreno-Bedmar, J.A., Company, M., Bover-Arnal, T., Salas, R., Delanoy, G., Martínez, R., Grauges, A., 2009. Biostratigraphic characterization by means of ammonoids of the lower Aptian Oceanic Anoxic Event (OAE 1a) in the eastern Iberian Chain (Maestrat Basin, eastern Spain). Cretaceous Research **30**, 864–872.

Moullade, M., Kuhnt, W., Bergen, J.A., Masse, J.P., Tronchetti, G., 1998a. Correlation of biostratigraphic and stable isotope events in the Aptian historical stratotype of La Bédoule (southeast France). Comptes Rendus de l'Académie des Sciences. Série 2. Sciences de la Terre et des Planètes **327**, 693–698.

Moullade, M., Masse, J.P., Tronchetti, G., Kuhnt, W., Ropolo, P., Bergen, J.A., Masure, E., Renard, M., 1998b. Le stratotype historique de l'Aptien inférieur (région de cassis-La Bédoule, SE France): synthése stratigraphique. Géologie Méditerranéene **25**, 289–298.

Mutterlose, J., 1991. Das Verteilungs- und Migrationsmuster des kalkigen Nannoplanktons in der borealen Unterkreide (Valangin – Apt). Palaeontographica B **221**, 27–152.

Mutterlose, J., 1992. Migration and evolution patterns of floras and faunas in marine early Cretaceous sediments of NW Europe. Palaeogeography, Palaeoclimatology, Palaeoecology **94**, 261–282.

Mutterlose, J., Wiedenroth, K., 1995. Die Bio- und Lithofazies der Unterkreide (Hauterive bis Apt) in NW-Deutschland. Berliner Geowissenschaftliche Abhandlungen **16**, 227–253.

Mutterlose, J., Böckel, B., 1998. The Barremian-Aptian interval in NW Germany: a review. Cretaceous Research **19**, 539–568.

Mutterlose, J., Bornemann, A., 2000. Distribution and facies patterns of Lower Cretaceous sediments in northern Germany – a review. Cretaceous Research **21**, 733–759.

Mutterlose, J., 2000a. Barreme. In: Stratigraphische Kommission Deutschlands, 2000. Stratigraphie von Deutschland III. Die Kreide der Bundesrepublik Deutschland. Courier Forschungsinstitut Senckenberg **226**, 16–18.

Mutterlose, J., 2000b. Apt. In: Stratigraphische Kommission Deutschlands, 2000. Stratigraphie von Deutschland III. Die Kreide der Bundesrepublik Deutschland. Courier Forschungsinstitut Senckenberg **226**, 18–21.

Mutterlose, J., Pauly, S., Steuber, T., 2009. Temperature controlled deposition of early Cretaceous (Barremian-early Aptian) black shales in an epicontinental sea. Palaeogeography, Palaeoclimatology, Palaeoecology **273**, 330–345.

Neuss, P., 1979. Zur Biostratigraphie und Fazies der Unterkreide-Serien (Hauterivium-Aptium) im Eisenerz-Tagebau "Morgenstern" N Goslar (SE-Niedersachsen). Mitteilungen aus dem Geologischen Institut der Universität Hannover Heft **17**, 155–222.

Ogg, J.G., Agterberg, F.P., Gradstein, F.M., 2004. The Cretaceous period. In: Gradstein, F.M., Ogg, J.G., and Smith, A.G. (Eds.), A geologic time scale 2004. Cambridge University Press, Cambridge, p. 344–383.

Ogg, J.G., Ogg, G., Gradstein, F.M., 2008. The concise geologic time scale. Cambridge University Press, 184 pp.

Perch-Nielsen, K., 1985. Mesozoic calcareous nannofossils. In: Plankton stratigraphy (eds Bolli, H.M., Saunders, J.B. and Perch-Nielsen, K.), p.329–426 (Cambridge University Press, Cambridge).

Price, G.D., Ruffell, A.H., Jones, C.E., Kalin, R.M., Mutterlose, J., 2000. Isotopic evidence for temperature variation during the early Cretaceous (late Ryazanian-mid-Hauterivian). Journal of the Geological Society (London) **157**, 335–343.

Price, G.D., 2003. New constraints upon isotope variation during the early Cretaceous (Barremian-Cenomanian) from the Pacific Ocean. *Geological Magazine* **140**, 513–522.

Raisossadat, S.N., 2004. The ammonite family Deshayesitidae in the Kopet Dagh Basin, north-east Iran. Cretaceous Research **25**, 115–136.

Rawson, P.F., Riley, L.A., 1982. Latest Jurassic-early Cretaceous events and the "late Cimmerian unconformity" in North Sea area. American Association of Petroleum Geologists Bulletin **66**, 2628–2648.

Reboulet, S., Hoedemaker, P.J., Aguirre-Urreta, M.B., Alsen, P., Attrops, F., Baraboshkin, E.Y., Company, M., Delanoy, G., Dutour, Y., Klein, J., Latil, J.L., Lukeneder, A., Mitta, V., Mourgues, F.A., Ploch, I., Raisossadat, N., Ropolo, P., Sandoval, J., Tavera, J.M., Vašiček, Z., Vermeulen, J., 2006. Report on the 2nd International meeting of the IUGS Lower Cretaceous Ammonite Working Group, the "Kilian Group" (Neuchatel, Switzerland, 8 September 2005). Cretaceous Research **27**, 712–715.

Renard, M., Rafélis, M.de, Emmanuel, L., Moullade, M., Masse, J.P., Kuhnt, W., Bergen, J.A., Tronchetti, G., 2005. Early Aptian $\delta^{13}C$ and manganese anomalies from the historical Cassis-La Bédoule stratotype sections (S.E. France): relationship with a methane hydrate dissociation event and stratigraphic implications. Carnets de Géologie/Notebooks on Geology Article **4**, 1–18.

Rosales, I., Robles, S., Quesada, S., 2004. Elemental and oxygen isotope composition of early Jurassic belemnites: salinity vs. temperature signals. Journal of Sedimentary Research **74**, 342–354.

Rückheim, S., Mutterlose, J., 2002. The Early Aptian radiation of planktonic foraminifera in NW Europe: the onset of the Mid-Cretaceous plankton revolution in the Boreal Realm. Cretaceous Research **23**, 49–64.

Ruffell, A., 1991. Sea-level events during the early Cretaceous in western Europe. Cretaceous Research **12**, 527–551.

Schott, W., Jaritz, W., Kockel, F., Sames, C.W., Stackelberg, V., Stets, J., Stoppel, D., Baldschuhn, R., Krampke, K.D., 1967/69. Paläogeographischer Atlas der Unterkreide von Nordwestdeutschland mit einer Übersichtsdarstellung des nördlichen Mitteleuropa. 306Kt., (Hannover). Hierzu Erläuterungen zum Paläogeographischen Atlas der Unterkreide von NW-Deutschland. 315 pp., Hannover.

Stolley, E., 1925. Beiträge zur Kenntnis der Cephalopoden der norddeutschen Unteren Kreide. I. Die Belemniten der norddeutschen Unteren Kreide. 2. Die Oxyteuthidae des norddeutschen Neokoms. Geol. Paläont. Abh., N.F. 14, **4**, 177–212, 8 Taf.; Jena.

Tremolda, F., Erba, E., 2002. Size analyses of Aptian *Assipetra infracretacea* and *Rucinolithus terebrodentarius* nannoliths: implications for taxonomy, bistratigraphy and paleoceanography. Marine Micropaleontology **44**, 77–92.

Vahrenkamp, V.C., 1996. Carbon isotope stratigraphy of the upper Kharaib and Shuaiba Formations: implications for the early Cretaceous evolution of the Arabian Gulf region. AAPG Bulletin **80**, 647–662.

van de Schootbrugge, B., Föllmi, K.B., Bulot, L.G., Burns, S.J., 2000. Palaeoceanographic changes during the Early Cretaceous (Valanginian-Hauterivian): evidence from oxygen and carbon stable isotopes. Earth and Planetary Science Letters **181**, 5–31.

Veizer, J., 1974. Chemical diagenesis of belemnite shells and possible consequences for paleotemperature determinations. Neues Jahrbuch für Geologie und Paläontologie, Abhandlungen **147**, 31–111.

Veizer, J., 1983. Chemical diagenesis of carbonates: Theory and trace element technique, In: Arthur, M.A., Anderson, T.F., Kaplan, I.R., Veizer, J., and Land, L.S., eds., Stable Isotopes in Sedimentary Geology. Society of Economic Paleontologists and Mineralogists Short Courses, Dallas, **10**, 3–1–3–100.

Weiss, W., 1995. Aptian planktonic foraminifers from the Wiechendorf 1/86 borehole. Geologisches Jahrbuch **A 141**, 113–131.

Weissert, H., Erba, E., 2004. Volcanism, CO_2 and palaeoclimate: a Late Jurassic-Early Cretaceous carbon and oxygen isotope record. Journal of the Geological Society (London) **161**, 695–702.

Weissert, H., Lini, A., Föllmi, K.B., Kuhn, O., 1998. Correlation of Early Cretaceous carbon isotope stratigraphy and platform drowning events: a possible link? Palaeogeography, Palaeoclimatology, Palaeoecology **137**, 189–203.

Weissert, H., Joachimski, M., Sarnthein, M., 2008. Chemostratigraphy. Newsletters on Stratigraphy, **42(3)**, 145–179.

Wierzbowski, H., Joachimski, M.M., 2009. Stable isotopes, elemental distribution, and growth rings of belemnopsid belemnite rostra: proxies for belemnite life habitat. Palaios **24**, 377–386.

Williams, J.R., Bralower, T.J., 1995. Nannofossil assemblages, fine fraction stable isotopes, and the paleoceanography of the Valanginian – Barremian (Early Cretaceous) North Sea Basin. Paleoceanography **10**, 815–864.

Wilson, P.A., Norris, R.D., Cooper, M.J., 2002. Testing the Cretaceous greenhouse hypothesis using glassy foraminiferal calcite from the core of the Turonian tropics on Demerara Rise. Geological Society of America **30**, 607–610.

Wissler, L., Funk, H., Weissert, H., 2003. Response of Early Cretaceous carbonate platforms to changes in atmospheric carbon dioxide levels. Palaeogeography, Palaeoclimatology, Palaeoecology **200**, 187–205.

Manuscript received: September 5, 2009, rev. version received: December 11, 2009, accepted for print: December 14, 2009.

Appendix 1–3: Trace elements and stable isotopes ($\delta^{13}C$, $\delta^{18}O$) of the analyzed belemnites

Rethmar	Belemnite Zone	$\delta^{13}C$ [‰]	± s	$\delta^{18}O$ [‰]	± s	Mg [ppm]	Sr [ppm]	Fe [ppm]	Mn [ppm]
Lower Aptian	*Neohibolites ewaldi*	0.93	0.14	0.19	0.17	1596	860	17	57
Lower Aptian	*Neohibolites ewaldi*	3.30	0.12	0.20	0.08	1624	804	48	100
Lower Aptian	*Neohibolites ewaldi*	0.66	0.17	0.09	0.18	1991	1411	88	58
Lower Aptian	*Neohibolites ewaldi*	1.20	0.10	0.19	0.18	1757	1267	1389	18
mean	***Neohibolites ewaldi***	**1.53**	**0.13**	**0.17**	**0.15**	**1742**	**1086**	**386**	**58**
Upper Barremian	*Oxyteuthis depressa*	1.68	0.15	−0.29	0.19	1715	1131	47	24
Upper Barremian	*Oxyteuthis depressa*	2.09	0.10	−0.30	0.09	2064	1295	118	7
Upper Barremian	*Oxyteuthis depressa*	1.85	0.21	−1.03	0.15	1483	1199	56	37
Upper Barremian	*Oxyteuthis depressa*	1.55	0.11	−0.54	0.19	1079	987	57	16
Upper Barremian	*Oxyteuthis depressa*	1.66	0.22	−0.75	0.19	2019	1299	48	13
mean	***Oxyteuthis depressa***	**1.77**	**0.16**	**−0.58**	**0.16**	**1672**	**1182**	**65**	**19**
Upper Barremian	*Oxyteuthis germanica*	1.40	0.13	−0.66	0.09	1565	1227	158	22
Upper Barremian	*Oxyteuthis germanica*	1.37	0.13	−0.35	0.10	2125	1356	75	10
Upper Barremian	*Oxyteuthis germanica*	0.99	0.09	−0.45	0.18	1172	1094	14	2
Upper Barremian	*Oxyteuthis germanica*	2.27	0.10	−0.45	0.18	972	1241	9	1
Upper Barremian	*Oxyteuthis germanica*	1.92	0.17	−0.37	0.16	2332	1245	19	4
Upper Barremian	*Oxyteuthis germanica*	1.09	0.14	−0.71	0.18	1279	1213	143	32
Upper Barremian	*Oxyteuthis germanica*	2.31	0.10	−0.30	0.17	1017	1124	44	9
Upper Barremian	*Oxyteuthis germanica*	0.93	0.09	−0.67	0.13	1960	1091	227	75
Upper Barremian	*Oxyteuthis germanica*	1.34	0.18	−0.46	0.13	1210	1055	146	15
Upper Barremian	*Oxyteuthis germanica*	1.17	0.10	−0.59	0.12	2499	1289	121	33
Upper Barremian	*Oxyteuthis germanica*	0.57	0.19	−1.04	0.15	1302	1297	23	7
Upper Barremian	*Oxyteuthis germanica*	0.76	0.19	−0.37	0.12	1700	1183	103	17
Upper Barremian	*Oxyteuthis germanica*	1.11	0.13	−0.61	0.09	1855	1103	252	37
Upper Barremian	*Oxyteuthis germanica*	1.29	0.19	−0.18	0.19	2008	1339	615	48
Upper Barremian	*Oxyteuthis germanica*	0.74	0.11	−0.85	0.26	1380	1415	1432	52
mean	***Oxyteuthis germanica***	**1.28**	**0.14**	**−0.54**	**0.15**	**1625**	**1218**	**225**	**24**
total mean		**1.42**	**0.14**	**−0.43**	**0.15**	**1654**	**1189**	**219**	**29**

Morgenstern	Belemnite Zone	$\delta^{13}C$ [‰]	± s	$\delta^{18}O$ [‰]	± s	Mg [ppm]	Sr [ppm]	Fe [ppm]	Mn [ppm]
Upper Aptian	*Neohibolites clava*	1.82	0.07	−0.18	0.07	1324	931	119	15
Upper Aptian	*Neohibolites clava*	1.91	0.10	0.34	0.13	1455	809	140	59
Upper Aptian	*Neohibolites clava*	1.74	0.08	0.05	0.09	1355	892	30	22
Upper Aptian	*Neohibolites clava*	1.78	0.14	−0.24	0.15	1867	819	334	136
Upper Aptian	*Neohibolites clava*	2.14	0.10	−0.10	0.10	1413	837	50	29
Upper Aptian	*Neohibolites clava*	3.93	0.09	0.42	0.12	1236	964	83	6
Upper Aptian	*Neohibolites clava*	3.38	0.09	0.32	0.10	1426	871	113	15
mean	***Neohibolites clava***	**2.39**	**0.09**	**0.08**	**0.11**	**1440**	**875**	**124**	**40**

Appendix 1–3: continued

Morgenstern	Belemnite Zone	$\delta^{13}C$ [‰]	± s	$\delta^{18}O$ [‰]	± s	Mg [ppm]	Sr [ppm]	Fe [ppm]	Mn [ppm]
Lower Aptian	*Neohibolites ewaldi*	4.27	0.10	0.65	0.12	1188	973	95	35
Lower Aptian	*Neohibolites ewaldi*	2.73	0.17	0.09	0.11	1890	842	79	21
Lower Aptian	*Neohibolites ewaldi*	2.71	0.15	−0.32	0.16	2594	886	193	54
Lower Aptian	*Neohibolites ewaldi*	3.21	0.10	0.13	0.05	1669	946	63	16
Lower Aptian	*Neohibolites ewaldi*	2.99	0.09	−0.34	0.10	1665	1006	155	26
Lower Aptian	*Neohibolites ewaldi*	3.50	0.08	−0.11	0.11	1555	889	104	43
Lower Aptian	*Neohibolites ewaldi*	3.57	0.11	−0.12	0.11	1282	987	94	44
Lower Aptian	*Neohibolites ewaldi*	3.94	0.14	−0.23	0.16	1443	1089	113	24
Lower Aptian	*Neohibolites ewaldi*	4.21	0.20	−0.10	0.21	1654	1085	201	66
Lower Aptian	*Neohibolites ewaldi*	3.60	0.17	0.01	0.15	1414	1042	99	27
Lower Aptian	*Neohibolites ewaldi*	3.56	0.12	−0.50	0.12	1610	1288	111	28
Lower Aptian	*Neohibolites ewaldi*	3.94	0.10	−0.20	0.11	1727	1047	98	20
Lower Aptian	*Neohibolites ewaldi*	5.15	0.16	0.29	0.20	1580	1125	242	69
Lower Aptian	*Neohibolites ewaldi*	3.90	0.15	−0.11	0.15	2083	999	80	23
Lower Aptian	*Neohibolites ewaldi*	4.10	0.11	−0.21	0.14	1886	1107	149	41
mean	***Neohibolites ewaldi***	**3.69**	**0.13**	**−0.07**	**0.13**	**1683**	**1021**	**125**	**36**
Upper Barremian	*Oxyteuthis depressa*	2.11	0.12	−1.17	0.14	1951	1141	724	339
Upper Barremian	*Oxyteuthis depressa*	3.06	0.15	−0.51	0.11	1008	1060	384	72
Upper Barremian	*Oxyteuthis depressa*	0.87	0.10	−1.10	0.15	1155	1078	784	621
Upper Barremian	*Oxyteuthis depressa*	−0.10	0.13	−0.65	0.07	942	1202	277	178
Upper Barremian	*Oxyteuthis depressa*	−0.83	0.12	−1.26	0.11	1586	1031	1595	1225
mean	***Oxyteuthis depressa***	**1.02**	**0.12**	**−0.94**	**0.12**	**1328**	**1102**	**752**	**487**
Upper Barremian	*Oxyteuthis germanica*	1.87	0.11	−0.16	0.12	1314	1170	240	54
Upper Barremian	*Oxyteuthis germanica*	0.87	0.12	−0.15	0.18	2065	1159	175	50
Upper Barremian	*Oxyteuthis germanica*	1.20	0.12	−0.74	0.16	1538	1224	448	55
Upper Barremian	*Oxyteuthis germanica*	0.26	0.16	−1.15	0.11	2298	1227	263	98
Upper Barremian	*Oxyteuthis germanica*	1.85	0.08	−0.79	0.10	1109	1244	70	19
Upper Barremian	*Oxyteuthis germanica*	1.17	0.11	−0.52	0.19	1386	1266	66	45
Upper Barremian	*Oxyteuthis germanica*	0.98	0.13	−0.67	0.15	2000	1258	292	38
Upper Barremian	*Oxyteuthis germanica*	0.98	0.13	−1.03	0.16	1880	1245	105	30
Upper Barremian	*Oxyteuthis germanica*	1.23	0.11	−0.51	0.11	1079	1088	129	28
Upper Barremian	*Oxyteuthis germanica*	1.44	0.13	−0.58	0.13	2035	1168	164	92
Upper Barremian	*Oxyteuthis germanica*	1.15	0.17	−0.42	0.12	2376	1209	115	51
Upper Barremian	*Oxyteuthis germanica*	1.44	0.20	−0.59	0.09	1917	1124	243	45
Upper Barremian	*Oxyteuthis germanica*	0.93	0.12	−0.82	0.14	1542	1130	300	102
Upper Barremian	*Oxyteuthis germanica*	1.22	0.17	−0.37	0.15	977	1155	107	29
Upper Barremian	*Oxyteuthis germanica*	1.84	0.22	−0.81	0.11	1880	1192	162	64
mean	***Oxyteuthis germanica***	**1.23**	**0.14**	**−0.60**	**0.13**	**1693**	**1190**	**192**	**53**
Upper Barremian	*Oxyteuthis brunsvicensis*	0.67	0.12	−0.77	0.19	2277	1147	366	50
Upper Barremian	*Oxyteuthis brunsvicensis*	1.46	0.12	−0.81	0.09	1439	1179	117	40
Upper Barremian	*Oxyteuthis brunsvicensis*	1.73	0.18	−0.60	0.17	1412	1207	70	35
Upper Barremian	*Oxyteuthis brunsvicensis*	0.96	0.16	−1.02	0.12	1394	1293	216	53
mean	***Oxyteuthis brunsvicensis***	**1.21**	**0.15**	**−0.80**	**0.14**	**1631**	**1207**	**193**	**45**
total mean		**2.18**	**0.13**	**−0.38**	**0.13**	**1606**	**1079**	**221**	**92**

Appendix 1–3: continued

A39	Belemnite Zone	$\delta^{13}C$ [‰]	± s	$\delta^{18}O$ [‰]	± s	Mg [ppm]	Sr [ppm]	Fe [ppm]	Mn [ppm]
Lower Aptian	*Neohibolites ewaldi*	1.75	0.01	0.15	0.01	2841	1329	134	6
Lower Aptian	*Neohibolites ewaldi*	4.12	0.01	−0.35	0.01	1461	1366	74	8
Lower Aptian	*Neohibolites ewaldi*	4.02	0.01	0.31	0.02	1809	1404	180	28
Lower Aptian	*Neohibolites ewaldi*	3.61	0.01	−0,01	0.02	1832	1284	179	23
mean	***Neohibolites ewaldi***	**3.38**	**0.01**	**0.03**	**0.02**	**1986**	**1346**	**142**	**16**
Upper Barremian	*Oxyteuthis depressa*	2.20	0.01	0.21	0.01	968	1225	107	6
Upper Barremian	*Oxyteuthis depressa*	2.16	0.01	0.19	0.01	1545	1224	120	6
Upper Barremian	*Oxyteuthis depressa*	1.53	0.01	0.21	0.01	1344	1158	382	31
Upper Barremian	*Oxyteuthis depressa*	0.91	0.01	−0.11	0.02	1024	1366	119	2
Upper Barremian	*Oxyteuthis depressa*	1.12	0.03	−0.55	0.02	1652	1436	149	5
Upper Barremian	*Oxyteuthis depressa*	2.03	0.02	−0.39	0.04	913	1336	95	33
Upper Barremian	*Oxyteuthis depressa*	1.62	0.01	0.22	0.02	1279	1452	102	5
Upper Barremian	*Oxyteuthis depressa*	1.73	0.01	−0.15	0.02	1469	1546	92	1
Upper Barremian	*Oxyteuthis depressa*	2.12	0.02	0.05	0.01	1899	1358	254	2
Upper Barremian	*Oxyteuthis depressa*	1.37	0.02	0.22	0.02	1652	1411	215	3
Upper Barremian	*Oxyteuthis depressa*	1.56	0.01	−0.18	0.02	1856	1404	198	3
Upper Barremian	*Oxyteuthis depressa*	1.60	0.02	−0.07	0.02	1632	1595	149	3
Upper Barremian	*Oxyteuthis depressa*	2.20	0.01	−0.31	0.02	1807	1465	81	1
Upper Barremian	*Oxyteuthis depressa*	1.66	0.01	−1.09	0.02	2365	1824	186	19
Upper Barremian	*Oxyteuthis depressa*	1.93	0.02	−1.28	0.02	1269	1446	99	1
mean	***Oxyteuthis depressa***	**1.72**	**0.01**	**−0.20**	**0.02**	**1512**	**1416**	**156**	**8**
Upper Barremian	*Oxyteuthis germanica*	1.13	0.02	−1.10	0.02	2156	1450	108	3
Upper Barremian	*Oxyteuthis germanica*	0.54	0.02	−0.44	0.01	2712	1839	197	16
Upper Barremian	*Oxyteuthis germanica*	0.52	0.04	−0.96	0.04	2271	1491	99	1
Upper Barremian	*Oxyteuthis germanica*	1.87	0.03	−0.08	0.02	1318	1466	198	34
Upper Barremian	*Oxyteuthis germanica*	1.19	0.02	−0.09	0.04	2488	1734	83	3
Upper Barremian	*Oxyteuthis germanica*	1.50	0.01	−0.78	0.02	1490	1777	131	17
Upper Barremian	*Oxyteuthis germanica*	3.43	0.02	−0.57	0.03	1104	1457	291	48
Upper Barremian	*Oxyteuthis germanica*	2.65	0.03	−0.50	0.04	1658	1547	105	34
Upper Barremian	*Oxyteuthis germanica*	1.95	0.02	−0.08	0.02	1673	1573	119	47
Upper Barremian	*Oxyteuthis germanica*	1.09	0.02	−0.81	0.02	2109	1788	227	33
Upper Barremian	*Oxyteuthis germanica*	1.14	0.01	−0.29	0.01	1449	1725	9	2
Upper Barremian	*Oxyteuthis germanica*	1.89	0.02	−0.04	0.02	1478	1675	76	12
Upper Barremian	*Oxyteuthis germanica*	1.81	0.02	−0.10	0.01	2821	1803	237	105
Upper Barremian	*Oxyteuthis germanica*	1.98	0.02	−0.39	0.01	1389	1486	105	34
Upper Barremian	*Oxyteuthis germanica*	1.83	0.02	−0.49	0.02	1436	1647	182	107
Upper Barremian	*Oxyteuthis germanica*	1.25	0.02	−0.38	0.03	2435	2435	500	24
Upper Barremian	*Oxyteuthis germanica*	1.16	0.01	−0.46	0.02	1287	1687	56	7
Upper Barremian	*Oxyteuthis germanica*	1.69	0.04	−0.84	0.03	1802	1520	777	59
Upper Barremian	*Oxyteuthis germanica*	1.22	0.03	−1.12	0.03	1899	1427	816	65
Upper Barremian	*Oxyteuthis germanica*	1.92	0.01	−0.69	0.02	1506	1798	246	45
Upper Barremian	*Oxyteuthis germanica*	1.23	0.02	−0.58	0.03	1800	1731	392	23
mean	***Oxyteuthis germanica***	**1.57**	**0.02**	**−0.51**	**0.02**	**1823**	**1669**	**236**	**34**

Appendix 1–3: continued

A39	Belemnite Zone	$\delta^{13}C$ [‰]	± s	$\delta^{18}O$ [‰]	± s	Mg [ppm]	Sr [ppm]	Fe [ppm]	Mn [ppm]
Upper Barremian	*Oxyteuthis brunsvicensis*	1.81	0.02	−0.11	0.02	1513	1655	37	3
Upper Barremian	*Oxyteuthis brunsvicensis*	1.47	0.01	−0.36	0.01	1576	1603	86	20
Upper Barremian	*Oxyteuthis brunsvicensis*	1.59	0.02	−0.39	0.03	1598	1723	38	9
Upper Barremian	*Oxyteuthis brunsvicensis*	1.62	0.02	−0.40	0.03	1536	1627	31	4
Upper Barremian	*Oxyteuthis brunsvicensis*	−0.26	0.05	−0.79	0.03	2094	2088	170	59
Upper Barremian	*Oxyteuthis brunsvicensis*	1.53	0.01	−0.17	0.01	1601	1653	318	26
Upper Barremian	*Oxyteuthis brunsvicensis*	0.43	0.02	−0.94	0.03	1368	1764	79	10
Upper Barremian	*Oxyteuthis brunsvicensis*	0.29	0.02	−1.25	0.02	1826	2109	97	16
Upper Barremian	*Oxyteuthis brunsvicensis*	1.46	0.01	−0.94	0.02	1671	1878	173	27
Upper Barremian	*Oxyteuthis brunsvicensis*	0.35	0.02	−0.63	0.01	2441	1592	328	12
Upper Barremian	*Oxyteuthis brunsvicensis*	0.53	0.02	−0.07	0.01	2189	1566	232	56
Upper Barremian	*Oxyteuthis brunsvicensis*	0.14	0.01	−1.07	0.01	1623	1635	188	21
Upper Barremian	*Oxyteuthis brunsvicensis*	−2.53	0.01	−3.17	0.01	3331	1297	3343	135
Upper Barremian	*Oxyteuthis brunsvicensis*	1.07	0.01	−0.84	0.01	1684	1554	152	4
mean	***Oxyteuthis brunsvicensis***	**0.68**	**0.02**	**−0.80**	**0.02**	**1861**	**1696**	**377**	**29**
Lower Barremian	*Aulacoteuthis* spp.	1.39	0.02	−0.83	0.02	885	1064	171	1
Lower Barremian	*Aulacoteuthis* spp.	1.51	0.02	−1.79	0.03	1494	1903	92	4
Lower Barremian	*Aulacoteuthis* spp.	0.69	0.02	−2.01	0.02	2056	1877	33	1
Lower Barremian	*Aulacoteuthis* spp.	0.84	0.01	−2.03	0.02	2845	2036	21	2
mean	***Aulacoteuthis* spp.**	**1.11**	**0.02**	**−1.67**	**0.02**	**1820**	**1720**	**79**	**2**
Lower Barremian	*Praeoxyteuthis pugio*	1.57	0.01	−1.16	0.02	1395	1740	195	19
Lower Barremian	*Praeoxyteuthis pugio*	1.60	0.02	−0.77	0.03	1521	1626	24	4
Lower Barremian	*Praeoxyteuthis pugio*	0.36	0.03	−0.41	0.03	1383	1874	17	3
Lower Barremian	*Praeoxyteuthis pugio*	1.10	0.03	−0.20	0.02	1383	1874	17	3
Lower Barremian	*Praeoxyteuthis pugio*	1.80	0.01	0.42	0.02	1487	1630	105	8
Lower Barremian	*Praeoxyteuthis pugio*	1.36	0.01	−0.15	0.01	1240	1568	48	4
Lower Barremian	*Praeoxyteuthis pugio*	−0.04	0.03	−0.20	0.02	2479	2238	7	10
Lower Barremian	*Praeoxyteuthis pugio*	1.19	0.02	0.05	0.04	4898	2074	380	49
mean	***Praeoxyteuthis pugio***	**1.12**	**0.02**	**−0.30**	**0.02**	**1973**	**1828**	**99**	**13**
total mean		**1.47**	**0.02**	**−0.51**	**0.02**	**1788**	**1620**	**216**	**21**

Appendix 1–3: continued

Upper Barremian	*Oxyteuthis germanica*	1.81	0.02	−0.10	0.01	2821	1803	237	105
Upper Barremian	*Oxyteuthis germanica*	1.98	0.02	−0.39	0.01	1389	1486	105	34
Upper Barremian	*Oxyteuthis germanica*	1.83	0.02	−0.49	0.02	1436	1647	182	107
Upper Barremian	*Oxyteuthis germanica*	1.25	0.02	−0.38	0.03	2435	2435	300	24
Upper Barremian	*Oxyteuthis germanica*	1.16	0.01	−0.46	0.02	1287	1683	56	7
Upper Barremian	*Oxyteuthis germanica*	1.69	0.04	−0.84	0.03	1802	1520	777	59
Upper Barremian	*Oxyteuthis germanica*	1.22	0.03	−1.12	0.03	1899	1427	816	65
Upper Barremian	*Oxyteuthis germanica*	1.92	0.01	−0.69	0.02	1506	1708	246	45
Upper Barremian	*Oxyteuthis germanica*	1.23	0.02	−0.58	0.03	1800	1731	392	23
mean	*Oxyteuthis germanica*	1.57	0.02	−0.51	0.02	1823	1669	236	34

Newsletter on Stratigraphy
Vol. **43/3:** 275–291, April 2010

Reassessment of the Zemorrian foraminiferal Stage and Juanian molluscan Stage north of the Olympic Mountains, Washington State and Vancouver Island

Elizabeth A. Nesbitt[1], Ruth A. Martin[1], Neil P. Carroll[1], and Jeff Grieff[1]

With 2 figures and 2 tables

Abstract. The Oligocene biozonation of marine formations exposed along the Straits of Juan de Fuca, western USA and Canada, are re-evaluated with a greatly increased fossil data set. The Pysht, Sooke and Clallam formations are the type sections of the Juanian and Pillarian molluscan stages, the *Liracassis rex* and *Liracassis apta* biozones of the Juanian Stage, and they have also been assigned to the Refugian, Upper and Lower Zemorrian and Saucesian benthic foraminiferal stages. Based on these stages, paleomagnetic signatures have been used to assign Chrons and numerical ages. Reassessment of the index fossils has resulted in the lack of definition of the biozones and the benthic foraminiferal stage boundaries and the entire Pysht and Sooke formations falls within the Zemorrian Stage, but could not be subdivided into early and late substages. The lack of delineation of subzones within the Oligocene in this region is attributed to both the original characterization of the stages/zones and complex faulting and folding of the exposed Tofina-Fuca depositional basin of the Cascadia subduction margin.

Key words. Oligocene, biostratigraphy, magnetostratigraphy, Tofino-Fuca basin, Cascadia

Introduction

The mid-Cenozoic Pysht, Clallam and Sooke formations, exposed along the Straits of Juan de Fuca, Washington State, USA, and Vancouver Island, Canada, are richly fossiliferous, but their ages have long been controversial. Along the southern coast of the Straits of Juan de Fuca the Pysht Formation is the youngest unit of the Twin River Group and is overlain by the Clallam Formation (Brown and Gower 1958; Snavely et al. 1978). The Sooke Formation, on the northwestern shores of the Straits, is the youngest unit within the Carmanah Group (Cameron 1980) overlying the Eocene Escalente and Oligocene Hesquiate Formations. These marine sedimentary sequences are part of the onshore exposures of the Tofino-Fuca depositional basin, part of the Cascadia subduction margin (Fig. 1) and they have variously been assigned ages from Eocene to Miocene based on biostratigraphic data from molluscan, foraminiferal and vertebrate fossil assemblages. Recent studies on the biostratigraphy of the offshore Tofino-Fuca basin, using sidewall core samples and cuttings from Shell Canada wells resulted in biostratigraphic systems based on foraminifera

Authors' address:
[1] Burke Museum of Natural History and Culture, University of Washington, Box 353010, Seattle WA 98,195, U.S.A. lnesbitt@u.washington.edu, ruthm2@u.washington.edu
Corresponding author: Elizabeth Nesbitt, address and E-Mail above, phone (206) 543-5949

DOI: 10.1127/0078-0421/2010/0043-0275
0078-0421/10/0043-0275 $ 4.25

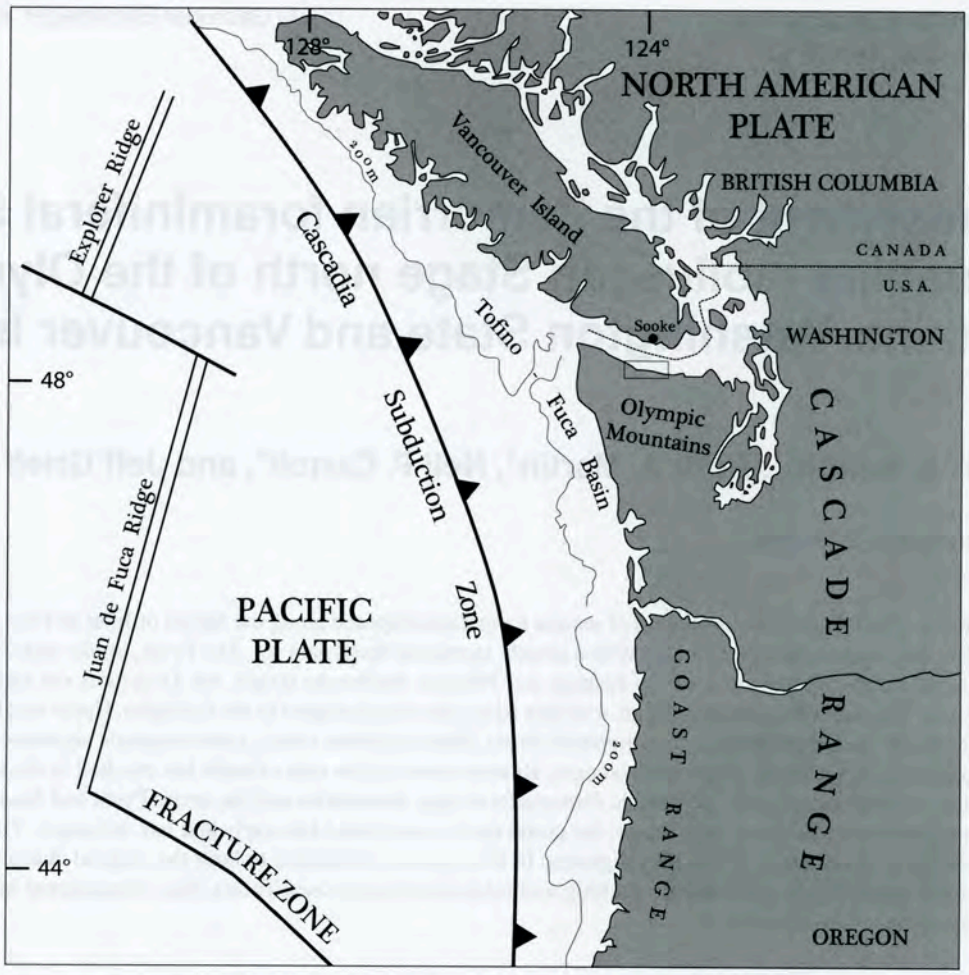

Fig. 1. Map of the Cascadia tectonic region showing the subduction zone of the Juan de Fuca Plate in relation to the North American Plate, the positions of the current divergent and convergent margins and the Cascade volcanic arc, and the Tofino-Fuca depositional basin off northwestern Washington, USA and Vancouver Island, Canada. The box represents the position of the Pysht and Clallam formation outcrops, as illustrated in Figure 2, and the locality of the Sooke Formation is marked with a dot.

(Narayan et al. 2005) and ichthyoliths (Johns et al. 2006), but these offshore wells do not correlate well with the onshore strata.

This study is a reassessment of the current status of the age and biostratigraphic correlation of these paleontologically important rocks, using much more comprehensive taxonomic collections than were previously available. Pinpointing the ages of the Pysht, Clallam and Sooke formations is critical for evolutionary studies of their marine mammal and bird taxa, evaluation of the published biozonal schemes, the stratigraphic placement of fossil methane seeps occurring in these formations, and the paleogeographic reconstructions of the Tofino-Fuca depositional basin. This reassessment is possible because of the accumulation of over 90 years of micro- and macrofossil collections since Charles Weaver's pioneering work in this region in 1916, and the consolidation of the paleontological repositories into the Burke Museum, University of Washington (UWBM) collections. The Pysht, Sooke and Clallam formations contain a high diversity of vertebrate, invertebrate and foraminiferal fossils, rare plant fossils, and chemosymbiotic assemblages, characteristic of methane seep settings.

Vertebrate specimens from the Pysht, Sooke and Clallam formations comprise a diversity of marine and littoral mammals and birds, most of them collected by James and Gail Goedert. Amongst the large collection of cetaceans (whale) mammals is the oldest known mysticete whale (with complete postcranial skeleton),

the toothed mysticete *Chonecetus goedertorum* which is the earliest known echolocating cetacean, and a large number of dolphin-size odontocete skulls (Barnes et al. 1994; Goedert and Barnes 1996; Barnes et al. 2001; Goedert et al. 2007; UWBM unpublished data). These formations have produced numerous critical specimens that illustrate whale evolution when the mysticete clade separated from the odontocetes and developed a toothless jaw with filter feeding baleen plates. In addition, this vertebrate fossil collection includes at least four genera of the herbivorous desmostylids including *Cornwallius sookensis*, *Behemotops proteus*, *?Kronokotherium sp.* and two different species of *Desmostylus* (Domning et al. 1986; Ray et al. 1994; Barnes and Goedert 2001), as well as one of three known specimens of the unique "sea bear" *Kolponomos clallamensis* and pinneped skulls (Tedford et al. 1994; Barnes and Goedert, 1996). Another important vertebrate taxon from the Pysht Formation is the rare marine plotopterid bird, *Tonsala howardae* (Olson 1980; Goedert 1988).

The major component of the invertebrate fauna from the Pysht, Sooke and Clallam formations is a high diversity of cool-water gastropods and bivalves and the last northeastern Pacific nautiloid, *Aturia augustata*. (Clapp and Cooke 1917; Clark and Arnold 1923; Durham 1944; Weaver 1943; Addicott 1976a, 1976b; Squires 1989). Coastal outcrops of the Pysht Formation form the type section for the regional Oligocene Juanian Stage and the *Liracassis* (formally *Echinophora*) *rex* and *Liracassis apta* biozones (Durham 1944; Addicott 1976c). Invertebrates from these formations also include rare brachiopods, solitary corals, spectacular beds of entire ophiuroids and crinoids, and a diversity of crustaceans including crabs, lobsters, deep water mud-shrimp, and the giant bathyal isopods, *Bathynomus goedertorum* (Rathbun 1926; Durham 1944; Wieder and Feldmann 1989; Berglund and Goedert 1996; Goedert et al. 1995; Schweitzer and Feldmann 1999; Fraaije et al. 2006; UWBM unpublished data).

Numerous fossil methane seep sites are located in Pysht and Sooke strata. These are characterized by authigenic carbonates and benthic foraminiferal tests with depleted $\delta^{13}C$ values (Martin et al. 2006). Methane seep sites in these formations are the result of active tectonic compression on organic-rich sediments within the forearc forcing methane enriched fluids up to the sediment-water interface via faults and folds. Active tectonism during the period of deposition for these strata resulted in numerous cold methane seepage localities that are now identifiable by the characteristic fauna and allochthonous calcite deposits. The fauna consists of assemblage of chemosymbiotic mollusks such as the bivalves *Adulomya chinookensis*, *Bathymodiolus willapaensis*, *Acharax dalli*, *Lucinoma hannibali* and *Conchocele bisecta* (Goedert et al. 2003; Kiel 2006; UWBM unpublished data). In addition, some of the chemosymbiotic mollusks occurred within the assemblages associated with the numerous whale falls, wood, and nekton falls in the Pysht Formation, including some wood-specific taxa such as *Thyasira xylodia* and *Xylodiscula okutanii* (Kiel and Goedert 2006; Kiel and Goedert 2007). It is critical for further research that the chronostratigraphic framework is robust for further study of these fossils and their evolutionary patterns.

Geologic setting

Western Washington and Oregon consist of a thick sequence of marine sedimentary rocks that formed in the accretionary wedge of the Cascadia forearc. This forearc that first developed in the Late Eocene as the remnants of the Farallon plate (the Juan de Fuca plate) subducted beneath the North American plate (Snavely and Wells 1996, Brandon et al. 1998; Haeussler et al. 2003). The Cascadia accretionary complex grew by frontal accretion and underplating of the forearc and it underlies the offshore continental margin of Oregon, Washington and western Vancouver Island (Brandon et al. 1998). Thick sequences of marine siliciclastic sediments were deposited into a basaltic basement in the forearc basin from Late Eocene to the Middle Miocene. A regional unconformity recorded in the late Middle Miocene extended across the entire shelf on the Cascadia margin (McNeill et al. 2000). Marine sedimentation into the forearc basin continued in the late Miocene through the Pliocene and was overlain by voluminous Pleistocene glacial debris. The forearc basin of northwestern Washington and southwestern Vancouver Island has been called Tofino-Fuca depositional basin and it is still an active depositional center for sediments derived from the Cascades volcanic arc, the Olympic Mountains and the Coast Range (Fig. 1). Because of oroclinal bending of the subducting plate, the Olympic Mountains rose rapidly about 14 Ma uplifting the accretionary complex which is now exposed as the Olympic Subduction Complex (Brandon et al. 1998). Continued oblique compressional tectonics distorted the basaltic basement unit and dividing the forearc depositional basin (Brandon et al. 1998, fig. 15;

Stewart and Brandon 2004). The stratigraphic section north of the mountains is separated from the Olympic core rocks by the Hurricane Ridge and Calawah fault zones (Tabor and Cady 1978). The Tofino-Fuca basin is now folded along a major east-west trending syncline and/or thrust fault that runs down the center of the Strait of Juan de Fuca (Snavely and Wells 1996; Dragovich et al. 2002) with outcrops on the north and south of the Straits of Juan de Fuca (Fig. 1). On the Vancouver Island side of the straits, the Leech River Fault separates the depositional basin from the Wrangallia Terrane in the north (Yorath et al. 1985).

Magnetostratigraphic studies of marine Cenozoic formations along the northeastern Pacific margin have revealed significant clockwise tectonic rotation for most of them (see compilation in Prothero and Nesbitt (2008). These include the highest rotation with respect to the Oligocene cratonic pole of North America, of $80° \pm 5°$ for the Late Oligocene Blakeley Formation, as well as the lesser motion of $49° \pm 6°$ for the Pysht Formation, and $46° \pm 15°$ for the Clallam Formation (Prothero et al. 2001, Prothero and Nesbitt 2008). These tectonic rotations indicate that the marine rocks now exposed along the Straits of Juan de Fuca were part of a strongly oblique convergence angle for the subducting slab. In contrast, the Sooke Formation records counterclockwise rotation of $35° \pm 12°$ which is consistent with the counterclockwise rotational data of the Eocene-Oligocene units on the northeastern-most part of the Olympic Peninsula, the Quimper Formation, Marrowstone Shale, and the underlying Port Townsend basalts. This rotation occurred in the Miocene, post-Sooke depositional time, and is related to the uplift of the Olympic Mountains (Prothero et al. 2008).

Pysht Formation

The Pysht Formation and overlying Clallam Formation on the southern side of the Straits of Juan de Fuca are the youngest onshore units in the Tofino-Fuca Basin and are exposed along the beaches and sea cliffs of the northern Olympic Peninsula. Rocks of the Pysht Formation have had numerous prior names and changing geographic boundaries since they were first described in 1913 by Arnold and Hannibal. These authors named these rocks the Twin River Formation based coastal exposures from Pysht Bay to east of Twin Rivers (Fig. 2). They correlated the underlying unit with the Seattle Formation in central Puget Sound, used this same name, and they designated the overlying rocks the Monterey Formation because of the faunal similarity with that formation on the central California coast. Weaver (1937) used the term Twin River Beds for these coastal outcrops and described the unit as cropping out "for a distance of 3 miles east and west on either side of Twin River". Based on the molluscan fauna, Weaver (1937) correlated these beds with the Blakeley Formation in central Puget Sound, included them in the definition of the Blakeley Formation, and discarded the name Seattle Formation. He used the Blakeley Formation, as well as the older Keasey and Lincoln formations as biostratigraphic units across western Washington and northwestern Oregon and not as essential lithostratigraphic mappable entities (Weaver 1937; Weaver et al. 1944).

Brown and Gower (1958) redefined the Twin River Formation because of the wide geographic gap with the type Blakeley Formation and the fact that the Blakeley fauna occurs only in part of the much more stratigraphically extensive unit on the Olympic Peninsula. This new definition also included older rocks on the north side of the Olympic Mountains that Weaver (1937) had incorporated into the Lincoln and the Lyre formations. The redefined Twin River Formation was named for outcrops along the northern Olympic Peninsula coast from Crescent Bay westward to the Clallam River, and extending inland for 8–13 km where they are only exposed in stream cuts (Brown and Gower 1958). The type section along Deep Creek was measured at 5,030 m thick and was divided into lower, middle and upper members. Subsequently Snavely et al. (1978) raised the Twin River Formation to the Twin River Group that consists of the lower Hoko River Formation, middle Makah Formation, and upper Pysht Formation. The Pysht Formation was mapped along the coast from Clallam Bay eastwards to the mouth of Whiskey Creek between Low Point and Agate Bay (Tabor and Cady 1978). It is also exposed along rivers and creeks that flow into the Straits of Juan de Fuca in this area (Fig. 2). The thickest section, at 870 m, is along the lower reaches of Deep Creek; however the contact with the overlying Clallam Formation is not present here (Brown and Gower 1958; Addicott 1976b, 1976c). The top of the Pysht Formation is exposed west of the Pysht River mouth where the thickness is 1,067 m. However, mapped faults, synclinal and anticlinal folds (Brown and Gower 1958) and confusing biozonal designations indicate that structural complexities probably make this thickness inaccurate. The contact between the Pysht and underlying the Makah formation is mapped at Whiskey Creek (Tabor

and Cady 1978) but this contact is now obscured by a long-lived landslide. Brown and Gower (1958) and Dragovich et al. (2002) mapped small faults along the coastal section of the Pysht Formation from East Twin River to Murdock Creek, most of them at right angles to the coast and numerous coast-parallel folds (Fig. 2). An additional east-west trending fault extending from the Pysht River west to the Clallam River, has juxtaposed pebble to boulder conglomerate units of the Pysht against deep water mudstones near the base of the section in the vicinity of Clallam Bay (Addicott 1976b).

Rocks of the Pysht Formation are generally massive mudstones and siltstones, with some thick, fine-grained sandstone beds (up to 100 m) towards its western extent. Calcite-cemented concretions occur throughout the mudstone and are frequently formed around macrofossils and burrows. From fossil evidence, most of the Pysht Formation was deposited on a submarine fan at outer shelf to slope in depths and turbidite beds are common. The depositional basin shallowed towards the top of the Pysht and into the Clallam and Sooke Formations.

Numerous methane seep sites are located in the Pysht coastal outcrops, including large limestone chemohermitic boulders at the mouth of Whiskey Creeks and smaller, scattered nodular deposits from east of Twin River to Deep Creek (Goedert et al. 2003; UWBM unpublished data). Outcrop-scale methane seep signatures include allochthonous calcites in the form of small nodules, vein fills, and narrow platforms along bedding surfaces, glendonite crystals and characteristic molluscan fossils such as species of *Vesicomya*, *Bathyodiolus*, *Acharax*, *Cryptolucina* and *Conchocele*.

Clallam Formation

The Clallam Formation conformably overlies the Pysht Formation (Fig. 2) and is exposed for ~7 km along the coast between Pillar Point and Slip Point, and west of Clallam Bay to the mouth of Sekiu River (Weaver 1937; Gower 1960; Addicott 1976b). Weaver (1937, p. 173) stated that the thickness of formation was ~700 m, and that the contact of the Clallam with the underlying Twin River Formation was concealed. However Addicott (1976a, 1976b) noted that west of Pillar Point the two formations were conformable and gradational, but reported a distinct change in molluscan taxa between the two formations. Large coast-parallel faults and transverse folds (Fig. 2) make it difficult to assess the formation's thickness, and to place the fossiliferous units in stratigraphic order. In general, the Clallam rocks are composed of sandstone and conglomerate with thin beds of coal near the top of the formation (Gower 1960; Addicott 1976c) as the basin shallowed upwards to supratidal depositional settings.

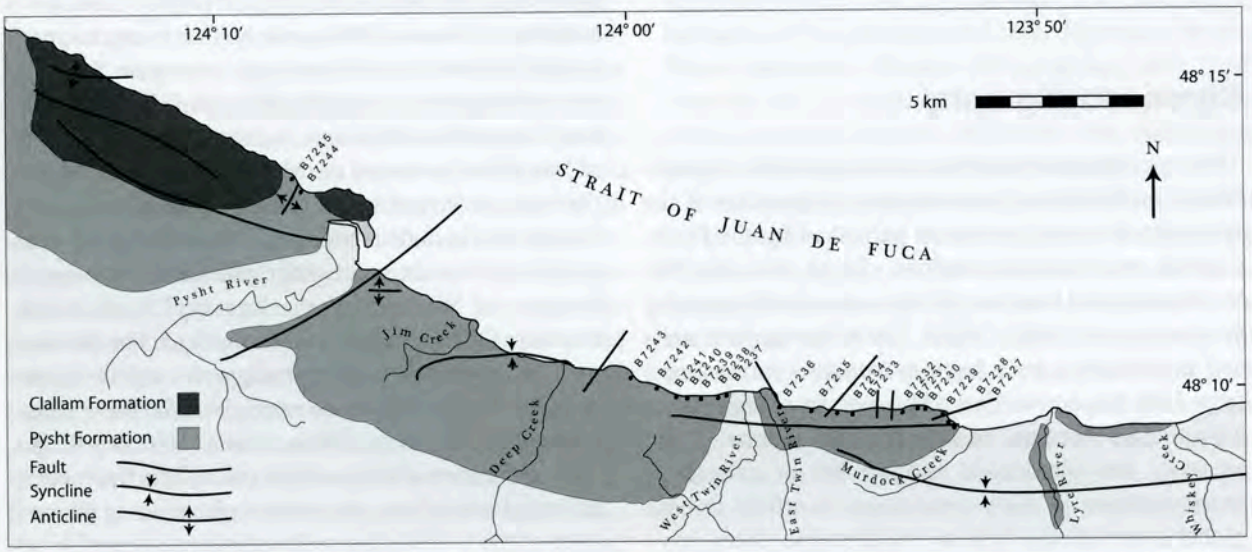

Fig. 2. Generalized geologic map of the Pysht and Clallam formations exposed along the south shore of the Straits of Juan de Fuca, showing reassessment fossil localities (UWBM numbers B7227 to B7245) and mapped faults and synclinal folds. Modified from Brown and Gower 1958; Brown, Gower and Snavely 1960; Gower 1960.

Sooke Formation

On the northern limb of the Tofino-Fuca Basin the three temporally equivalent formations to the Twin River Group are the Escalate, Hesquiat and Sooke Formation (the Carmanah Group) that crop out along the coast from Sooke Bay eastwards to Tachu Points (Cameron 1980). The Sooke Formation was first mapped by Clapp and Cook (1917) and described from exposures along beaches and creeks west of Sooke Bay to San Juan Point, southern Vancouver Island. The type section of the Sooke Formation is ~ 45 m thick, consisting primarily of inner neritic to intertidal cross-stratified sandstones and conglomerates, grading into supratidal and terrestrial. Debris-flow pebble to boulder conglomerates and cross-bedded and laminar sands with abundant wood debris indicate high energy, inner neritic depositional environments. These intertidal strata include a diversity of molluscan fossils, most notably with taxa from the rocky shoreface (Clap and Cooke 1917; Prothero et al. 2008). A few strata of mudstone are preserved west of the type section and these sediments indicate low energy regimes, perhaps protected regions behind sea stacks (Cameron 1980). A small outcrop of this sandy siltstone and mudstone was exposed at Sombrio Beach, 25 km northwest of Sooke, which included a single diffuse methane seep site. This site is characterized by a single bedding plane with discontinuous carbonate nodules. No mollusks were seen here but stable isotope ratios from allochthonous carbonate samples and benthic foraminifera are indicative of methane seepage (Martin and Nesbitt 2007).

Chronostratigraphy

Three stratigraphic systems, based on benthic foraminifera, mollusks and paleomagnetic signatures of the sedimentary rocks, have been published for the Pysht, Clallam and Sooke formations, dating from the first by Arnold and Hannibal (1913) to the most recent by Prothero et al. (2001, 2008). These lithological units and the biozones have been assigned to various ages from Late Eocene to Early Miocene from correlation with the Californian biostratigraphic scheme. There are very few planktonic foraminifera or calcareous nannoplankton in these formations on which to base global correlations, and no radiometric dates have been obtained. The global climate reorganization during the Late Eocene and early Oligocene resulted in increased provinciality in temperate latitudes, hindering biostratigraphic correlations. In the northern hemisphere at this time, warm-water organisms were forced southwards, new endemic taxa evolved and other taxa migrated in from higher latitudes. This is documented along the eastern Pacific margin in the molluscan faunas (Hickman 2003; Nesbitt 2003) and benthic foraminifera must have been subject to the same biogeographic realignment. These problems only exacerbate the difficulties of applying California stages to the northern Washington sections, some 1,500 km north.

Molluscan and benthic foraminiferal biozonations were erected for the coastal outcrops of the Pysht and Clallam Formation (Weaver 1937; Durham 1944; Addicott 1976a, 1976b, 1976c; Rau 1964, 1981). The stratigraphically-restricted Sooke Formation was not correlated with either of these, but instead with the geographically limited Blakeley Formation in central Puget Sound (Clark and Arnold 1923). Prothero (2001), in summarizing numerous studies on magnetostratigraphy of Cenozoic fossiliferous units the northeastern Pacific margin, noted that incompleteness of the stratigraphic record is the rule rather than the exception, and that the Oligocene units were amongst the most incomplete known.

Molluscan Biozonation

The historical account of terminology used for Cenozoic biozones along the west of North America is complex and variable, some of which is documented in Prothero (2001). Only a brief history of those schemes that are pertinent to the rocks north of the Olympic Mountains is noted here. Weaver (1916) was the first to erect a stratigraphic scheme for Cenozoic units in western Washington and Oregon by identifying three molluscan biozones based on richly fossiliferous, but stratigraphically isolated, strata that he named the *Molopophorus lincolnensis*, *Turritella porterensis* and *Acila gettysburgensis* zones. These zones included the fossils from five distinct stratigraphic units in different geographical areas of western Oregon and Washington: the Keasey, Lincoln Creek, Blakeley, Quimper, and Pysht formations. The biozones were directly tied to the lithostratigraphic units and those considered to be Oligocene were given the same names as the rock units, Keasey, Lincoln and Blakeley Stages, making them invalid by modern rules of the International Stratigraphic Code. As in other places along the west coast of the U.S.A., the rock unit names were also utilized as time-stratigraphic names and these were published in the first official correlation charts of the west coast marine Cenozoic rocks (Weaver et al. 1944).

Weaver's original 1916 zonation was refined by Durham (1944) with six molluscan biozones for what he considered to be Oligocene rocks in Washington State. However, the zonal type sections that Durham (1944) defined are geographically widely separated, and not in stratigraphic contact with underlying or overlying units. Two of the these six molluscan biozones included fossils from the coastal outcrops of the Pysht Formation (at the time called the Upper Member of the Twin River Formation) that he called the *Echinophoria rex* and *E. apta* zones, and an unnamed seventh biozone was tentatively suggested for the overlying Clallam Formation fauna. Durham (1944) noted that the mollusks from the Sooke Formation, Vancouver Island, were originally considered to be most similar to those from the Blakeley Formation, central Puget Sound, and therefore within the *E. rex* zone. Durham (1944) also noted that the Sooke molluscan taxa had more in common with faunas from unnamed units considered Blakeley Formation equivalents at Lake Sammamish and in Snohomish County (east of the Blakeley Formation outcrops on Puget Sound) which he attributed to the *E. apta* zone, and he correlated it with the Refugian foraminiferal zone. The problem is that the mollusks from these unnamed units are all from intertidal embayment settings and have little in common with the type section of either the Blakeley or the Pysht formations, both of shelf/slope depositional depths. Durham's (1944) youngest, unnamed biozone was based on the Clallam Formation that he correlated with the Miocene Temblor Formation in southern California.

Later, with the recognition of post-Eocene biogeographic provinciality along the west coast, Armentrout (1975) proposed the Late Eocene/Early Oligocene Galvinian Stage and the Oligocene Matlockian Stage, based on overlapping ranges of molluscan species from the Keasey Formation (northwest Oregon) and Lincoln Creek Formation (southwest Washington). In this biostratigraphic scheme the Matlockian Stage replaced the "Blakeley" Stage that was divided into the *E. rex* and *E. apta* zones, and correlated lower and upper Zemorrian foraminiferal stages and the middle and upper Oligocene age, respectively. Armentrout (1975, p. 28) noted that exposures of Durham's (1944) type section of the *E. apta* zone in the upper Twin River Group (Pysht Formation) are "discontinuous, structurally complex and lacking superpositional controls".

At the same time Addicott (1976a, 1976c) erected six Late Paleogene and Neogene molluscan stages for Oregon and Washington, and correlated them with California benthic foraminiferal stages. The lowermost was the regional Juanian Stage based on the *E. apta* zone, with the type section in the coastal outcrops of the Pysht Formation, from 3 km east of the East Twin River to the several meters above the base of the Clallam Formation west of at Pillar Point. However the Juanian Stage in this scheme overlapped with the Matlockian Stage of Armentrout (1975) and so the latter was amended to include only the early Oligocene time (Armentrout 1981). Moore (1963, p. 30) had assigned *Echinophoria fax*, *E. rex* and *E. apta* to the genus *Liracassis* and subsequently the two biozones were renamed *Liracassis rex* and *Liracassis apta* zones.

The regional Juanian Stage was erected to replace the rock stratigraphic name "Blakeley" stage (Addicott 1976c), and it was equivalent to the *Liracassis apta* biozones of Durham (1944). This did not, however, include the fauna from the Blakeley Formation itself which he considered to be older. The biostratigraphic description of the Juanian Stage is based on concurrent range of the following gastropod species: *Liracassis apta*, *Neptunea teglandae*, *Bathybembix turbonata*, and *Aforia clallamensis* that were found along the coast exposures of the Pysht Formation east of East Twin River. The Juanian Stage was also recognized in part of the Lincoln Creek Formation (southwestern Washington), the Scappoose and Yaquina Formations (western Oregon) and the Sooke Formation. Addicott (1976b) then redefined the subjacent Matlockian Stage of Armentrout (1975) to include the fauna from the Blakeley Formation which was equivalent to the *Liracassis rex* zone of Durham (1944). Armentrout's (1975) description of the *L. rex* zone included the restricted occurrence of the gastropods *L. rex*, *Neptunea landesi*, *Perse teglandae*, *Fusinus (Priscofusus) foxi*, *F. (P.) stewarti* and *Turritella blakeleyensis*. However, many of the restricted species and those with overlapping ranges do not occur in the Pysht Formation.

The boundary between the Juanian and younger Pillarian Stages is at the contact between the Pysht and Clallam formations on the coast, and the type section for the Pillarian was designated as the Clallam Formation (Addicott 1976c). The Clallam fauna is very different from that of the underlying Pysht Formation being characteristically inner neritic and littoral, and from warmer water. The most abundant and conspicuous taxon in the Clallam Formation is the giant pectinid, *Vertipecten fucanus*, which is restricted to this stage. Other taxa listed as restricted are found in other units, but the Pillarian is also defined by the overlapping range occurrences of numerous molluscan species (Addicott, 1976c, p. 14 and 15).

Table 1 Results of the "blind test" of individual samples of the gastropod genus *Liracassis* from the Lincoln Creek, Pysht, Makah and Blakeley Formations, western Washington State. *Liracassis rex* and *L. apta* were characteristic zonal indicators of the molluscan Juanian Stage, and data from these formations show that both species range throughout the entire stage.

Test sample #	Stratigraphic section	UWBM localities	*Liracassis* species
I. Samples collected without the authors' knowledge of localities i.e. blind test			
Lincoln Creek Formation a) Canyon River section in stratigraphic order			
1	Canyon River *L. rex* zone (weathered)	B0284	*L. apta*
7	Canyon River *L. rex* zone	B0285	*L. rex*
5	Canyon River *L. rex* zone	B0297	*L. apta*
2, 9	Canyon River C *L. rex* zone	B0298	*L. rex*
6	Canyon River *L. rex* zone	B0300	*L. rex*
3	Canyon River *L. apta* zone	B1320	*L. rex*
8	Canyon River *L. apta* zone	B1323	*L. rex*
4	Canyon River *L. apta* zone	B0322	*L. rex*
10			*L. apta*
Lincoln Creek Formation b) Middle Fork Satsop River section in stratigraphic order			
15, 18	Middle Fork Satsop River *L. fax* zone	B0356	*L. rex*
12	Middle Fork Satsop River *L. fax* zone	B0357	*L. apta*
13, 16			*L. rex*
14, 21, 26, 28, 28, 30, 31, 32	Middle Fork Satsop River *L. fax* zone	B0367	All *L. rex*
11, 17, 22, 27	Middle Fork Satsop River *L. rex* zone	B0372	All *L. durhami*
20	Middle Fork Satsop River *L. apta* zone	B0384	*L. rex*
Twin River Group a) Makah Formation, subjacent to Pysht Formation			
23	Shipwreck Point		*L. rex*
111	Jensen Creek		*L. apta*
Twin River Group b) Pysht Formation			
24	700 m west of Murdock Creek	B7229	*L. rex*
25			*L. apta*
76	Float at Murdock Creek		*L. fax*
33	West of UWBM B7232, concretionary ledge	Field no. JLG77	*L. fax*
II. UWBM collection from Twin River/Pysht Formation			
	Gettysburg, Lyre River mouth: *L. rex* zone	A9880	*L. rex*
	160 m east of E Twin River *L. apta* zone	A3072	*L. apta*
	350 m W of W Twin River *L. apta* zone	A3091	*L. rex*
	Ideal Cement Quarry *L. apta* zone: 30 specimens *L. apta* and 12 specimens *L. rex*	B5378	*L. apta* and *L. rex*
	Ideal Cement Quarry, *L. apta* zone: 10 very large individuals	B6562	*L. apta*
UWBM collection from Blakeley Formation, Bainbridge Island, Puget Sound			
	Restoration Point *L. rex* zone: 9 specimens are *L. rex*, 3 specimens are *L. apta*	W13	*L. rex* and *L. apta*
	Restoration Point *L. rex* zone: 3 specimens	B1383	*L. rex*
	Fort Ward *L. rex*	B2109	Both *L. rex* and *L. apta*

New data from both the Lincoln Creek and Pysht formations (Table 1) show that differentiation of *Liracassis rex* and *L. apta* are not possible. Tegland (1931) noted in her description of the species *L. apta* (as *Galeodea apta*) that it was morphologically very variable, particularly in the expression of rounded to tabulate shoulder curves, and variations in the expression of the nodes on the final whorl. Moore (1963) suggested that these may be sexually dimorphic characteristics. New collections of *Liracassis* individuals from along the Canyon River, Satsop River and Porter Bluffs sections of the Lincoln Creek Formation, and from the Pysht Formation showed that both typical *L. rex* and *L. apta* forms are found throughout the sections, in general with the larger individuals attaining the *L. apta* form and the smaller individuals the *L. rex* form.

To investigate this we conducted a "blind test" of *Liracassis* specimens from both the Lincoln Creek and coeval formations in Washington. James Goedert supplied 34 specimens collected from the type section of all three *Liracassis* biozones in the Lincoln Creek Formation for identification, without providing locality data. An additional 68 individuals were taken from museum collections of five geographically separate sections of the Lincoln Creek Formation, as well as from the Pysht Formation, the Makah (stratigraphically below the Pysht) and the coeval Blakeley Formation. These were set out for identification without their relevant locality information. Our species level identification of these fossils is presented in Table 1. The fossils were then matched to the original collection locality. These data indicate a lack of biozonal integrity. In addition to the evidence that *L. rex* and *L. apta* occur through both biozones in all Oligocene formations in western Washington, *L. apta* was also found in the *L. fax* biozone that is subjacent to the *L. rex* zone (Table 1). It was also apparent from the museum collections that the larger individuals were preferentially collected in the field and the smaller, and somewhat distorted, individuals are left in the outcrop. Large individuals of *Liracassis* are more likely to have the *L. apta* morphology. In the collections from the Pysht Formation, the biggest and best preserved individuals that express the *L. apta* form were collected mostly from those areas where cold methane seeps have been subsequently identified, most particularly from the now defunct Ideal Cement Quarry (600 m west of the mouth of West Twin River).

Additional problems are apparent with other biozone index species. Durham (1944) described *Fusinus (Priscofusus) foxi* from the Lincoln Creek Formation but did not compare it to the morphologically closest taxon, *F. (P.) hannibali*. The only two specimens of *F. (P.) foxi* the Lincoln Creek Formation in the museum collections are in fact *Turricula kincaidi*, and none have been recorded from the Pysht or Sooke formations. Thus *F. (P.) foxi* can no longer be a zonal index species. Other zonal index species, *F. (P.) stewarti*, *Neptunea goodspeedi* and *N. landesi* are all rare but have been collected throughout the coast outcrops of the Pysht Formation from Murdock Creek to the top of the formation. Thus, in the Tofino-Fuca basin the *Liracassis rex* and *L. apta* biozones of the Matlockian Stage cannot be reliably differentiated.

Macrofossils of the Clallam Formation are the basis for the Pillarian Stage (Addicott 1976b) that overlies the Juanian stage, and the stage boundary is set at the Clallam-Pysht formational boundary. The top of the Pillarian Stage could not be defined because the Clallam is the youngest onshore unit exposed along the northern Olympic Peninsula. The Pillarian Stage is characterized by the restricted occurrence of the giant pectinid *Vertipecten fucanus* as well as *Mytilus* cf. *tichanovich*, *Macoma optiva*, *Aforia tricarinata* and *Priscofusus geniculus*, as well as concurrent range zones of other mollusks (Addicott 1976b; Moore and Addicott 1987). The common molluscan taxa reflect both the inner neritic to intertidal depth of deposition and an incursion of warmer water compared with the characteristically cooler water Pysht fauna. The Clallam Formation was correlated with the type section of the Astoria Formation and the upper Nye Mudstone, western Oregon, the lowest section of the Astoria Formation in southwestern Washington, and the uppermost Poule Creek Formation, Gulf of Alaska (Addicott 1976c).

The Sooke Formation was more difficult to place within the molluscan biostratigraphic framework as all macrofossil-bearing sections are of intertidal and shallow subtidal paleodepths. Previously the Sooke has been assigned to the Miocene based on molluscan taxa (Clapp and Cooke 1917). However the Sooke fauna has the closest taxonomic similarity to that of the inner neritic to marginal marine bay facies that have been attributed to the Blakeley Formation exposed near Lake Sammamish, east of Seattle. Molluscan taxa from the Sooke Formation are listed in Clark and Arnold (1923) and Prothero et al. (2008). The only biozonal indicator species found in Sooke sediments are *Liracassis apta* and *Fusinus (Priscofusus) hannibali* and, as stated above, these are now shown to be present throughout the Oligocene sedimentary rocks here.

Benthic Foraminiferal Biozones

Benthic foraminifera from the coastal and river outcrops of the Pysht Formation were assigned to the upper Zemorrian Stage by Rau (1964). The Zemorrian Stage was defined for southern California (Kleinpell 1938) with the type section along Zemorra Creek, near Bakersfield, Kern County. Kleinpell (1980) discussed the controversies associated with the Zemorrian type section and the biostratigraphic interpretation made in other southern California coeval localities, and he stated that "Superpositional discipline, in terms of its overlaying the Refugian Stage, is lacking in the type locality of Zemorrian Stage, though observable at the type locality of the Refugian Stage." (Kleinpell 1980, p. 17). The Refugian -Zemorrian stage boundary was based on last appearance in these strata (LAD) of the following species: *Uvigerina vicksburgensis*, *U. cocoaensis*, *U. atwilli*, *Plectofrondicularia packardi robusta* and *Cibicides haydoni* (Kleinpell 1938, 1980). The Zemorrian Stage was recognized by the first appearance of species in these strata (FAD) and the LAD of many species of which only a few are found in northern Washington and Vancouver Island:

- FAD of *Uvigerina gallowayi*, *U. obesa* (including the subspecies *U. obesa impolita*), *Bolivina marginata marginata*, and *Cassidulina crassipunctata*.
- The lower *U. gallowayi* Zone was further recognized on the LAD of *Cibicides hodgei*, *Gyroidina condoni* and *Eponides kleinpelli*.
- The upper *U. sparsicosta* Zone was recognized by the restricted occurrence of the nominal species and the FAD of *Nonion incisum*, *Eponides kleinpelli*, and *Uvigerina kernensis*.
- The superjacent biozone is the *Siphogenerina transversa* Zone of the Saucesian Stage (Kleinpell 1938, 1980). The definition of this zone included the FAD of *Bolivina adelaidana*, *B. advena*, *Bulimina alligata*, and *Nonion costiferum*.

Almost all the published descriptions of benthic foraminiferal biozonation in Washington and northwestern Oregon are attributed to Weldon Rau, who published papers from 1948 to 2000, and his large collection of fossils from both drill cores and surface projects is now available in the Burke Museum, University of Washington. Rau (1958) originally named the upper Refugian biozone in Washington State the *Eponides kleinpelli* Zone but with additional data he changed the name to the *Cassidulina galvinensis* Zone (Rau 1981). In his study of the foraminifera from the Twin River Group, Rau (1964) noted that the age and correlation assignments are hampered by scarcity of fossils and poor preservation. He assigned the entire Twin River Group to four faunal divisions from Late Eocene to the Early Miocene boundary and in reviewing his prior biostratigraphic system, he noted the difficulty of defining the Refugian-Zemorrian boundary in this region. Rau's (1981) revised system of biozonal indicators is further confused by typological errors on the symbols for species' FAD and LAD. In this updated scheme for Washington and Oregon, the following species are important in the defining the biozones:

- The Refugian-Zemorrian stage boundary is set at the LAD of *Cassidulina galvinensis*, *Cassidulina kernensis*, *Eponidies kleinpelli*, and *Guttelina hantkeni*.
- The Zemorrian Stage is characterized by the FAD of *Anomalina californiensis*, *Bucella mansfieldi oregonensis*, *Bolivina marginata adelaidana*, *Bulimina alsatica*, *Cassidulina crassipunctata*, *Quinqueloculina weaveri*, *Elphidium minutum*, *Plectofrondicularia californica*, and the common occurrence of *P. packardi multilineata*.
- The upper Zemorrian-Saucesian boundary was not defined, but the lower Saucesian biozone is marked by the "common occurrence" of *Bolivina advena*, *Bucella mansfieldi oregonensis*, *Siphogenerina kleinpelli*, *Uvigerina obesa impolita* and *Plectofrondicularia californica*.

In a review of the foraminiferal stages of the Pacific Northwest, taking into account facies restrictions, McDougall (1980, p. 30) placed the Refugian-Zemorrian boundary at the FAD of *Cibicides elmaensis*, *Buccella mansfieldi oregonensis*, *Ceratobulimina washburnei*, *Valvulineria willapaensis* and *Uvigerina californica*, and that the members of the *U. cocoaensis* species group are not restricted to Refugian strata but range up into the lower Zemorrian. She also noted that *Cassidulina galvinensis* and some samples of *C. crassipunctata* were the same taxon (McDougall 1980, plate 25, fig. 1, 2). Data from the Shell Canada wells drilled in the Tofino Basin off Carmanah Point, western Vancouver Island (Narayan et al. 2005, fig. 1) show that only two penetrated below the Miocene. The Pluto I-87 well reached mudstones with *Cassidulina galvanensis* and *Plectofrondicularia packardi* but no other species typical of the onshore Refugian assemblage were recorded. The Zeus I-65 well penetrated ?Oligocene-middle Miocene strata that are dominated by agglutinate taxa with two poorly preserved Oligocene age calcitic species. From these data Narayan et al. (2005)

could identify the Refugian- Zemorrian boundary as the *Cassidulina galvinensis* Zone but could not subdivide the overlying Zemorrian Stage (their *Turrilina alsatica* zone) further.

For the reassessment study presented here, foraminifera were collected from the coastal section of the Pysht Formation, from Murdock Creek to Deep Creek, and west of Pillar Point to the formational contact with the Clallam Formation (Table 2). Along the coastal outcrops, 24 localities were resampled and 19 sites provided stratigraphically useful taxa. Only those taxa that have stratigraphic significance are listed in Table 2, along with taxa from 5 previously unpublished localities originally identified by Weldon Rau for a Washington State Department of Natural Resources mapping project (unpublished UWBM data). This new set of samples provided a much greater number of individuals per species which a) now records the co-occurrence of species previously considered to be useful stratigraphic indicators, and b) shows examples of great intra-taxon variability that necessitated the combination some of these species into a single species or a species group. The major points from this reassessment of the benthic foraminiferal assemblages are:

1. *Plectofrondicularia packardi packardi* and *P.p.multilineata* are found together in a number of samples from the Pysht Formation, thus the subspecies cannot be used for stratigraphic separation. In addition, the illustrations in Rau (1964, plate 5 figures 13 and 1) are transposed. The original description of *P.packardi* (Cushman and Schenck 1928, p.311, figures 14 and 15) from the Bastendorf Shale, Oregon, show the morphologies of these two subspecies are the microspheric and megalospheric forms that occur together.
2. In the same paper Cushman and Schenck (1928, p.321, figures 17, 18, and 19) illustrated three morphological varieties of *Uvigerina cocoaensis* that co-occur in the Bastendorf Shale. These three morphologies were assigned to separate species, *U.cocoaensis*, *U.vickburgensis* and *U.atwelli*. McDougall (1980, plate 16, figs.4–13) combined them into the *U.cocoaensis* group. Thus they cannot be used separately as stratigraphic indicators.
3. *Cassidulina galvinensis*, *C.kernensis* and *Eponides kleinpelli* do not occur in any of the Pysht samples. These three species are index fossils for the Refugian Stage, thus the coastal outcrops of the Pysht Formation are all younger than the Refugian Stage.
4. *C.crassipunctata* is present and common in all of the new samples, and the reviewed samples from Pysht localities, and this species co-occurs with *Buccella mansfieldi oregonensis*, *Cibicides elmaensis* and *Nonion incisum*, all of which are Zemorrian index species.
5. The new samples are all indicative of the Zemorrian Stage as a whole and there is no data to separate them into lower and upper biozones.
6. *Bolivina advena*, previously used as an index species for the lower Saucesian, is present in places across the outcrop (in localities UWBM B7230, B2732, B2741–2743) together with the Zemorrian species listed above. This suggests that here in the Tofino-Fuca Basin this species is not restricted to the Saucesian Stage.

This study did not include resampling the Pysht coastal sections from west of the mouth of Murdock Creek eastwards to Whiskey Creek, but the assemblages from these strata in museum collections were reassessed. Rau (1964) assigned the rocks that crop out from East Twin River to Murdock Creek to the Upper Zemorrian biozone and designated this section to be the reference section for the substage. These assemblages contain the same suite of taxa that occur in the section west of Murdock Creek including *Bolivina advena*. No Refugian index species are present and this section of the coastal strata is similarly assigned to the entire Zemorrian stage and cannot be subdivided.

Rau (1964) assigned the easternmost coastal outcrops of the Pysht Formation (east of the Lyre River) to the Refugian Stage. Refugian index species *Cassidulina galvinensis*, *C.kernensis*, and *Eponides kleinpelli* do not occur in any of these samples. The presence of *Guttulina hantkeni* in one sample, the additional presence of *Anomalina californiensis*, *Gyroidina condoni* and *Quinqueloculina weaveri* together with the absences of the common Zemorrian taxa *Uvigerina obese*, *Bolivina marginata marginata*, and *Cassidulina crassipunctata* indicates that these outcrops should be placed at the base of the Zemorrian. Benthic foraminifera from two vertebrate-bearing localities at the mouth of Murdock Creek (Barnes et al. 2001), do not include taxa that restrict them to the Refugian as discussed above. These small assemblages from Murdock Creek resembles those listed in Rau (1964) from this area, and are also assigned to the Zemorrian Stage.

The three conclusions from this reassessment of the benthic foraminiferal data are that

1. the Pysht Formation was most likely deposited during the Zemorrian, but the marine vertebrate fauna from Whiskey Creek are probably older than those

Table 2 Biozonal index species of benthic foraminifera from new sampling of the coastal outcrops of Pysht and Clallam formations, northern Olympic Peninsula, Washington (B7227–B7245 are UWBM locality numbers, and GP locality numbers are from the U.S. Geological Survey). This data indicate that the Zemorrian Stage in the Straits of Juan de Fuca sedimentary rocks cannot be subdivided divided into biozones, and that the Zemorrian-Saucesian boundary is not identifiable.

	B7227	B7228	B7229	B7230	B7231	B7232	B7233	B7234	B7235	B7236	B7237	B7238	B7239	B7240	B7241	B7242	B7243	B7244	B7245	GP56–101	GP56–10A	GP56–80C	GP56–80D	GP56–53
Anomalinoides californiensis (d'Orbigny)	x	x							x				x			x		x	x					
Bolivina advena Cushman				x								x			x	x	x				x			
B. adelaidana Cushman and Kleinpell			x		x																			
Bucella mansfieldi oregonensis (Cushman Stewart & Stewart)											x	x	x	x	x		x			x		x	x	x
Cassidulina crassipunctata Cushman & Hobson	x			x	x	x	x	x	x	x	x	x		x	x	x	x	x	x		x			x
Cibicides elmaensis Rau	x			x	x	x	x	x		x			x		x	x								
Elphidium minutum Ruess										x		x	x				x	x	x	x	x	x	x	
Gaudryna alazaensis Cushman	x	x		x						x		x	x	x		x				x				
Gyroidina condoni Cushman & Simonson	x	x				x																		
Gyroidina orbicularis planate Cushman	x	x				x	x				x		x	x	x	x			x					
Melonis pompiliodes (Fitchel & Moll)		x				x			x	x	x	x											x	
Nonion incisum (Cushman)	x	x		x	x	x		x		x		x				x	x	x	x					
Plectofrondicularia packardi packardi Cushman & Schenk				x	x	x				x	x													
Plectofrondicularia packardi multilineata Cushman & Simonson	x	x		x		x			x	x		x	x	x		x			x	x				
Quinqueloculina weaver Rau												x	x		x	x								
Uvigerina cocoaensis Cushman species group	x	x		x	x	x				x														
Valvulinaria willapaensis (Rau)	x					x				x														

from the more western exposures, dating from early in the Stage;
2. coastal exposures cannot be divided into upper and lower Zemorrian biozones;
3. taxa confined to the Saucesian Stage in more southerly rock units overlap with Zemorrian Stage taxa in this more northerly depositional basin.

Foraminifera from outcrops of the Sooke Formation in the vicinity of Muir Creek were indicative of inner neritic facies and had no stratigraphic utility (Muller et al. 1981). New collections of foraminifera from the deep-water facies that includes the cold-seep site at Sombrio Beach yielded 21 species, including all the Zemorrian index species found in the Pysht Formation such as *Cassidulina crassipunctata*, *Cibicides elmaensis*, *Elphidium minutum*, *Uvigerina cocoaensis*, *Plactofrondicularia packardi*, *Gyroidina orbicularis planata*, and *Bucella mansfieldi oregonensis*. These rocks are clearly the same age as those exposed south of the Straits of Juan de Fuca in the Pysht Formation.

The only published study of benthic foraminifera from the Clallam Formation is a short list of taxa from 3 localities by Rau (1964) and unpublished data (UWBM). *Nonion costiferum* and *Bolivina mansfieldi adelaidana* present in all published samples and GP56–101 of Rau's unpublished notes. Kleinpell (1980) designated the FAD of these species to be the base of the Saucesian. However in northern Washington and southern Vancouver Island these species co-occur with other typically the Zemorrian taxa and the Zemorrian-Saucesian boundary is not easily defined.

Magnetostratigraphy

Paleomagnetic signatures from the Pysht, Clallam and Sooke formations were tied to molluscan and benthic foraminiferal biozones (Prothero and Burns 2001; Prothero et al. 2001; Prothero et al. 2008). Samples for the Pysht Formation were collected along the coastal outcrops of the Straits of Juan de Fuca, in approximately the same localities as Durham's original biostratigraphic sampling sites, as well as samples taken from the short beach outcrops of the Pysht Formation west of Pillar Point to the contact with the Clallam Formation. These are the same sites that were re-sampled for benthic foraminiferal assemblages (UWBM B7227–B7245). Sampling for both studies resulted in a gap from B7243 to Pillar Point because of restricted access and lack of outcrop. Of the 32 paleomagnetic sites sampled, 17 were considered statistically distinct from random distribution at the 95% confidence level (Prothero et al. 2001). These results show 4 normal and 4 reversed magnetozones; the Pysht Formation was correlated with Chron 11r to Chron C6n, and the collecting hiatus was inferred to include Chrons C8r to C6r (Prothero et al. 2001, Fig. 3).

Nine paleomagnetic sites were sampled across 210 m stratigraphic meters of the Clallam Formation (Prothero and Burns 2001). Four of these were considered statistically distinct from random distribution at the 95% confidence level. They show a single reversal and were correlated to Chron C6Cn3n to C6Cn2r based on the molluscan biozones, and therefore the entire sequence spans only the time 24.2 to 23.8 Ma (Prothero and Burns 2001). The type Sooke Formation is a short (10 m) section exposed between Muir and Kirby Creeks, with of beds dipping 5–10° SW. Samples from the four localities sampled showed reversal. Based on correlations with the *Liracassis apta* molluscan biozones, and the presence of the marine vertebrates *Kolponomos* sp. and *Cornwallius sookensis*, Prothero et al. (2008) correlated the Sooke with the Clallam Formation and placed it in Chrons C6Cr (24.1–24.8 Ma).

The problems associated with index taxa in both molluscan and benthic foraminiferal zonal schemes for these formations, as described above, make correlations difficult. In addition, Prothero and Ressuguie (2001) noted that, based on their paleomagnetic study, the type Zemorrian section and the type Saucesian section in southern California, both stages overlap the Oligocene/Miocene boundary and thus are at least partially coeval.

Additional problems arise in the correlation of the Zemorrian benthic foraminiferal stage with global planktonic schemes and therefore with the global paleomagnetic chronology. Noting that calcareous nannoplankton and planktonic foraminifera are "scarce and erratic in occurrence in the Paleogene of the northeastern Pacific margin", Warren and Newell (1980, p. 245) assigned the late Zemorrian benthic foraminiferal stage in Los Sauces Creek, southern California, to the *Spenolithus ciperoensis* nannoplankton zone, equivalent to NP24–25 of Martini's (1971) zonation scheme. This indicates that the Oligocene/Miocene boundary occurs very near the top of the Zemorrian Stage there, and not at a benthic foraminiferal species turnover event. In addition, Warren and Newell (1980) assigned the uppermost Zemorrian strata at Los Sauces Creek to the *Globigerina ampliapertua* planktonic foraminiferal zone, equivalent to P19–20 zone of Blow (1969). Berggren et al. (1995) placed P19 at Chrons C12r–C11r or late Early Oligocene and NP24–25 spans the late Early and

entire Late Oligocene Chrons C11n–C6C3n (30–24 Ma). This contradiction has not yet been resolved. Nevertheless, the entire Zemorrian Stage, with the lowermost Saucesian Stage, was considered to span the Oligocene, and the Zemorrian was correlated with the European Rupelian and Chattian Stages (Warren and Newell 1980).

A third problem with these paleomagnetic correlations is the structure of the coastal outcrops. Prothero and Burns (2001) discuss the problems of faulting and folding of coastal units in the Clallam Formation, noting that from this investigation, the Pillarian molluscan biozone extends for less than half a million years, and they suggest that a denser sampling protocol may change these results. This is equally true for the coastal outcrops of the Pysht Formation which are exposed parallel to major east-west trending synclines (Brown et al. 1960; Tabor and Cady 1978), show inconsistent dips, and display ample evidence of small northwest-trending faults that result in long-lived landslides. In addition, the section west of the Ideal Cement Quarry for a distance of 1,700 m along the beach that was studied for its ubiquitous diffuse methane seepage signatures is virtually horizontal in attitude (Martin and Nesbitt 2007).

Conclusions

The Zemorrian benthic foraminiferal stage defined for Southern California spans 10 million years, from 33.7–23.8 Ma (Prothero 2001). This a critical time period for marine mammal evolution, and fossils collected along the Straits of Juan de Fuca include some highly significant specimens for understanding the cladogenesis of odontocete and mysticete whales. In addition, at this time unusual marine vertebrates lived along the shores of the then northeastern Pacific: a diversity of desmostylids and the "sea bear", *Kolponomos*, and the giant penguin-like plotopterid birds. The evolution of these novel mammals and birds was apparently connected to the cooling event that characterized the Oligocene in temperate latitudes. These taxa, from the Pysht, Sooke and Clallam formations are relatively rare but well-preserved. Methane seep-specific invertebrate fauna, and similar taxa associated with from whale falls, are also unique components of the same formations. Cold methane seep sites are the result of active tectonic compression of methane-rich sediments and provided faults and folds for fluid-flow pathway to the seabed (Campbell 2006). It is critical that the chronostratigraphic framework of these fossiliferous units is robust.

New foraminiferal and molluscan sampling of the Oligocene sedimentary package along the Straits of Juan de Fuca illustrates the difficulty of using biozonation developed in southern California for the rock record of the Pacific Northwest. This is the result of both the ~ 1,500 km separation (latitudinal), and the fact that the Eocene-Oligocene cooling event resulted in distinct biogeographic differentiation of both micro- and macrofaunal assemblages. Studies of many other Cenozoic marine sedimentary units along the northeastern margin of North America have shown that they generally span a much shorter time than originally proposed, and that there are more gaps than rock record in this region (see discussion in Prothero 2001; Prothero et al. 2008). Outcrop evidence and mapped folds and faults indicate that the Pysht and Clallam formations are not structurally continuous sections, and that both biostratigraphic and magnetostratigraphic patterns should not be interpreted as defining complete sections. New biostratigraphic evidence suggests that either the rocks under investigation span the entire 10 million years of the Oligocene with no distinctive taxa that allow zonal sub division, or, more likely, that these formations span a much shorter time period.

Acknowledgements. We thank James and Gail Goedert for their extraordinary fossil collections, both vertebrate and invertebrate, donated to the Burke Museum. We thank Donald Prothero for initiating and working for so many years on the magnetostratigraphy of West Coast marine sedimentary units, Nick Pyenson for discussions on aspects of the marine mammal fauna, and Steffen Kiel for his very helpful review. Partial funding for this study was provided by the Barbara Chapple Endowment Fund, Burke Museum.

References

Addicott, W.O., 1976a. Molluscan paleontology of the lower Miocene Clallam Formation, north-western Washington. U.S. Geological Survey Professional Paper **976**, 1–44.

Addicott, W.O., 1976b. New molluscan assemblages from the upper Twin River Formation, western Washington: significance in Neogene biostratigraphy. U.S. Geological Survey Journal of Research **4**, 437–447.

Addicott, W.O., 1976c. Neogene molluscan stages of Oregon and Washington. In: The Neogene Symposium, selected papers on paleontology, sedimentology, petrology, tectonics and geologic history of the Pacific Coast of North America. Pacific Section SEPM, Los Angeles, California, p. 95–115.

Armentrout, J.M., 1975. Molluscan biostratigraphy of the Lincoln Creek Formation, southwest Washington. In: Weaver, D.W., Hornaday, G.R., Tipton, A., (Eds.), Future energy horizons – Paleogene Symposium and Technical Papers, SEPM, Pacific Section, Los Angeles, California p.14–48.

Armentrout, J.M., 1981. Correlation and ages of Cenozoic stratigraphic units in Oregon and Washington. Geological Society of America Paper **184:** 137–148.

Arnold, R., Hannibal, H., 1913. The marine Tertiary stratigraphy of the north Pacific Coast of America. Proceedings of the American Philosophical Society **52**, 559–605.

Barnes, L.G., Goedert, J.L., 1996. Marine vertebrate paleontology on the Olympic Peninsula. Washington Geology **24**(3), 17–25.

Barnes, L.G., Goedert, J.L., 2001. Stratigraphy and paleoecology of Oligocene and Miocene desmostylian occurrences in western Washington State, USA. Ashoro Museum of Paleontology Bulletin **2**, 7–22.

Barnes, L.G., Kimura, M., Furusawa, H., Sawamura H., 1994. Classification and distribution of Oligocene Aetiodedidae (Mammalia; Cetacea; Mysticeti) from western North America and Japan. The Island Arc **3**, 393–431.

Barnes, L.G., Goedert, J.L., Furusawa, H., 2001. The earliest known echolocating toothed whales (Mammalia; Odontoceti): preliminary observations of fossil from Washington State. In: McCord, R.D., Boaz, D. (Eds.), Western Association of Vertebrate Paleontologists and Southwest Paleontologists Symposium, Proceedings. Mesa Southwest Museum Bulletin **8**, 91–100.

Berggren, W.A., Kent, D.V., Swisher, C.C.III, Aubry, M.-P., 1995. A revised geochronology and chronostratigraphy. SEPM Special Publication **54**, 129–212.

Berglund, R.E., Goedert, J.L., 1996. A new crab (Brachyura; Cancridae) from lower Miocene rocks of the northwestern Olympic Peninsula, Washington. Journal of Paleontology **70**, 830–835.

Blow, W.H., 1969. Late Middle Eocene to Recent planktonic foraminiferal biostratigraphy. Proceedings 1st International Conference on Planktonic Microfossils **1**, 199–422.

Brandon, M.T., Roden-Tice, M.K., Garver, J.I., 1998. Late Cenozoic exhumation of the Cascadia accretionary wedge in the Olympic Mountains, northwest Washington State. Geologic Association of America Bulletin **110**, 985–1009.

Brown, R.D., Jr., Gower, H.D., 1958. Twin River Formation (redefined), northern Olympic Peninsula, Washington. America Association of Petroleum Geologists Bulletin **42**, 2492–2512.

Brown, R.D., Jr., Gower, H.D., Snavely, P.D., Jr., 1960. Geology of the Port Angeles-Lake Crescent Area, Clallam County, Washington. U.S. Geological Survey Oil and Gas Investigation Map **OM – 203**.

Cameron, B.E.B., 1980. Biostratigraphy and depositional environment of the Escalante and Hesquiat formations (Early Tertiary) of the Nootka Sound area, Vancouver Island, British Columbia. Geological Survey of Canada Paper **78**, 9–28.

Campbell, K.A., 2006. Hydrocarbon seep and hydrothermal vent paleoenvironments and paleontology; past developments and future research directions. Palaeogeography, Palaeoclimatology, Palaeoecology **232**, 362–407.

Clapp, C.H., Cook, H., 1917. Sooke and Duncan map areas, Vancouver Island. Geological Survey of Canada Memoir **96**, 1–445.

Clark, B.L., Arnold, R., 1923. Fauna of the Sooke Formation, Vancouver Island. University of California Publications, Department of Geological Sciences Bulletin **14**, 123–234.

Cushman, J.A., Schenck, H.G., 1928. Two foraminiferal faunules from the Oregon Tertiary. University of California Publications, Department of Geological Sciences Bulletin **17**, 305–324.

Domning, D.P., Ray, C.E., McKenna, M.C., 1986. Two new Oligocene desmostylians and a discussion of tethytherian systematics. Smithsonian Contributions to Paleobiology **59**, 1–56.

Dragovich, J.D., Logan, R.L., Schasse, H.W., Walsh, T.J., Lingley, W.S., Jr., Norman, D.K., Gerstel, W.J., Lapen, T.J., Schuster, J.E., 2002. Geologic map of Washington – Northwest Quadrant. Washington Division of Geology and Earth Resources Geologic Map GM-50.

Durham, J.W., 1944. Megafaunal zones of the Oligocene of northwestern Washington. California University Publications, Department of Geological Sciences Bulletin **27**, 102–211.

Fraaije, R.H.B., Van Bakel, B.W., Jagt, J.W., Coole, Y., 2006. Two new Paleogene species of mud shrimp (Crustacea, Decapoda, Upogebiidae) from Europe and North America. Bulletin of the Mizunami Fossil Museum **33**, 77–85.

Goedert, J.L., 1988. A new late Eocene species of Plotopteridae (Aves: Pelecaniformes) from northwestern Oregon. California Academy of Sciences Proceedings **45**, 97–102.

Goedert, J.L., Barnes, L.G., 1996. The earliest known odontocete; a cetacean with agorophiid affinities from latest Eocene to earliest Oligocene rocks in Washington State. Paleontological Society Special Publication **8**, p.148.

Goedert, J.L., Squires, R.L., Barnes, L.G., 1995. Palaeoecology of whale fall habitats from deep-water Oligocene rocks, Olympic Peninsula, Washington State. Palaeogeography, Palaeoclimatology, Palaeoecology **118**, 151–158.

Goedert, J.L., Thiel, V., Schmale, O., Rau, W.W., Hamburg, M., Peckmann, J.M., 2003. The Late Eocene 'Whiskey Creek' methane-seep deposit (western Washington State) Part I: geology, palaeontology, and molecular geobiology. Facies **48**, 223–240.

Goedert, J.L., Barnes, L.G., Furusawa, H., 2007. The diversity and stratigraphic distribution of cetaceans in early Cenozoic strata of Washington State, USA. 11th conference of Australasian Vertebrate Evolution, Paleontology and Systematics, Geological Society of Australia, p.44.

Gower, H.D., 1960. Geologic Map of the Pysht Quadrangle. U.S. Geological Survey, Map GQ 129.

Haeussler, P.J., Bradley, D.C., Wells, R.E., Miller, M.L., 2003. Life and death of the Resurrection plate: evidence for its existence and subduction in the northeastern Pacific in Paleocene-Eocene times: Geological Society of America Bulletin **115**, 867–880.

Hickman, C.S., 2003. Evidence for abrupt Eocene-Oligocene molluscan faunal change in the Pacific Northwest. In: Prothero, D.R., Ivany, L.C., Nesbitt, E.A. (Eds.) From Greenhouse to Icehouse: the Eocene Oligocene Transition, Columbia University Press, New York, p.71–87.

Johns, M.J., Barnes, C.R., Narayan, Y.R., 2006. Cenozoic ichthyolith biostratigraphy; Tofino Basin, British Columbia. Canadian Journal of Earth Sciences **43**(2), 177–204.

Kiel, S., 2006. New Records and species of mollusks from Tertiary cold-seep carbonates in Washington State, USA. Journal of Paleontology **80**, 121–137.

Kiel, S., Goedert, J.L., 2006. Deep-sea food bonanzas: early Cenozoic whale-fall communities resemble wood-fall rather than seep communities. Proceedings of the Royal Society B **273**, 2625–2632.

Kiel, S., Goedert, J.L., 2007. Mew mollusks associates with biogenic substrates in Cenozoic deep-water sediments of Washington State. Acta Palaeontologica Polonica **52**, 41–52.

Kleinpell, R.M., 1938. Miocene stratigraphy of California. American Association of Petroleum Geologists, Tulsa Oklahoma, 450 p.

Kleinpell, R.M., 1980. The Miocene stratigraphy of California revisited. American Association of Petroleum Geologists Studies in Geology **1**, 1–182.

Martin, R.A., Nesbitt, E.A., 2007. Characteristics of methane-influenced fluid-flow in Oligocene-Miocene sediments of the Cascadia margin. Geological Society of America Abstracts and Proceedings **39**(6), 304.

Martin, R.A., Nesbitt, E.A., Campbell, K.A., 2006. Benthic foraminiferal characterization of two Cenozoic cold seeps, Cascadia accretionary margin. Third International Symposium on Hydrothermal Vent and Seep Biology, La Jolla, California p.27.

Martini, E., 1971. Standard Tertiary and Quaternary calcareous nannoplankton zonation. Proceedings of the 2nd Planktonic Conference, p.739–785.

McDougall, K., 1980. Paleoecological evaluation of the late Eocene bio stratigraphic zonations of the Pacific Coast of North America. Paleontological Monograph **2**, 46 p.

McNeill, L.C., Goldfinger, C., Kulm, L.D., Yeats, R.S., 2000. Tectonics of the Neogene Cascadia forearc basin: investigations of a deformed late Miocene unconformity. Geological Society of America Bulletin **112**, 1209–1224.

Moore, E.J., 1963. Miocene mollusks from the Astoria Formation in Oregon. U.S. Geological Survey Professional Paper **419**, 109 p.

Moore, E.J., Addicott, W.O., 1987. The Miocene Pillarian and Newportian (molluscan) stage of Washington and Oregon and their usefulness in correlations from Alaska to California. U.S. Geological Survey Bulletin **1664**, A1–A13.

Muller, J.E., Cameron, B.E.B., Northcote, K.E., 1981. Geology and mineral deposits of the Nootka Sound area map (92E), Vancouver Island, British Columbia. Geological Survey of Canada Paper **80–16**, 1–53.

Narayan, Y.R., Barnes, C.R., Johns, M.J., 2005. Taxonomy and stratigraphy of Cenozoic foraminifers from Shell Canada wells, Tofino Basin, offshore Vancouver Island, British Columbia. Micropaleontology **51**(2), 101–168.

Nesbitt, E.A., 2003. Changes in shallow-marine fauna from the Pacific Margin across the Eocene/Oligocene boundary. In: Prothero, D.R., Ivany, L.C., Nesbitt, E.A. (Eds.), From Greenhouse to Icehouse: the Eocene Oligocene Transition. Columbia University Press, New York, p.57–70.

Olson, S.L., 1980. A new genus of penguin-like pelecaniform bird from the Oligocene of Washington (Pelecaniformes: Plotopteridae). Natural History Museum Los Angeles County Contributions in Science **330**, 51–57.

Prothero, D.R., 2001. Chronostratigrpahy calibration of the Pacific Coast Cenozoic: a summary. Pacific Section SEPM Book **91**, 377–394.

Prothero, D.R., Burns, C., 2001. Magnetic stratigraphy and tectonic rotation of the upper Oligocene-?lower Miocene (type Pillarian Stage) Clallam formation, Clallam County Washington. Pacific Section SEPM Book **91**, 234–241.

Prothero, D.R., Nesbitt, E.A., 2008. Paleomagnetism and tectonic rotation of the Restoration Point Member of the Blakeley Formation (Type Blakeley Stage) Bainbridge Island, Washington, and the Pacific Coast Oligocene-Miocene boundary. New Mexico Museum of Natural History and Science Bulletin **44**, 315–322.

Prothero, D.R., Ressuguie, J.L., 2001.Magnetic stratigraphy of the Oligocene Zemorrian Stage, Temblor Formation, Kern County, California. Pacific Section SEPM Book **91**, 210–223.

Prothero, D.R., Streig, A., Burns, C., 2001. Magnetic stratigraphy and tectonic rotation of the upper Oligocene Pysht Formation, Clallam County, Washington. Pacific Section SEPM Book **91**, 224–233.

Prothero, D.R., Draus, E., Cockburn, T.C., Nesbitt, E.A., 2008. Paleomagentism and counterclockwise tectonic rotation of the Upper Oligocene Sooke formation, southern Vancouver Island, British Columbia. Canadian Journal of Earth Sciences **45**, 499–507.

Rathbun, M.J., 1926. The fossil stalk-eyed Crustacea of the Pacific slope of North America. Bulletin of the United States National Museum **138**, 114–117.

Rau, W.W., 1958. Stratigraphy and foraminiferal zonations in some Tertiary rocks of southwestern Washington. U.S. Geological Survey Oil and Gas Investigation Chart OC-57.

Rau, W.W., 1964. Foraminifera from the Northern Olympic Peninsula, Washington. U.S. Geological Survey Professional Paper **374-G**, p.33.

Rau, W.W., 1981. Pacific Northwest Tertiary benthic foraminiferal biostratigraphic framework – an overview. Geological Society of America Special Paper **184**, 67–84.

Ray, C.E., Domning, D.P., Mckenna, M.C., 1994. A new specimen of *Behemotops proteus* (order Desmostylia)

from the marine Oligocene of Washington. Proceedings of the San Diego Society of Natural History **29**, 205–222.

Schweitzer, C.E., Feldmann, R.M., 1999. Fossil decapod crustaceans from the late Oligocene to early Miocene Pysht Formation and late Eocene Quimper Sandstone, Olympic Peninsula, Washington. Annals of Carnegie Museum **68**, 215–273.

Snavely, P.D., Jr., Niem, A.R., Pearl, J.E., 1978. Twin River Group (upper Eocene to lower Miocene) – defined to include the Hoko River, Makah, and Pysht formations, Clallam County, Washington. U.S. Geological Survey Bulletin **1457A**, 111–120.

Snavely, P.D., Jr., Wells, R.E., 1996. Cenozoic evolution of the continental margin of Oregon and Washington. U.S. Geological Survey Professional Paper **1560**, 161–182.

Squires, R.L., 1989. Pteropods (Mollusca: Gastropoda) from Tertiary formations of Washington and Oregon. Journal of Paleontology **63**, 443–448.

Stewart, R.J., Brandon, M.T., 2004. Detrital-zircon fission-track ages for the "Hoh Formation": implications for late Cenozoic evolution of the Cascadia subduction wedge. Geological Society of America Bulletin **116**, 60–75.

Tegland, N.M., 1931. The fauna of the type Blakeley, Upper Oligocene of Washington. California University Publications, Department of Geological Sciences Bulletin **23**, 81–174.

Tabor, R.W., Cady, W.M., 1978. Geologic map of the Olympic Peninsula, Washington. U.S. Geological Survey Miscellaneous Investigations Series Map MI-994.

Tedford, R.H., Barnes, L.G., Ray, C., 1994. The Early Miocene littoral ursoid carnivoran *Kolponomos*: systematics and mode of life. Proceedings of the San Diego Society of Natural History **29**, 11–32.

Warren, A.D., Newell, J.H., 1980. Planktonic biostratigraphy of the Refugian and adjoining stages of the Pacific Coast Tertiary. Cushman Foundation Special Publication **19**, 233–251.

Weaver, C.E., 1916. Tertiary faunal horizons of western Washington. University of Washington Publications in Geology **1**, 1–67.

Weaver, C.E., 1937. Tertiary stratigraphy of western Washington and northwestern Oregon. University of Washington Publication in Geology **4**, 1–266.

Weaver, C.E., 1943. Paleontology of the marine Tertiary formations of Oregon and Washington. University of Washington Publications in Geology **5**, 1–789.

Weaver, C.E., 22 Others, 1944. Correlation of the marine Cenozoic formations of western North America. Geological Society of America Bulletin **55**, 569–598.

Wieder, R.W., Feldmann, R.M., 1989. *Palaega goedertorum*, a fossil isopod (Crustacea) from Late Eocene to Early Miocene rocks of Washington State. Journal of Paleontology **63**, 73–80.

Yorath, C.J., Green, A.G., Clowes, R.M., Brown, A.S., Brandon, M.T., Kanasewich, E.R., Hyndman, R.D., Spencer, C., 1985. Lithoprobe, southern Vancouver Island: seismic reflection sees through Wrangalia to the Juan de Fuca plate. Geology **13**, 759–762.

Manuscript received: August 29, 2009, rev. version received: September 28, 2009, accepted for print: October 28, 2009.

NEWSLETTERS ON Stratigraphy

Volume
43

With 91 figures, 5 plates and 11 tables

Gebrüder Borntraeger · Berlin · Stuttgart 2010

ISSN 0078-0421

♾ Printed on permanent paper conforming to ISO 9706-1994.

Printer: Laupp & Göbel, Nehren/Tübingen – Printed in Germany

Contents

Newsletters on Stratigraphy – News

Call for papers

Authors are invited to submit their original papers or short notes to the editors.
Interested in publishing your paper in Newsletters?

Please use the Newsletters Online Review System
(https://www.schweizerbart.de/submit/newsletters/index.php)

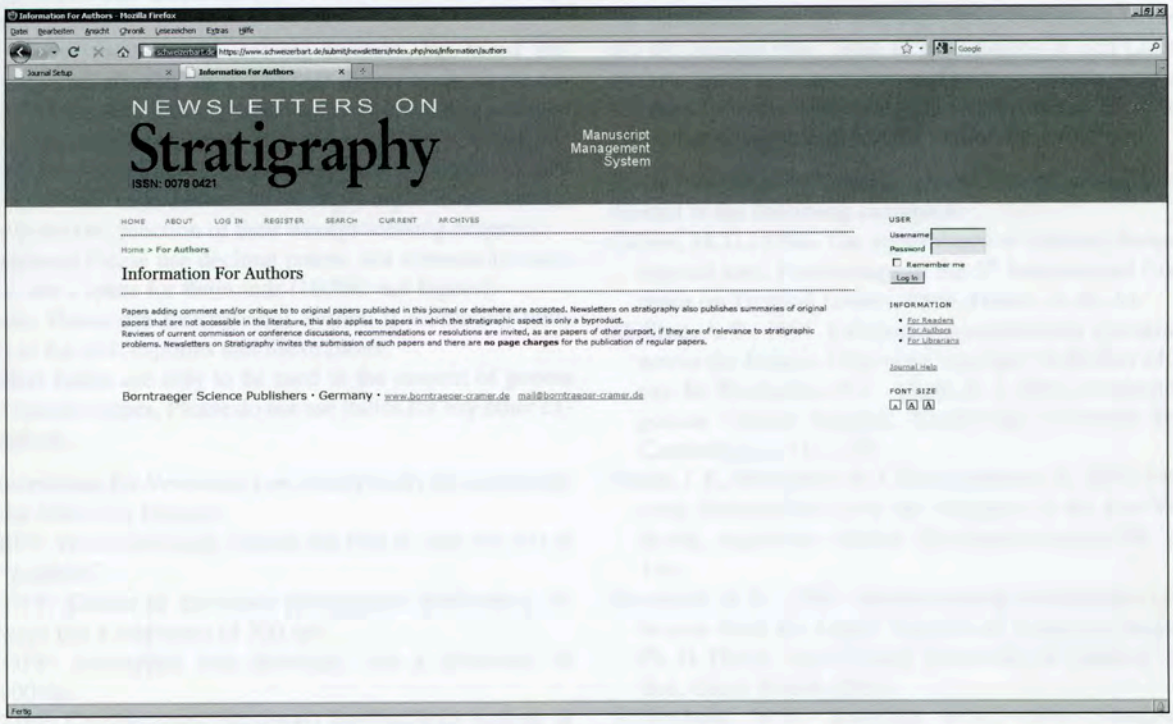

This procedure simplifies and speeds up the review process, accelerates communication, and enables authors, editors and reviewers to maintain an excellent overview about the status of all review processes.

For further information on submission please visit:
www.schweizerbart.de/journals/nos

Gebrüder Borntraeger · Berlin · Stuttgart

A "Present address" may be indicated as a footnote to an author's name if that author has changed his address since the work presented in the article was carried out. The address where the author actually carried out the work needs to be retained as the main affiliation address.

Corresponding Author. Please indicate which author will handle correspondence throughout the refereeing and publication processes. For the corresponding author, E-Mail address, telephone and fax numbers (including country and area code), and the complete postal address are required.

Abstract. An abstract exceeding not more than 400 words is required. Please consider that an abstract is often presented separate from the article, so it must be able to stand alone. References should be avoided. In the rare cases they are essential, they must be fully cited in the abstract. If such a reference does not re-occur later in the manuscript text, it will not be included into the reference list. Abbreviations should be avoided unless they are commonly used (such as, e.g., SI units).

Keywords. After the abstract, provide a maximum of 6 keywords.

We accept most wordprocessing formats, but Word and WordPerfect are preferred. The text should be in single-column format and double spaced. All text lines and pages must be consecutively numbered. Please use bold face, italics, etc. where needed. To avoid unnecessary errors and thus to ease the reviewers' task, authors are strongly urged to activate the 'spellchecker' function of their wordprocessing program.

Numbers: Please use decimal points, not commas in numbers; use a space for thousands (10,000 and higher).

Units: Please use International System (i.e., metric) units (SI) in the text, captions and illustrations.

Italics: Italics are only to be used in the context of genera and species names. Please do not use italics for any other expressions.

Illustrations for *Newsletters on Stratigraphy* are acceptable in the following formats:

- EPS: Vector drawings. Embed the font or save the text as "graphics".
- TIFF: Colour or greyscale photographs (halftones): always use a minimum of 300 dpi.
- TIFF: Bitmapped line drawings: use a minimum of 600 dpi.
- TIFF: Combinations bitmapped line/half-tone (colour or greyscale): a minimum of 300 dpi is required.
- DOC, XLS or PPT: If your illustrations are created in any of these Microsoft Office applications please supply "as is".

Please do not supply embedded graphics in your wordprocessor (spreadsheet, presentation) document when submitting the final accepted article;

Avoid GIF, BMP, PICT, WPG and Corel graphics, ensure readability of graphics when reduced to page size.

If pdf files are submitted, please ensure that all fonts are embedded and figures are resolved with a minimum resolution of 300 dpi (colour/grey scale figures) and 600 dpi (line drawings), respectively.

Colour illustrations will be printed against costs; please ask the publishers for details.

References. All references cited in the text need to be listed at the end of the paper in a "References" section. Please check carefully that the spellings of author names and publication years are consistent within the text and the "References" section. Do not type author and editor names in capitals.

In the text, please refer to an author's study as indicated in the following examples:

- ... referring to the study of Fischer et al. (2003), Stone and Waller (2005) argued that ...
- ... these observations are in line with the results of earlier workers (e.g., Smith et al. 1990, Miller et al. 1997, Willis and Morrison 2000).

References in the text are to be given in chronological order. References in the "References" section are to be arranged alphabetically based on the authors' names; there, the last names and initials of all co-authors are required. Please give the full names of journals in the "References" section; do not use abbreviations.

For publications in any language other than English, please use the original title. Titles of publications in non-Latin alphabets (such as, e.g., Chinese, Greek, Japanese, or Russian) need to be transliterated, and a note such as '(in Chinese)' needs to be included at the end of the reference.

In the **"References"** section, please list publications as indicated in the following examples:

Calvin, M.D., 1986. The significance of climate change on tropical ants. Proceedings of the 5th International Conference on Tropical Insects, Paris, France, p. 38–54.

Shilling, A.S., 1991. Calcareous nanoplankton stratigraphy across the Eocene-Oligocene boundary in the Bay of Biscay. In: Fleckstein, D.C., Mann, E.E. (Eds.), Eocene-Oligocene Climate Records. Cambridge University Press, Cambridge, p. 111–128.

Smith, J.P., Elbrächter, H.I. Gudmundsson, S., 2001. Planktonic foraminifera from the Neogene of the Los Valles Basin, Argentina. Marine Micropaleontology **24**, 111–126.

Wareland, A.B., 2000. Spatiotemporal relationships in paleosols from the Upper Permian of Southwest England. Ph.D. Thesis, Agricultural University of London, London, Great Britain, 245 p.

Zonenshain, M.S., Berglund, G.V., 1999. Stratigraphy Through Space and Time. Schweizerbart, Stuttgart, 245 p.

Online access for all subscribers: Beginning in 2004, **Newsletters on Stratigraphy** is available online through Ingenta. Articles are included in the CrossRef Services which allow direct access to referenced papers (published in this or other journals which are available online). Conversely, papers in other journals are able to reference papers published in Newsletters on Stratigraphy by placing direct reference links. Please contact Ingenta.

Reprints. First authors will receive 25 reprints free of charge or alternatively a pdf file of their article for personal use only.

March 2010

NEWSLETTERS ON
Stratigraphy Volume 43 No. 3

Contents

NEWSLETTERS ON
Stratigraphy

ISSN 0078-0421
Available online via **www.schweizerbart.de/journals**
Indexed in Science Citation Index Expanded®, ISI Altering Services